NASA CONTRACTOR REPORT

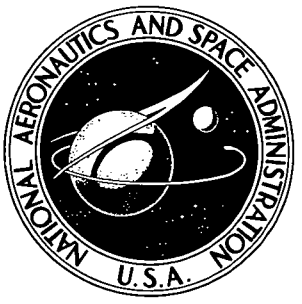

NASA CR-2309

NASA CR-2309

SIMULATOR TESTS TO STUDY HOT-FLOW PROBLEMS RELATED TO A GAS CORE REACTOR

by John W. Poole, Mark P. Freeman, Kenelm W. Doak, and Merle L. Thorpe

Prepared by
HUMPHREYS CORPORATION
Concord, N.H. 03301
for Lewis Research Center

NATIONAL AERONAUTICS AND SPACE ADMINISTRATION • WASHINGTON, D. C. • OCTOBER 1973

1. Report No.	2. Government Accession No.	3. Recipient's Catalog No.
NASA CR-2309		

4. Title and Subtitle	5. Report Date
SIMULATOR TESTS TO STUDY HOT-FLOW PROBLEMS RELATED TO A GAS CORE REACTOR	October 1973
	6. Performing Organization Code

7. Author(s)	8. Performing Organization Report No.
John W. Poole, Mark P. Freeman, Kenelm W. Doak, and Merle L. Thorpe	None
	10. Work Unit No.

9. Performing Organization Name and Address	11. Contract or Grant No.
Humphreys Corporation Concord, New Hampshire 03301	NAS 3-15710
	13. Type of Report and Period Covered
12. Sponsoring Agency Name and Address	Contractor Report
National Aeronautics and Space Administration Washington, D.C. 20546	14. Sponsoring Agency Code

15. Supplementary Notes

Project Manager, Chester D. Lanzo, Nuclear Systems Division, NASA Lewis Research Center, Cleveland, Ohio

16. Abstract

The report presents the results of an advance study of materials, fuel injection, and hot-flow problems related to the gas core nuclear rocket (GCNR). Not all the tasks planned were completed because of contract termination. The first task was to test a previously constructed induction heated plasma GCNR simulator above 300 kW. A number of tests are reported operating in the range of 300 kW at 10,000 cps. A second simulator was designed but not constructed for cold-hot visualization studies using louvered walls. A third task was a paper investigation of practical uranium feed systems, including a detailed discussion of related problems. The last assignment resulted in two designs for plasma nozzle test devices that could be operated at 200 atm on hydrogen.

17. Key Words (Suggested by Author(s))	18. Distribution Statement
Induction heated gases; Plasmas; Radiofrequency heating; High-temperature gases; Gas core reactors	Unclassified - unlimited

19. Security Classif. (of this report)	20. Security Classif. (of this page)	21. No. of Pages	22. Price*
Unclassified	Unclassified	115	$3.00

* For sale by the National Technical Information Service, Springfield, Virginia 22151

TABLE OF CONTENTS

TABLE OF CONTENTS (Cont'd)

SUMMARY

A series of four tasks formed the basis of the subject investigation for the purpose of an advance study of hot-flow problems related to the Gas Core Nuclear Rocket Engine. A portion of the study was an upgrading of proposed simulator systems for the follow-on program at the Arnold Engineering Development Center.

Task I included a refinement of design features in order that the GCNR simulator, previously constructed by TAFA, could be operated at power levels of 300 kW and above. Successful design changes were completed including the long sought permeable inner wall--the confinement region for the plasma. The test runs reached power levels of 350 kW but attempts to operate at higher power levels were unsuccessful. The simulator was found to be extremely sensitive to additives in the arc gas, i.e. the smallest air leak made starting impossible. In addition, it was found that inductance inherent in the long transmission line from the power source did not have capacitive compensation which resulted in very high starting voltages.

Task II was directed towards the design and test of a cold-hot flow simulator that could be used for visualization studies, evaluation of fuel expansion characteristics, and a variety of flow patterns and seeding studies. The latter was a significant activity because of earlier success with this method for radiation absorption. Following a thorough investigation, a simulator was conceived that included a variable area louvered cylindrical shaped inner wall made from clear quartz. The cold flow investigation and the hot flow studies scheduled for the new simulator were not conducted because the contract was terminated for the convenience of the government.

The problem addressed in the third task was an in depth study of practical approaches to the uranium feed system in the final engine design. This study included an analysis of the four major areas related to the feed system namely the cavity region, the moderator region, uranium storage and the actual feed mechanism. Following an in depth discussion of these problem areas, four feed

systems are presented--identified as wire feed, liquid jet feed, pellet feed, and cartridge feed. None of the proposed systems appear to have major critical problem areas. It was also established that the feed must be introduced radially through multiple ports. The concept of a halide feed was abandoned because of the corrosion problem.

A detailed design study to develop a four megawatt hot hydrogen nozzle for use in the follow-on study was the assignment for Task IV. The first design follows the d.c. approach and is based on proven arc constrictor design concepts. The second approach is an r.f. induction heater design that relies on a cesium vapor plus an argon fuel region to provide necessary plasma resistivity. While the d.c. approach would involve less technical risk, both designs could be successfully operated.

INTRODUCTION

The Gas Core Nuclear Rocket has a variety of unique design requirements that have been or are currently being investigated by various organizations. The TAFA Division of the Humphreys Corporation has been involved in a number of these programs to test design principles and possibly define solutions. The purpose of the work reported herein, as defined in a series of four tasks, was to simulate as closely as possible, with induction plasma heating, the heat transfer and flow characteristics of a Gas Core Nuclear Rocket (GCNR) including solid feed techniques, and the development of a system for propellant seeding.

Specifically, the purpose of the first task was the operation of a GCNR simulator, previously constructed by TAFA[1], at power levels of 300 kW and above. Following additional work with feed systems, a series of at least ten data runs would be made at the TOCCO Division of Park-Ohio Industries where a 10 KHz power supply was available.

In the second task, a modified version of the simulator was to be designed and constructed that would duplicate the features of the device used in a study conducted by Aerojet Nuclear Corporation. The Aerojet activity was confined to a cold flow investigation while both hot and cold tests were scheduled for this contract. Twenty documented cold flow runs and twenty hot flow runs were to be made.

Task III was directed primarily towards designing alternate uranium feed systems for the gas core engine. Guidelines included the concept of injecting enriched U-235 in powder or wire form, or a uranium halide liquid or gas. Activity included preparing four designs and/or options along with appropriate discussions of potential advantages and disadvantages.

Lastly, Task IV was established as a design activity to develop a 4 MW hot hydrogen nozzle tester suitable for use with the Arnold Engineering Development Center 4 MW r.f. power supply under construction. The design was to include an induction heater coil assembly and the nozzle interior gases were to be seeded in order to provide protection to the walls from radiation of the hot core gases. Included in the assignment was the task of identifying and/or designing instrumentation to provide heat balance measurements and surface temperatures along the inside surface of the nozzle.

The contract was terminated for the convenience of the government before the program was completed. With the exception of the second task (hot and cold studies), the results of the various investigations are being presented in reasonably complete form. As the test portion of Task II was not undertaken, only the results of the design portion are being reported.

TASK I - DESIGN REVISION AND HIGH POWER TESTING

Prior to the higher power test program for the combined principles simulator (CPS), several areas of the basic design needed additional study directed towards improved performance. These included an investigation of materials for the permeable inner wall and refinement of the fuel injection system and the method of seeding. For reference purposes Figure 1 is an assembly drawing of the CPS previously constructed.[1] A permeable wall, roughly spherical in shape, surrounds the plasma region and is contained within an outer pressure vessel. The fuel inlet-end flange provides for penetration of the solid fuel feed mechanism and injection of the seeding for the propellant gas stream. The nozzle-end flange supports the nozzle and provides for transpiration cooling and seeding flow to the nozzle. Adequate cooling and space for a large coil are provided for high power operation.

In the following paragraphs the various studies required prior to the test program are discussed.

A. Permeable Inner Wall

The permeable wall of the CPS, Figure 1, serves as the confinement region for the plasma and is probably the most significant test item in the simulator. Since energy is coupled into the plasma from an electromagnetic field, the wall material must have a very high electrical resistivity. In addition, due to the sudden increase in radiant heating upon establishment of a plasma, the material must have good thermal shock properties. Uniformity of permeability is necessary to avoid distortion of the plasma and to provide cooling of the entire wall. Therefore, a permeable silica should be the ideal material for the inner wall due to its excellent electrical and thermal shock properties.

The permeable wall material originally used in the CPS constructed for this investigation was AlSiMag 447, a cordierite material.[2] This material has a thermal expansion coefficient similar to silica and has appropriate electrical properties. The straight circular cylinders of AlSiMag 447

used for laboratory tests were supplied without any discernable internal cracks. Unfortunately, cracking of the more complex shape for the CPS became a very severe problem.

To correct this difficulty, prior to the high power test runs, a strenuous effort was undertaken to find a more reliable wall material. To assist in this investigation, an experimental setup was constructed (Figure 2), where a permeable wall of fused silica was located inside of the pressure shell in the plasma generator. Figure 3 shows an end view of the permeable wall which had a wall approximately 0.636 cm thick and is about 10.2 cm in diameter and 26.6 cm long. A small penetration was made through the back of the device for introduction of the fuel material.

During a difficult search, lasting almost two years, only one material was found that provided acceptable wall performance--VX grade silica produced by Western Gold & Platinum Co. The material has been tested to every extent possible on the smaller plasma devices and has been found to stand up very well. Its success as a transpiration cooled wall involves a combination of high reflectivity, moderately good heat transfer, and the characteristically low thermal expansion of fused silica. Its thermal conductivity is approximately six times that of the silica foam walls (tested earlier in the program) that were found to glaze on the inside surface. However, the thermal conductivity is only about 60 percent of that for AlSiMag 447 but the white color of the VX silica compared to the tan color of the 447 should make enough of a difference in absorption so that the materials will behave much the same. The big advantage with the VX material would be that it can be processed into sound parts without the cracking that has been a problem with the AlSiMag 447.

During the initial shakedown tests at TOCCO, the AlSiMag 447 walls were utilized. The AlSiMag walls cracked badly as the power was raised above 250 kW utilizing a transpiration flow of 9400 cm^3/sec. At this point, the VX silica walls were substituted and no further cracking problems were experienced even with ignition at 250 kW. In some tests, the silica walls were yellow hot and, once the arc extinguished, the gas continued to transpire through the wall without causing cracking. It thus can be concluded that the silica walls performed very satisfactorily and were an excellent choice for this design.

B. Fuel Injection - Wire

As the GCNR concept requires the introduction of the uranium fuel into the fissioning fuel region, several injection techniques were investigated in earlier work.[1] The CPS used in Task I incorporated a wire feed approach that has continued to function with a minimum of difficulty.

This system incorporates a simple variable speed motor drive propelling the wire between two rollers from a storage reel. Downstream from the drive wheels is a close fitting gas barrier which prevents leakage from the plasma chamber. The uranium wire is introduced through a boron nitride tip into the core of the plasma. A small quantity of chlorine gas is passed around the wire to form uranium chlorides that vaporize at temperatures of about 870°K. This is significantly below the vaporization temperature of uranium (4073°K). If chlorine is not used, the high melting point and vaporization temperature of uranium prevents the formation of a vapor in the plasma device. In the GCNR, the high temperatures and pressures during operation will circumvent this problem. However, the injection of chlorine does suggest an ignition technique at lower temperatures.

Initial work with the wire feeder indicated a very smooth operation with well controlled injection. Continued use of the feeder, however, developed a control problem which was traced to a leak in the gas block seal. This seal is designed to prevent chlorine from escaping from the torch through the wire feed. This problem was cured by introducing a ceramic seal to prevent gas leakage and consequent dilution of the chlorine feed. It is now possible to obtain a very uniform, continuous metallic vapor feed for the plasma. For the 10.16 cm i.d. clear quartz tube that has been used for the checkout of the wire feeder, a feed rate of approximately 0.1 g/min. with a chlorine feed rate of about 1.34 cm^3/sec was established as a very smooth operating point.

Continued work with the wire feeder established the limiting characteristics of operation. With iron wire as a substitute for uranium, extensive testing in the TAFA laboratory at 4 MHz and 100 kW was conducted with chlorine feed rates and injection tip location as variables to determine optimum values. Understanding of the characteristics

exhibited by these variables will enable smoother operation of the combined principles simulator. The final evaluation of the proposed fuel feed injection system could not be made because of inadequate power at TOCCO during the tests reported here and program cancellation which prevented further tests.

C. Propellant Seeding

Since the ultimate design of the GCNR requires propellant seeding in the boundary layer to intercept the high radiant energy from the fuel region, a continuing effort has been made in the TAFA simulator programs to refine the seeding system. The CPS, shown in Figure 1, has provision for propellant seeding along the permeable wall and again at the entrance to the nozzle.

Since thermal protection of the permeable wall requires the injection of a powder between the plasma and the wall, a significant effort was devoted to checking out the powder feed system. The clear walled device, shown in Figure 4, was used with a high intensity tungsten lamp located on the centerline of the device to measure the radiation absorption during powder feed runs at various flow rates. It was determined that the TAFA Model PI-104 feeder, operating by itself, could not supply adequate powder to intercept more than 50 percent of the radiation from the lamp. Consequently, two new Plasmadyne Model 1000A powder feeders were purchased. When the new powder feeders were first run with silicon powder, severe abrasion of certain parts was experienced. Apparently the form of the silicon was the primary problem. It was supplied as flat platelets which filled all close clearance areas, causing parts seizure and galling. Therefore, the decision was made to shift to a more uniformly shaped tungsten powder of approximately 15 microns in diameter for additional tests.

During the test work at TOCCO, submicron tungsten was fed to the seed system, but the runs were of such short duration it was not possible to establish the effectiveness of radiation barrier. A more detailed description of seed performance, in a similar plasma environment, is discussed in Reference 1.

D. Induction Coil Design

As the program called for testing the CPS at 10 KHz and at a power level above 300 kW, a new coil design was required. Using a calculator program, developed in earlier work[1] for optimizing coil configuration, a four turn coil, 24.8 cm in diameter and 17.0 cm in length, was found to be optimal for coupling the available power into the plasma at the anticipated load diameter. The coupling efficiency would be approximately 60 percent for a 12.7 cm diameter plasma and 77 percent for a 15.2 cm diameter plasma within the 20.3 cm diameter permeable wall. Therefore, with the 1600 V available from the auto-transformer, it appeared possible to operate at the maximum output of the motor generator sets. (The experimental setup has been discussed in previous reports.[3])

During the final design stage, it was determined that the turns of the coil for the TOCCO test program were of such a large diameter (coil currents 8000 amperes) that they completely obscured the sight paths through the CPS. This, in turn, prevented the transmission of x-rays to be used for fuel density measurements in the plasma ball. A solution was found by modifying the coil design with a mitered step that produced a 2.54 cm space at the mid-point of the total coil --two coils above and below.

E. High Power Test

Instrumentation.- The instrumentation required for the program in the higher power phase was designed to provide the following information:

1) a complete heat balance,
2) feed rates for the solid rod, propellant gas and seed material flow rates,
3) temperature of the plasma, and
4) average discharge temperature from the torch.

The heat balance measurement is accomplished in the conventional manner of noting temperature rise and cooling water

flow rate. Variable area type water flowmeters and bimetallic spring type temperature sensors are used to make the required measurements. The heat balance includes flow and temperature rise measurements on five water cooling circuits. These are discussed in more detail in Reference 1. There is also a water cooled calorimeter for measuring the heat flux on the permeable wall (Figure 1).

Fuel retention in the plasma was to be established by using x-ray radiography. The x-ray radiography technique involves exposing film by x-rays and examining the resultant film with a densitometer. Exposure times are on the order of 1-1/2 minutes. For visual discrimination on the film, there must be at least two percent difference in density between the area being examined and the background. Figure 5 shows the result of a calculation of absorption for various fuel loadings. It can be noted that at about three grams of uranium or greater in the plasma region, sufficient absorption would be experienced to make radiography attractive.[1]

Electrical measurements included input current, voltage, kW and KVAR. These are continuously recorded on a visicorder which permitted observation of ignition and extinguishment transients as well as a direct record of length of run. Heat balance temperature differentials were also recorded.

A calculator program has been written to determine the heat balance and flow input in order to provide all of the desired data in appropriate form as outputs. Thirty-nine individual inputs are used in the program for each of the runs made. Not all of these inputs are used on each run but are included in the program to maintain consistency.

Test Facility.- The experimental setup is shown in Figures 6, 7, and 8. The power supply and capacitor bank were the same as that used previously.[4] The power supply consisted of two 175 kW (continuous rating) 210 kW (intermittent) 10,000 Hz motor generator power units connected in parallel and appropriately synchronized to produce a clean wave-form. These power units were connected by standard busses to the test facility shown in the photographs. The output busses of the power supply were connected in the test area to an autotransformer to double the 800 V buss voltage. This higher voltage, in turn, was connected across a large bank of capacitors which could be connected in various numbers by

conventional linkage to a maximum of 13,000 KVAR although only 11,205 KVAR were used. The output of the capacitors was connected by heavy 0.635 x 30.48 cm copper busses to the four-turn open center coil referred to previously and shown in Figure 7.

Experimental Procedure.- All tests followed a similar pattern.

1) The ignition procedure required a pressure in the range of 2.64 N/m^2 to establish a glow. To assure leak-tight operation, a pre-vacuum check was made. This involved connecting the o-ring sealed calorimeter to the exit nozzle (the calorimeter was placed in the vacuum line to cool the plasma gases before they entered the pump). With the calorimeter in place, the vacuum pump was turned on to evacuate the torch. Three to five back fills with argon were required to achieve a suitably pure atmosphere.

2) Once it was demonstrated that the low pressure could be maintained, the power was applied to the coil and a bright glow would appear if the torch atmosphere was free of diatomic gases.

3) With the glow operating, the argon flows were turned up, at an experimentally determined rate, to approximately 9400 cm^3/sec through the porous wall.

4) As the gas flow increased, chamber pressure rose and at approximately 106 N/m^2 the glow automatically switched to an arc while the pressure continued to rise. Finally, the pressure in the chamber reached atmospheric and the calorimeter dropped automatically from the nozzle permitting the plasma to issue from the torch, Figure 9.

5) Once atmospheric operation was achieved, additional items were varied as the test schedule directed; for example, wire feed was started, power increased, gas flow increased, etc.

6) After 15-35 sec, the unit was shut off to prevent wall failure since no seeding was used.

The entire procedure from glow through formation of an atmospheric plasma took approximately 10 sec. The complete ignition sequence, including pump down, was repeated for each test.

Discussion of Experimental Results.- It had been expected to complete all the tests required under Task I during the first test period. This was not accomplished and, hence, the test period was somewhat disappointing. The main causes for failure to achieve all the test objectives centered around the limited power available which manifested itself in two main areas. The first stems from a design compromise made in 1971 to permit initial checkout on the 189 kW, 4 MHz power supply at the TAFA laboratory. At that time, it was felt that the 20.3 cm diameter cavity would permit simple operation at TAFA while units much larger would prohibit effective coupling of the 4 MHz power. This design compromise was further confirmed when it was determined that the only acceptable available material at that stage, AlSiMag 447, could not be fabricated in diameters larger than 20.3 cm i.d. Secondly, the less favorable load to coil ratio (plasma diameter/coil diameter = 0.51) and/or the nearness of the simulator end flanges to the coil, which, in turn, may have reduced the field strength available for glow ignition within the torch, produced unfavorable conditions which made ignition very difficult with the power available. It should be noted that the previous cylindrical wall torches tested permitted ignition at much lower powers; for example, a glow was established in the 30.48 cm i.d. uncooled quartz tube at only 65 kW during the 1971 tests as noted below. The minimum sustaining powers (MSP) listed below refer to the minimum power at which a one atmosphere plasma can be maintained in argon.

Glow Ignition Powers and Minimum Sustaining Powers (MSP) of Various Torches at 10 KHz

	Ignition Energy	MSP
15.24 cm i.d. cylindrical torch	190 kW	145 kW
30.48 cm i.d. cylindrical torch	65	80
20.32 cm i.d. CPS	250	190

Powers above 350 kW could not be drawn from the 10 KHz power unit because of the load conditions produced by the CPS even though operation at 420 kW was theoretically possible. This was irrespective of the number of coil turns or the amount of capacitance used. This limited power, coupled with less

than optimum plasma stabilization, produced a situation where all the tests during this period had to be run relatively close to the MSP and, thus, extinguishment. This, in turn, produced a situation where only slight variations in the plasma environment would produce extinguishment. For example, when chlorine was added, either its slightly less plasmagenic nature (higher resistivity) or the fact that it was injected into the center of the plasma, caused extinguishment. Therefore, the scheduled uranium plasma core tests were not conducted.

The tests were plagued with many periods (some as long as two days in length) where a successful ignition could not be achieved, and these occurred at unpredictable intervals. As the tests progressed, it was determined that vacuum leaks through a slightly porous fiber glass wound pressure vessel and certain seals permitted air to enter the system and produce an atmosphere with a high enough resistance to prevent an acceptable glow to be established. Once these leaks were eliminated, reproducible ignition was achieved.

It should also be noted that sensitivity and extinguishment with minor addition of diatomic gases is to be expected with the power supply and frequency used. Figure 11 shows the effect of frequency on MSP. This figure indicates that 3000 kW is required to sustain a pure air plasma, thus, we are operating in a power region where small additions of air could be expected to produce extinguishment. It is also interesting to note from Figure 11 that a higher frequency, which was to be available at AEDC, would have produced a much more favorable condition; for example, 50,000 Hz reduces the MSP on air to 1000 kW. If twice as many ampere turns had been available during the TOCCO tests, i.e. a larger power supply, the field strength would have been adequate to alleviate this problem.

Approximately twenty completely documented runs were conducted during the test period. Data for 12 of these tests are presented in Table I. In summary, the following highlights were observed:

1) A maximum power of 350 kW was achieved. This was caused by the limitations described previously, i.e. torch diameter with associated coupling efficiency at 10,000 Hz and load/coil ratio.

2) With a properly sized load and coil at 10,000 Hz the heat balance should look something like that shown in Figure 12 with 50-75 percent ending up in the arc within the coil. By comparison, all the tests at TOCCO were in the 27-54 percent range. This further demonstrates mismatch of the CPS load at 10,000 Hz, i.e. primarily too small a diameter for efficient coupling at 10,000 Hz and a poor load/coil ratio (Figure 13 indicates 80 percent coupling efficiency).

3) Coil losses varied from 29-47 percent. This illustrates the sensitivity of the I^2R losses in the circuit to load diameter. This coil loss can be decreased by 12 percent when the arc diameter is increased from 11.4 to 12.7 cm, again drawing attention to the fact that the larger diameter CPS will show dramatic improvements in efficiency.

4) It was shown, both theoretically and experimentally, that the capacitor loss in the circuit was one-half that of the coil loss. This is confirmed throughout the data sheets. The high losses in the circuit with small load diameters results from the fact that circulating capacitor losses will also increase the coil loss since they are caused by the same phenomenon.

5) Torch losses recorded were in the range of 1-4 percent. This is a low number since the only portion of the device which is water cooled and in contact with the plasma is the seed-wire injection port at the rear.

6) Intuitively one would feel that the nozzle loss should be greater than the loss in the seed injection region; however, this was not the case. It is felt that the nozzle losses were actually lower for three reasons. First, the cold wall transpiration flow probably continued through the nozzle, thus, reducing convective losses. Secondly, the surface area of the nozzle was small compared with the inlet region (approximately one-half). Thirdly, it has been observed with transparent units that

the buoyant effect of the plasma tends to keep it close to the inlet end, thus increasing the convective and radiant energy in this area.

7) The percentage of power in the gas stream leaving the torch was in the range of 40 percent. This number is encouraging when one compares operation with a water cooled device, i.e. even with the most efficient standard TAFA torches 50-55 percent is a very acceptable efficiency. This improved efficiency, even at low powers, obviously comes about because of transpiration wall cooling.

8) Exhaust gas enthalpies ranged from 2.5×10^6 to 9.5×10^6 J/kg. This is reasonably respectable as standard plasma torches go. The 9.5×10^6 J/kg enthalpy corresponds to a temperature of 9300°K. It should be noted that this is Run No. 5 and was recorded at 238 kW with 11.38 g/sec wall gas flow.

9) As indicated previously, argon gas flows through the wall above 22 g/sec produced arc extinguishment within the limits of the power supply. Wall heat load calculation (assuming 10,000 Hz plasma at 300 kW) indicates 78.5 g/sec is required to maintain a wall temperature below 800°K. It was, thus, no surprise that wall temperatures rose above this level during the longer runs and prohibited continuous operation. The maximum wall temperatures were achieved during a 46 sec, 300 kW run. At this point the wall was bright yellow internally with an estimated temperature in the range of 1200°K. Extrapolating the data of MSP versus gas flow would indicate that 650 kW would be required to operate in the 78.5 g/sec range, at which point the required wall flow for cooling would have again doubled. It is also obvious, from past torch experience, that higher power operation would have produced a more stable, spatially consistent plasma, similar to that produced in the cylindrical torches. Again, it cannot be over emphasized that we were operating in a corner of the stability diagram shown in Figure 14.

10) It was envisioned that later tests would utilize helium as the propellant to emphasize the buoyancy effect and more closely simulate hydrogen. Some experiments were run with helium during this test period. A glow could be formed and transformation to an arc occurred; however, extinguishment occurred above 250 mm chamber pressure. This is not an unexpected result based on the fact that we were operating close to extinguishment with argon and the additional point that helium operation requires a slightly higher MSP. It is expected that if higher powers were available, helium operation would not be a problem.

11) A similar picture can be painted for chlorine. It was introduced through the wire feed port on the axis of the chamber. This, in turn, introduced a less plasmagenic gas into a very critical region of the plasma. In addition, past experience at TAFA has indicated that any introduction of a gas on the axis of a plasma tended to disturb its stability and, thus, it would be expected that even argon injected here would tend to raise the MSP slightly. The tests in which chlorine was run at TOCCO resulted in immediate extinguishment even when small amounts were added (argon wall gas). However, it is expected that chlorine operation, on the basis of our laboratory work at TAFA, should be possible with higher powers.

Regular and high speed movies were taken through a fiber optics fish eye (Figure 15) that was aimed at the arc cavity throughout many runs. Most of the movies show poor definition of the plasma because of reflection from the upper domed part of the porous wall which became yellow hot during operation. This would indicate the plasma was quite transparent. The reflection from the liner was of some help, however, since it placed a known lighted geometry within the view field. Preliminary evaluation of these movies would indicate the plasma diameter was in the range of 12.70 cm. A general conclusion which can be drawn here was that additional film, at different exposures, must be taken, and along with some time exposures to produce a more definable plasma geometry. Even with this,

additional calibration work will be required to permit significant plasma geometry data to be obtained. One of the disadvantages of the present CPS design and proposed future remote nuclear powered devices is the opaque wall which prohibits either visualizing flow patterns or making any type of optical measurements. It, obviously, would be very attractive to determine the plasma diameter and average temperature through electrical measurements in the induction circuit or in a coil surrounding a nuclear heated device. This appears to be possible and Appendix A addresses itself to this possibility. Basically, known induction heating formulas can be utilized to determine plasma diameter and resistivity (temperature) by measuring capacitor voltage and the real and imaginary power dissipated in the circuit with and without the plasma operating.

To more fully understand the interrelationship of the power supply at TOCCO and the CPS, an analysis of the electrical factors influencing operation was undertaken. The purpose was to determine if changes in electrical parameters would greatly reduce MSP or reduce sensitivity to ignition with small concentrations of diatomic gases in argon. This complete analysis is included in Appendix B.

TASK II - HOT FLOW SIMULATION OF COLD TESTS

The object of the Task II assignment was to provide as direct a comparison as is possible between hot flow and cold flow in a transparent spherical geometry test section with features duplicating the louvered spherical inner wall used in cold-flow tests conducted by Aerojet Nuclear Corporation (Interagency Agreement C-54558B).

A. Basic Design Criteria

The initial study involved a review of the Aerojet Nuclear work in order to determine the best way to incorporate a louvered inner wall into the combined principles simulator.[1] Note was made of the apparent difference in core expansion characteristics between hot flow and cold flow in test work completed previously. A preliminary step in the program involved construction of a simulator with a clear, non-porous, center section (Figure 4) for visualization of fuel expansion and flow patterns developed by the porous wall surrounding the fuel injection system. This intermediate design also permitted cold flow seeding studies.

Using a technique for calculating the performance of various induction coupled plasma generator configurations at low frequency, it was determined that a hot flow test device providing for a 15 to 18 cm plasma would be ideal for a three turn coil with the existing r.f. power supply in the TAFA laboratory, while a 45 to 46 cm diameter device would be ideally suitable for the AEDC power supply. Unless two different sized devices were built, it would not be possible to run hot and cold flow tests at both locations.

The decision was made to proceed with the smaller device to permit tests at TAFA and to provide for designing, at a later date, a different set of louvered segments for the inner wall to enlarge it for operation on the AEDC power supply. New drawings of affected parts of the torch assembly were prepared with significantly increased water cooling provisions.

During the final approval stages of the torch design, additional modifications were made to provide:

1) An injection system suitable for cold and hot operation. This would permit continuous runs by starting cold with gas visualization, then heating up the core gas plasma and proceeding into seeding all without shut-down.

2) A louvered wall assembly design to permit operation in an up or down position. This modification was desired so that it would be possible to reverse gravitational effects on the density differences of the simulating gases to check the effect of acceleration on the intended operation of the rocket engine.

3) Adaptations to a uranium wire feed device similar to the one in use on the combined principles simulator for Task I.

It was also planned to run air as a propellant gas, with air plus smoke visualization in the core gas, for one set of observations and to compare this set with a similar set using argon in the core gas. It was felt that if the similar performance that was expected was actually achieved, anticipated hot-cold test correlation problems would be easily solved.

B. Cold-Hot Flow Simulator

The simulator design, as shown in cross section in Figure 15, evolved from the constraints imposed by the frequency range of the existing high frequency power supply. The top and bottom aluminum flanges were provided with water cooled copper shields to protect them from plasma radiation. Within the quartz outer wall, directly water cooled surfaces were employed as top and bottom thermal barriers. Two concentric gas manifolds were provided in the top cover to supply and distribute propellant gas. Plastic foam diffusing discs were used to provide for more uniform gas flow. The central seeder was designed along the same principle as the seeder assembly used on the combined principles simulator. It

provides for uniform radial seed injection along the inner wall into the path of the incoming propellant gas. The design provided for cylindrical and an alternate spherical high temperature gas injector as well as a wire feed system, all of which could be used interchangeably. The water cooled exit nozzle assembly was designed for one atmosphere operation and was sized to permit attachment of an exit gas calorimeter. The top and bottom flanges were positioned by four large fiber glass reinforced epoxy rods. These tie rods were to be protected from the high radiation level present immediately outside the torch with high efficiency thermal insulation held in place with high reflectivity fiber glass tape. The outer wall of the simulator was a sleeve of fused silica 0.2 cm thick. The sleeve was sealed at the top and bottom flange assemblies with o-rings.

The inner wall of the simulator assembly was designed to consist of 12 separate overlapping fused silica segments, each 0.15 cm thick, that were formed on contours to provide a nominal 0.32 cm space between segments for each of the 11 annular inlet paths for the propellant gas.

C. Louver Adjustment Method

The object of the cold flow test portion of the study was to quickly achieve cold flow conditions that would duplicate, as closely as possible, the Aerojet Nuclear results mentioned previously. Toward this end, a number of different concepts were considered. An important objective was to eliminate all sighting obstructions after proper pressure drops had been determined. It was apparent that the concentricity of the quartz segments was very important and that the initial and final spacing dimensions should be such as to help maintain this concentricity. Since it was desirable to achieve optimum louver spacing prior to final fabrication of the quartz spacers to be used in the hot flow tests, temporary plastic spacers were used.

The first approach considered involved establishing four separate gas inlet areas directing gas flow to separate channels with provisions for adjusting and maintaining the flow to each zone. By manipulating the flow rates to the

various zones during operation, the optimum flow distribution could be determined and these results transferred to louver spacing.

The aim in changing louver spacing was to avoid the necessity for complete disassembly every time an adjustment was desired. During the course of studying the best means to accomplish this adjustment, it was planned to introduce a temporary plastic box enclosure which would be large enough to provide for adjustable spacers that could be reached by simply removing the front or rear (or both) sides of the box.

The second approach resulted in the final design shown in Figure 17. The louver adjustment fixture provided adjustment for each louver segment from the outside of a segmented plastic outer wall with an inside diameter the same as the fused silica wall to be used in the final tests. The clear plastic outer wall was provided in three sections, with a nominal 2.54 cm gap between sections, to provide for penetration of support rods attached to the louvers on the inside and to a spring clip on the outside. The spring clip provided positive support of each louver segment, while allowing for vertical motion to change the inlet channel dimensions. A temporary seeder body assembly was made with additional height adjustment provisions to allow for sufficient motion to accommodate the vertical take-up that could be required. Horizontal concentricity is maintained by the adjustable support arms.

To contain the propellant gas outside the inner louvered wall within the three section plastic enclosure, light gauge latex sheet was obtained. This sheet exhibits extreme elasticity and, when fastened to the plastic enclosure and provided with undersized holes for the louver support rods, would provide the combined features of gas containment and the freedom of rod motion desired. In this manner, the time required to achieve the cold flow optimization, with smoke visualization techniques, would be minimized inasmuch as propellant gas would be introduced in the same manner as in the final cold and hot flow tests. The final louver settings would be achieved without an intermediate step requiring translation of differing gas flow rates to corresponding louver spacings as had been contemplated. Further, comparison of air and argon in the gas core could be made

prior to fabricating the permanent quartz louver support spacers. To facilitate measurements for the spacers, the three temporary plastic outer wall segments could be removed without affecting the settings of the spring clip mounted louver support rods.

It was planned to run preliminary experiments to determine the number density of smoke particles as a function of radius, with the adjustment fixture in place, by arranging a laser beam and related apparatus in a horizontal plane in front of the simulator. This technique is described in some detail in Appendix C. The number density data would be used to verify visual observations and to insure that proper settings are made before proceeding to the final fabrication of the quartz spacers.

For the TAFA tests, the range of propellant gas flow rates, derived from scaling the Aerojet Nuclear values to the simulator dimensions, varied from 4000 to 16,200 cm^3/sec. Working with propellant to fuel ratios of 200:1 to 25:1, the target fuel flow rates (smoke-air) would range from 80.3 to 160.6 cm^3/sec.

D. Laboratory Tests

Experimental Procedure.- After initial cold flow tests for sizing the separators for the quartz louver sections, the assembled simulator was to be mounted on the 189 kW, 4 MHz Lepel power supply. The first runs would determine the final procedure for converting from cold flow to hot flow without interrupting core gas and propellant gas flows. Argon core gas would be utilized with ammonium chloride fumes for visualization. After re-establishing good core gas expansion characteristics, induction power would be applied to initiate a plasma. This direct conversion from cold flow to hot flow should provide the clearest indication of the relative behavior of the two core gas conditions and as direct a comparison as possible between cold and hot flow. After heating with argon plasma alone, seeding would be initiated and the affects of this step would be observed. In this case, seeding is as vitally important in simulation as will be in the final engine design in order to absorb radiation and prevent overheating of the louvers and outer wall enclosure.

The seeding experiment was of unique importance as many possibilities have been advanced to predict the behavior of seeding material in the louvered wall configuration. For example, photoionization effects may cause seed particles to be driven to the louver walls and adhere to them thus negating any shielding effect and possibly adding to overheating problems on the louver walls. From Task I results, it also appeared that the louver design approach might provide a more stable flow pattern than the use of porous walls for the design of larger test units and/or the final GCNR.

Cold-Hot Flow Simulation Runs.- The prime objective of the cold flow tests was establishing the degree that cold flow characteristics in the r.f. simulator were comparable to the Aerojet Nuclear results. This work would be the basic preliminary to the hot flow tests where data on mass flow of the propellant and rod feed were to be determined as well as the overall heat balance of the system and utilization of the plasma power generated. Additional information sought included plasma temperature, rod material distribution, and the effect of the radio frequency field on plasma/helium mixing.

The termination of the contract precluded any of the desired information being obtained.

TASK III - DESIGN OF A URANIUM FEED SYSTEM

In the most successful simulation to date,[5] an induction arc was maintained in argon coaxially surrounded by a flow of hydrogen with 1.67 the mass flow of the argon (~24 times the volume flow under isothermal conditions). Eight centimeters downstream from the point where the two streams had come in contact, the intermixing of the streams was still minimal (as opposed to their cold flow tendencies). This reluctance of a cold gas and a plasma to mix, frequently qualitatively noted if not explained by arc plasma jet investigators, is presumably the phenomenon on which the success of the GCNR is to depend.

Although a fissioning plasma and an induction arc have many features in common, the feed problems substantially differ. The fission reactor has to be supplied with gaseous uranium. Only very limited attempts have been made to operate induction arcs on metal vapors, especially heavy metal vapors. Although a coaxial flow arc can be supplied through a coaxially situated tube at low velocity, this would not be at all appropriate for the nuclear situation where proximity of the fireball to any wall surface would be catastrophic. In addition, any plating out of the feed material, however small, on any cooled surface would quickly result in catastrophic failure of the nuclear device.

It was only after this task was well underway that it became clear that the contract on the one hand had underspecified the constraints on the problem and on the other hand that complete engineering drawings would not be feasible until the actual physical problems involved were clarified to the point they could be solved or circumvented. A further complication is that in recent months more advanced reactor studies[6] have drastically revised the feed system requirements. In addition, a shift to a lower thrust, higher specific impulse engine introduced a new regimen of problems.

At the half way point in the contract, a series of meetings with NASA personnel were held in which modified specifications were generated. The following points were established:

1) The concept of a halide feed was abandoned because of the corrosion problem.

2) The pressure requirement was changed to 400 atm. as the earlier specification of 1000 atm. failed to take the negative worth of the propellant into account.

3) The cavity neutron flux of $0.25\phi \times 10^{14}$ sec^{-1} was computed from the criticality density and mass calculations of C. Whitmarsh[7] for a 4000 MW core.

4) A 62 cm moderator thickness was specified because of the real possibility of encountering substantial design problems in this area which must clearly be shielded from the neutron flux in the moderator region, that was assumed to peak at about 0.6×10^{15} sec^{-1}.

5) The (fast neutron) radiation damage exposure of 1.5×10^{20} N/cm^2 per mission is for materials of construction and shielding that would be used in the moderator region.[7]

In the discussion to follow, it will develop in the analysis of the problem that there are many useful design concepts that could be explicated by mathematical modeling that fall outside the purview of the present contract. Thus, additional assumptions, based at least in part on common sense, will be made as necessary to circumvent this problem. However, adoption of any of the feed methods proposed here would require extensive further work using digital simulation of the flow field. Therefore, it no longer seems appropriate to work out complete engineering details for any of the methods prescribed. Rather, the alternative methods will be presented in greater or lesser detail along with a discussion of advantages and disadvantages and a bare presentation of the areas of minimum technical background as they appear at first inspection.

Figure 18 presents a visual comprehension of the current problem specifications as defined in the last meeting with NASA personnel. The nature, quality and feed rates of fuel are accepted as design points even though some or all should probably be changed in view of current activity by the contractor. In any event, there are four major areas to be

considered in the design study, each with separable and unique problems. They are:

Cavity region flow problems

Moderator transit problems

Actual feed mechanisms

Uranium storage problems

In the following analysis, each of these problem areas will be individually discussed. The first two areas may be discussed independently of a specified feed mechanism. The remaining areas will be concurrently discussed for each of four apparently viable alternatives presented.

A. Cavity

It is important to realize that from the instant the fuel enters the cavity it will be subjected to the full thermal neutron flux and will generate heat at the same rate as the fireball itself. Thus, for a 4000 MW fireball containing a critical mass of 33 kg of U-235, the nuclear heat generated per gram, η, will be 122 kW. This will be liberated regardless of temperature or physical state of the uranium.

The propellant hydrogen is an excellent heat conductor and when it is seeded for opacity, it becomes even better at temperatures over 4000°K where radiative heat transfer takes over. It is clear that a feed rate that is too slow will generate a disruptive amount of heat too close to the walls for the propellant to carry it away. Viscous drag will ensure that some of the propellant will follow the feed stream carrying heat in the direction of the fireball. Also, as the fuel traverses the temperature gradient in the propellant, it will undoubtedly acquire heat in the beginning and subsequently surrender it to its surroundings. Because the cooling of the feedstream is always better than that of the fireball, it will never exceed its 28,000°K surface temperature but that is still too high a temperature to tolerate in the vicinity of the wall.

As a further consideration, if the rule of Guldberg and Gage is used, multiply the normal boiling point of uranium (see Table II)[8] by 1.5 to estimate the critical temperature (6150°K). Straightforward application of the Clausius Clapeyron equation then gives an estimated critical pressure of 136 atm. This calculation could be somewhat in error, as it is for many materials, but not of sufficient magnitude that it would alter the conclusion that a condensed stream of uranium entering the reactor would turn into a vapor somewhere between 6000 and 7000°K without undergoing a phase transition. This too must happen far enough from the wall that deposition of uranium on the walls is absolutely precluded.

Clearly some criterion must be established to ensure the protection of the reactor walls on both counts. The criterion that suggests itself is to have the adiabatic temperature rise of the feed stream be such that the initial temperature rise of the feed stream exactly match the temperature profile in the propellant in the vicinity of the wall. This choice is preferable because if the stream went any slower it would increase heat flux to the wall. If the stream went any faster, it would be heated by conduction from the propellant. Thus, in the region between the fireball radius, r_N, and the wall, R, temperature is regulated by the radial heat flux and a sort of thermal conductivity (including convective and radiative components). LaPlace equations for spherical radial symmetry have been developed and are presented in Appendix D.

In summary, allowing that Grier's computed thermal conductivity function for hydrogen at 500 atm. is a reasonable approximation, Eq. D6 can be used to compute the minimum velocity with which the uranium feed stream can enter the cavity without danger of overheating the walls or depositing uranium by sublimation. Using Figure 19 and the parameters of Figure 18, the minimum velocities are found to be 5.22 m sec^{-1} for the assigned mission where T_N is 12,000°K. For the revised mission (T_N + 36,000°K), the velocity reduces to the modest value of 0.66 m sec^{-1}.

Proceeding further, as a continuous stream, the cross section necessary to transport 0.05 lb/sec (222.7 g sec^{-1}) of uranium at this velocity can be specified.

$$\delta A = \frac{\dot{m}}{\rho_{vel}} = \begin{cases} 0.24 \text{ mm}^2 & \text{(assigned mission)} \\ 1.89 \text{ mm}^2 & \text{(revised mission)} \end{cases} \quad (1)$$

Clearly both of these areas correspond to wires of reasonable dimension (0.55 mm and 1.55 mm, respectively) moving at reasonable velocities.

B. Fuel Flow

One of the most critical problems in the development of the Gas Core Nuclear Rocket is physically stabilizing the position of the fireball. There would seem to be no dynamic stabilizing forces. It can at best be thought of as an extremely slow flow of uranium vapor in the center of a coaxial flow. The forces tending to accelerate this flow and thus disrupt the fireball are:

1) Buoyancy effects due to acceleration[9]
2) Viscous drag on the fireball due to the surrounding accelerating propellant.
3) Fuel injection momentum.

The buoyancy forces are currently under study.[9] The viscous drag is amenable to numerical calculation which again falls outside the purview of the present task. The drag on horizontal components of the feed stream must be included. However, the vertical component of the injected fuel will be of immediate concern here.

Taking the core, for the moment, as a cylinder of one meter radius containing monatomic gas at 10^5°K and 400 atm. through which 0.0227-0.454 kg sec^{-1} of U-235 flows, one can compute the corresponding allowed axial components of the injection velocity. For the minimum rate:

$$v = \frac{\dot{m}}{\rho A} = \frac{\dot{m}RT}{\pi \rho r^2} = .63 \times 10^{-3} \text{ m sec}^{-1} \quad (2)$$

This is one thousandth the minimum velocity of the revised mission and about one ten thousandth the minimum velocity calculated for the assigned mission by Eq. D6. Thus, axial feeding of fuel, as shown in Figure 18, is categorically excluded. Just the vertical component added by expansion of the feed stream would far exceed this value. Therefore, only horizontal injection is admissible. Indeed, detailed evaluation of the other forces mentioned above may well indicate that horizontal injection with a slightly reversed vertical component could render the most nearly stable fireball.

Given the inescapable conclusion that the feed stream must be horizontal, other considerations immediately apply. For example, there must be a multiplicity of feed streams, symmetrically arranged, so that all horizontal components of force cancel. One might suggest as many as 24 which would supply redundancy and greatly simplify attenuation of the fireball as the submultiples 2, 3, 4, 6, 8, and 12 jets could also be used to symmetrically feed the fireball.

As a further argument for multiplicity, the more streams that are active at high mass flows, the more nearly the fuel can be fed at its minimum velocity. This is important because the kinetic energy of the fuel goes up as the square of the velocity. It will appear in the fireball as vorticity which must be dissipated by normal viscous processes.[10] An actual computation of the rate at which this energy can be dissipated without seriously disrupting the cohesiveness of the fireball is again beyond the purview of the present task. However, we proceed on the assumption that the requirement can be met as the alternative is to abandon the problem which is not in the spirit of the assigned task. It seems inescapable at this point that at least some of the fuel will find its way to a wall. At the very least, this possibility should be admitted. However, in the context of its use as a rocket, the reactor need only be designed for finite lifetime and it would therefore seem reasonable and appropriate to inject a small amount of a halogen gas into the propellant for scavenging any deposited fuel. The concommitant erosion of the reactor walls could be taken in account in the cavity design.

C. Moderator

For this discussion, the moderator region is taken to be 0.61 m thick and is extremely intractable as an environment. Having essentially no structural strength, it has nearly an order of magnitude higher flux of slow neutrons than in the cavity. Nor can nuclear reactions, brought about by these neutrons, be directly used in feed mechanisms as there would be no limit on temperature in the event of a feed mechanism failure. Thus, the moderator region is most simply handled by effectively isolating it neutronically from the feed mechanisms, whatever their type.

Shielding the feed mechanism from slow neutrons is not difficult. An attenuation of 10^6 in the slow neutrons is all that is required. As an example, a three percent boronated stainless steel shield 0.267 cm thick will produce this much attenuation.[11]

The exposure to fast neutrons of 1.5×10^{20} per mission is not inconsequential in terms of material damage.[12] Insofar as no attempt has been made to stop the fast neutrons, their effect on the structural integrity of the neutron shield should be considered. However, the various stainless steels exhibit remarkably good radiative stability and will mainly increase in hardness. Therefore, it seems unlikely that this will constitute a serious problem in the final design stages. With minimal planning, the feed mechanism shield will almost certainly decompose less rapidly than the cavity pressure shell.

The heat generated in the shield is not trivial. For example, n, α reactions of the boronated shield mentioned earlier liberate about 3 meV (4.8×10^{-13} J) per event. If 0.6×10^{15} neutrons are absorbed per second in each square centimeter, this represents a real heat liberation density of about 300 W cm^{-2}. It is clear that to conduct this heat away will require a good bond to say a copper or tungsten shell which in turn would be connected to the high capacity space radiator concommitant to the engine. The heat load is high but well within known art.

No matter how carefully the feed system is shielded, it must always have some "Offnungswinkel" for cavity

neutrons. However, unless one wants to design a heat leak (i.e. to keep plugs from forming in a liquid jet feeder) this is no problem for continuous flow systems. U-235 is one of the better shielding materials itself. However, this point does require discussion for discontinuous flow systems.

D. Feed Assemblies

The constraints on the feed assemblies are fairly well defined with gaseous and powder feeds categorically excluded. The uranium must be injected in a condensed state with a minimum velocity of 5.22 m sec^{-1} for the assigned mission (0.66 m sec^{-1} for the revised mission) but it should be capable of double these speeds in either case. The injection should be radial with perhaps a slight negative axial component. Preferably as many as 12 (24 gives greater redundancy) feed stations should be symmetrically located about the periphery of the upper end of the fireball. The feed may either be continuous or intermittent but in either case minimum speeds should be adhered to so as to minimize vortical disruption of the fireball on the one hand and damage to the reactor wall on the other.

In addition, it will be assumed that the feed mechanisms will be located within the moderator region and effectively isolated from it. Given these constraints, four viable alternatives are presented.

1) Wire feed
2) Liquid jet feed
3) Pellet feed
4) Cartridge feed

The last two alternatives (essentially the same) are only briefly discussed insofar as work on this contract was terminated during the time of their conception.

Wire Feed.- For a beginning, 24 feed ports are assumed each capable of introducing wire in the range from 5.2 to 8.7 m sec^{-1}. The wire will be 0.0392 cm in diameter so that each port, operating at minimum speed, delivers 11.3 gm/sec. For

example, two ports, at minimum speed, deliver 22.6 gm/sec. Twenty-four ports, at maximum speed, deliver 454 gm/sec. The required range is thus bracketed. Naturally, if vortical energy dissipation turns out not to be a problem then fewer ports could be used with a greater range in velocities to achieve the same goal.

In Figure 20, the principle features of a wire feed system are shown for a single port axial feed engine. Although this type of feed is unworkable, the figure served to illustrate, in simple form, the following features:

1) The wire storage chamber and the entire feed system is pressurized with e.g. EuF_2 or some other neutron absorbing gas. Pressurization is necessary, on the one hand, because sealing a wire entry against a 400 atm. differential seems impossible and, on the other, a gas other than hydrogen must be present to preclude its attack on the stored uranium.

2) Although uranium wire is dead soft when properly annealed it should pass through a straightener, as shown, to insure the absence of stray axial components in the feed.

3) Each of the ports will be fed from an inside spool spinning off wire much as a spinning reel lets out fishing line. The clamp will control and prevent coil collapse due to the constant pull on the wire. The clamp automatically adjusts as the wire is used.

4) Each wire spool, assuming 24 ports are used, contains only 42 kg (19.2 km) of 0.0392 cm U-235 wire. Each spool will be filled with EuF_2 gas under pressure to poison spontaneous fission, but enough of some solid poison (e.g. B^{10}) should also be incorporated in the mechanism to provide a fail safe condition in case of loss of pressure.

5) Speed is controlled by the primary wire feed mechanism in which a grooved idler wheel assembly is forced against a knurled feed

roll by a pressure spring sandwiching the uranium wire. A cylindrical cam causes the knurled feed roll to reciprocate thereby distributing the wear across the contact surface of the feed roll.

The disadvantages of the wire feed system are clear. First, the entire feed system must be pressurized which for 24 feed ports could imply substantial excess weight depending on how its done. Second, the question of what to do in the case of a break or tangle would have to be resolved. Neither of these problems appear insurmountable--merely difficult. This is probably the most promising feed concept to date.

Liquid Jet Feed.- A feed system concept that circumvents the need for a sealing system would be the uranium liquid jet (Figure 21). In this concept a fuel rod is forced through an extrusion die into a melting region. The pressure on the rod is such that a jet of liquid is forced from another die into the cavity with the required velocity.

Again a multiplicity of jets is used. For discussion, consider 24 jets, 0.038 cm in diameter with a velocity of 5.2 m/sec. The required hole in the jet plate is then just twice that of the diameter[13] or 0.076 cm. The trivial pressure differential required is easily computed by equating the work of extrusion and the kinetic energy of the jet:

$$\Delta P \cdot A \cdot v = \frac{1}{2} \dot{m} v^2 \tag{3}$$

$$\text{or } \Delta P = \frac{mv}{2A} \tag{4}$$

Using the specified parameters, we find a differential of about 2.5 atm. with of course a linear dependence on velocity. Given the built in 400 atm. pressure differential to start with and the not trivial pressure required for the entrant extrusion die, the problem here will mainly be one of control.

The device must be held above the melting point of uranium (1405°K). This may be accomplished by insulating the feed device from the shield and electrically heating

it or conceivably pipe heat in from an absorber external to the shield that is thermostatted by heat loss to the space radiator. Going one step further, a combination of an electric heat for start-up and a designed heat leak for more reliable sustained operation may be practical.

The obvious flaw with a liquid jet feeder is the possible problem of plugging. A controlled nuclear leak around the exit jet should cause any plugs to vaporize out but these problems can only be satisfactorily studied in a test program.

Note that corrosion problems could be severe in such a feeder. Most refractory metals are slightly soluble in liquid uranium.[14] However, it seems likely that this is a problem that will yield to development. It would also appear highly desirable to lower the temperature of the melt through alloying, but again no suitable high uranium eutectics have been found.[14]

The feeding of the rods to the entrant extruder is clearly a problem. However, a viable system for coping with the problem is shown in Figure 22 (for clarity--a single axial feed engine). Again, the details of how to feed 24 extruders, using a minimum of equipment, will be an interesting problem. Certainly not many rods will be required for the 42 kg to be fed through each feeder. A one centimeter rod, one meter long, weighs 1.5 kg. Therefore only 28 rods of this size are required. Poisoning the storage compartments against criticality with e.g. gadolinium would, in this case, be quite simple.

Pelletized Feed Systems.- An alternative to the processes described would be a "pinball" type feed mechanism. There is nothing in the cavity constraints precluding this concept although it would of course cause discrete radial momentum impulses that may be harder to dissipate, without disrupting the fireball, than the steady vortical input of a continuous feed. It must be remembered that, because of the peculiar conditions in the cavity, the "bullet", however it is driven, will arrive in the vicinity of the fireball as a gas cloud without having undergone a phase change. This is difficult to visualize but an ideal situation for pelletized feed.

Using, for example, a solenoid driven plunger, the balls would be entering the cavity at the required speed. Or perhaps a chemical reaction, generating propulsive gas in a cartridge case, would achieve the same goal.

Storing the fuel would now be relatively trivial. In either case, the entire fuel storage and feed system could be pressurized so that the pellets can be brought into the feeder through a non-sealed opening. The cartridge concept is a particularly attractive one from the fuel handling and storage standpoint as the cartridge belt is ideal for holding a poison for nuclear reaction while the loading of machine gun ammunition from storage cassettes is an old art. Also, the balls could be stored in storage bins, in isolated tubes, and easily sent down a common feed tube, one at a time, like a feed mechanism for a BB gun.

The obvious objection to a pellet feeder is the premature exposure of the fuel to the cavity neutrons through the "Offnungswinkel" of the feeder. It seems likely that some sort of shutter device would be required to preclude this or possibly a "poison" gas, such as EuF_2, could be used to fill the barrel of the feeder. Indeed, if the feed area is pressurized, as indicated with EuF_2, it would be difficult to keep it out of the barrel. This may not be an unsolvable problem.

If this program were to proceed, it should be concerned with much finer mathematical models of all the flow and transport properties in the cavity. If, as indicated in this preliminary study, no insurmountable problems appear, one or all of these fuel injection schemes should be evaluated in a simulated fireball.

TASK IV - DESIGN OF A HEATING SYSTEM FOR A HOT HYDROGEN NOZZLE

The goal of Task IV was to design a heating system to subject a nozzle to very high heat fluxes in a hydrogen environment simulating those of the GCNR. Wall boundary layer seeding was included to test the capability of this technique to shield the nozzle. Previous efforts in this area demonstrated the value of propellant seeding for radiation absorption but were conducted at modest heat fluxes.[1,15] Since the maximum specific impulse at which the nuclear rocket can be operated is directly related to exhaust temperature, a more rigorous testing program was required. The equipment to be designed in this task would be adaptable to the multi-megawatt power supply at AEDC.

A. Basic Design Criteria

The task specifies the design of a system to produce a hydrogen flow at 200 atm. pressure and 4700°K through a 0.407 cm diameter throat. The power supply to be utilized is the 3.56 MW plate power, 5-50 KHz oscillator being constructed at AEDC. The hydrogen flow was to include seeding upstream of the nozzle for radiation shielding. A maximum of 10 percent diluent was allowed to enhance the electrical properties of the gas stream.

These specifications are not consistent in that the power required to heat a hydrogen flow necessary to fill a 0.407 cm throat diameter, at the given pressure and temperature, would be 3.18 MW in the gas. The AEDC unit, as designed, would produce a maximum of 2.5 MW output under an ideal load match with full utilization of the available current and voltage. This problem was reviewed with NASA personnel and a decision made to reduce the throat diameter of the nozzle to a diameter that would allow the pressure and temperature specifications to be met. Calculations indicate that this throat diameter would be approximately 0.20 cm. This calculation neglects the 10 percent diluent allowed by NASA and would be adjusted depending on final design parameters.

Two designs are proposed; one powered with d.c. and the second with high frequency.

B. Design of The DC Torch

Developments over the last several years have provided the high power, high pressure d.c. plasma generator experience necessary to undertake the design for this task. For example, development of the segmented constrictor design at NASA/Ames greatly assisted this effort. Investigation of techniques for utilizing multiple cathodes for the arc current at low cathode erosion rates has been made by NASA/Ames and NASA/Langley. NASA/Langley also developed the use of a contoured magnetic field for anode spot rotation.[16] In addition, an investigation of electrode erosion phenomena, sponsored by NASA, provided improved materials for the cathode.[17] By combining all of these technologies with the high voltage, low current power supply available at AEDC it has been possible to generate a d.c. torch design that should be capable of meeting the current specification. The proposed design is illustrated in Figure 23 and described in some detail in the following paragraphs.

Experience at 100 atm. with a 1.5 MW nitrogen plasma indicates that anything over 200 amperes leads to rapid erosion on conventional thoriated tungsten cathodes. This occurs as a result of the concentrated heating produced by the constricted arc column, and the high voltage gradient. Because of this phenomena and the desirability of operating at 500-800 amperes for the hydrogen heater, it was decided to utilize a four cathode geometry. This approach is similar to the one utilized by Carter in his MHD accelerator.[16] Proper distribution of the current to the various cathodes requires water cooled resistors. The system has been designed so that the resistors are the dropping resistors for the stabilization of the power supply.

The material selected for the cathode is a barium, calcium aluminated tungsten alloy reported by NASA in a sponsored investigation of cathode materials.[17] The material was found to have significantly longer life in demanding cathode applications at high pressure.

The anode duct would be a water cooled constrictor design, that includes boron nitride insulators similar to the approach used by NASA/Ames in the 5 MW arc head. An anode duct diameter of approximately 2 cm is anticipated for the unit. This configuration requires that the unit be pulled down to a vacuum in order to establish the arc. This is only a minor inconvenience as the pump required is very small and the low pressure is only momentarily established for ignition.

For the anode end of the arc, three design features will avoid the high arc spot erosion that normally takes place on copper in a high pressure hydrogen plasma generator.[18] The first feature will be a contoured magnetic field to provide rapid rotation of the anode footpoint of the arc. The design reported in Reference 16 will be used because it has the added feature of positioning the anode footprint downstream of the leading edge of the anode. The second feature will be to shield the anode as completely as possible with a flow of argon gas. This helps to diffuse the arc and to produce multiple striking points which reduces erosion. The third feature is rhodium vapor plating of the anode insert. As reported in Reference 18, when this high melting point metal is vapor deposited on copper, it reduces markedly the arc erosion when operating in a hydrogen environment. The combined effect of these three features should provide reliable anode operation for the device.

The constrictor segmented insulator design is greatly simplified by providing an external pressure to counterbalance the operating pressure within the torch. This is provided by a liquid insulating material so regulated that its pressure matches the pressure inside the torch. This minimizes the constraint problems relative to the constrictor segments and also provides a low energy storage buffer between the high pressure gas operation inside the heater and the laboratory. The pressure outside the torch would be maintained higher than the gas pressure by a high pressure regulator.

It is proposed that before proceeding with fabrication of the system, the final duct length and diameter be established using a modified version of the NASA/Ames ARCFLO computer code for d.c. arc heater design.[19] The code iteratively solves the continuity, momentum and energy equations axially along the constrictor column. Radiative

heat transfer losses to the constrictor walls are accounted for in the program and, in addition, radial convection effects are included in the gas flow analysis. Gas property input is available for nitrogen and air, hydrogen and argon. The parameters computed for each axial station by this method include average enthalpy, efficiency, radial heat flux, voltage gradient, radial distributions of enthalpy, velocity and mass flux. Thus, it is readily seen that an analysis of the proposed design would be most advantageous in establishing the constrictor diameter and length and to confirm the overall efficiency of the unit.

C. Nozzle Design

The specification states that the nozzle be water cooled copper and have a throat diameter of 0.406 cm. Calculations based on throat conditions of 4723°K and 100 atm. pressure indicates that 3.3 MW would be required to heat the hydrogen gas flow passing through the nozzle. Thus, the throat diameter specified was apparently a holdover from earlier work when the facility at AEDC was planned for 20 MW. Discussions with NASA established the fact that the nozzle throat diameter could be reduced to match the power level and estimated efficiency of the facility actually being constructed.

The design provides fin cooling on the outside with a reducing flow area to provide high velocity turbulent flow for throat cooling. The inside configuration involves a radius for convergence to the throat and a throat contour at the same radius as the throat diameter.

The design provides that thermocouples, for nozzle surface temperature measurement, penetrate through the water cooling passage at the outside edge of the cooling fins. An insert through the nozzle housing makes a metal to metal seal on the outside of the fin. The thermocouple is made from a platinum-rhodium material with beryllia insulators to provide good heat transfer.

As the expected heat transfer rates are above the maximum acceptable by the water cooled copper, it is apparent that a radiation intercepting shroud of powder will be required.

D. Powder Feeding

It is required that the interior gases at the nozzle be seeded to provide protection to the walls from the radiation of the hot core gas. This is the heart of the test facility, since to survive the proposed nuclear rocket nozzle heat loads, the radiation from the propellant gas stream must be intercepted by a cloud of particles. The purpose of the test facility is to measure the effectiveness of the protection technique.

It is planned that the powder storage and feed system would be similar to the one used by United Aircraft Research Laboratory.[20] Basically, a high pressure container is filled with the appropriate seed particles with the powder kept in suspension by mechanical agitation. The powder particles are submicron in size and consequently will float in the atmosphere if agitated.

There are two major problems in this portion of the design. The first will be to prevent pressure fluctuations in the torch, due to variations in the heating rate of the plasma load, from adversely effecting the flow of powder into the unit. This means that the feed lines must be kept small and the powder supply line operate at double the pressure inside the torch. This is believed necessary so that the flow can be fed through an orifice that prevents pressure fluctuations upstream. This, of course, represents a serious problem in that the 200 atm. operating pressure of the chamber requires a powder feed pressure in excess of 400 atm. Standard gas supply facilities would not be adequate for the facility. Hopefully a less severe solution would suffice in the final design.

The other requirement is that the powder be fed uniformly across the surface of the nozzle. It is anticipated that a dual truncated chamber powder feed system similar to that used in the combined principles simulator[1] would be used. The arrangement has been found to provide a smooth and controllable powder injection in the reference configuration. Certainly, preliminary test runs should be made, without a plasma operating, at the design pressure with light sensors along the wall of the nozzle measuring the instantaneous radiation interception by the powder flow.

Only in this way will it be possible to completely check out the facility. If necessary, a second set of injection slots could be added upstream with an overlapping pattern to improve the uniformity of the flow field.

E. Design of Induction Heated Torch

Several induction coupled heater designs were considered for this application. The possibility of using a susceptor for the induction coupled energy was most attractive since it would provide a constant load for the oscillator. The two logical choices of susceptor materials are tungsten and graphite. Unfortunately, neither is capable of operating at the gas temperatures required for this system.

The possibility of a hybrid system incorporating both induction and d.c. operation was another possibility. A tungsten mesh wall inductively heated to a temperature of approximately 3000°K would provide the first stage of heating for a transpired hydrogen flow. Then an internal radial d.c. arc, operating inside the cavity, would raise the hydrogen temperature to the 4800°K required. Unfortunately, this design concept requires two different uses of the available d.c. power supply; one at high voltage and one at low voltage. This complication is not easily circumvented and consequently the approach was ruled out.

The final induction coupled design is shown in Figure 24. This system includes the injection of the cesium vapor at the center of the unit and hydrogen propellant injection through the cylindrical permeable wall. As it is impossible to inject enough hydrogen to cool the wall directly, an inner row of radiation absorbers is required to shield the permeable wall from the arc. The crucial items in this design would be wall cooling and the fuel injector system.

The unit was designed with a radiation barrier of small diameter quartz tubes. Coolant for the quartz tubes would be water doped with nigrozine dye, the approach used by United Aircraft in their nuclear light bulb engine simulators.[21]

A unique feature in the design is the provision for ceramic rods to be installed in the cavity in front of the

quartz tube wall. These rods would act as radiation absorbers and would be cooled by radiation and conduction to the hydrogen gas flow around the periphery of the plasma cavity. Therefore the rods have the potential for a significant improvement in efficiency by returning radiated heat to the hydrogen stream. The possibility exists, however, that the rods may become conductive at high temperature. In addition, heating by the induction field may occur. This could block some of the field causing extinguishment of the plasma. Therefore, the rods are included only as an optional feature.

The induction coil is located immediately outside of the permeable wall. This presents some design difficulties in bringing the leads out of the high pressure shells, but does provide the advantages of a closer coupling to the load. In addition, hydrogen now surround the coil for arc suppression. The coil would be manufactured using a new teflon coated copper tube which has ideal insulation characteristics. It is planned that the coil would be wound as a split helix with the high voltage lead connected at the center. In this manner, the two ends of the coil would be at ground potential which would avoid the possibility of arcing to the flanges at the end of the heater.

The high temperature electrical properties of cesium vapor indicate that the fuel feed will have to be diluted in order to achieve the proper resistivity for maximum coupling at 50,000 Hz. Provision for dilution with argon is made in the feeder. Diffusion of hydrogen will also increase the resistivity of the plasma region. The exact cesium feed rate and argon flow requirement will be adjusted to provide smooth operation of the operating system. The thermodynamic properties of cesium dictate an injection temperature of 2473°K or higher to maintain the metal as a vapor at 200 atm. pressure.[22] This would require very careful cesium injector design with a molybdenum heating element providing the final vaporization energy. Fuel injector heating would be controlled by a platinum-rhodium thermocouple temperature sensor. The complete system could be built and checked out prior to actual installation in the hydrogen heater.

In summary, the induction coupled hydrogen heater involves completely proven basic design criteria in all respects. The only questionable areas are the stability of

the fuel mixture in the load region and achieving appropriate resistivity with cesium-argon fuel mixture at 200 atm. pressure. It should be noted that a cesium plasma, at 200 atm., has approximately the same resistivity as graphite.

F. Operating Sequence for The DC Arc Heater

The d.c. arc heater would be started by pulling down to a vacuum and back filling with argon to create an easily ionized gas column. A low flow of argon around the cathodes and in the main injector ports would be used during the starting. Special connections would initiate the starting arc from the cathodes to a duct segment near the cathodes. This would generate a plasma stream down the center of the torch. Next, the connection to the starter anode would be opened causing the arc to transfer away from the duct to the operating anode. This would be carried out at relatively low power and pressure. Next, the power would be increased, the main injector gas flow switched to hydrogen, and the power and gas flow increased together to achieve the design operating point. An argon gas flow would continue around the cathode segments and the shield gas across the surface of the anode. Experience gained in operation may dictate that the unit be operated with a nitrogen-hydrogen mixture or with a nitrogen gas flow only during a portion of the pressure buildup. This would not be difficult to accomplish, however, and would not alter the design. It would simply make the pressure increase sequence less sensitive by substituting a more easily ionized gas in the main arc stream.

The power control for different operating points would use the tap changing transformer for input voltage control. This is the same power control that is used with the rectifier unit. In order to fine tune the system to a particular operating point, it may be necessary to add a variable water cooled ballast resistor.

The gas metering system for the facility would be an in-line turbine flowmeter. This alleviates the necessity of supplying the operating gases at the significantly higher pressure required for critical orifice metering. Correction of the readout for pressure variation would be handled electrically using a pressure sensor adjacent to

the turbine flowmeter. Metering systems of this type are available as off-the-shelf items from several suppliers.

G. Instrumentation

The specification requires that provision be made for a surface temperature measurement along the inside surface of the nozzle from a point upstream of the throat to a point at least two nozzle diameters downstream. The purpose of this measurement is to allow accurate assessment of the effectiveness of powder feeding for intercepting radiation, thereby cutting down the incident heat flux on the nozzle.

The ideal measurement technique would be to use a finely focused radiation pyrometer looking at the actual surface of the nozzle. Unfortunately, this is impossible due to the configuration of the nozzle and the fact that the effluent from the nozzle would be highly radiative.

The proposed technique includes five standard thermocouple elements using the copper of the nozzle as one side of the couple and a welded on constantan wire as the other side of the circuit. This would provide an accurate measurement at a point approximately sixty three thousands of a centimeter below the surface. By careful calibration of the element, using radiant heating and surface pyrometers, it would be possible to calibrate the probes.

The only shortcoming in this particular approach is the possibility of electrical pickup on the signal leads due to the electromagnetic field of the work coil. Appropriate shielding techniques would be utilized to minimize the extent of the pickup and an integrating digital voltmeter would be used to remove the common mode signal. As an example of the type of instrument that might be used, the Hewlett-Packard Model 2402A digital voltmeter provides average reading over a preselected time span which greatly reduces the factor of superimposed noise. A floated and guarded input circuit eliminates common mode noise error. In combination, these techniques yield effective common mode noise rejection greater than 126 db (two million to one) at any frequency and d.c.

A small scanner unit would be used to measure the five thermocouple temperatures on the nozzle plus any other heat balance thermocouples that might be used in the system. With an integration time appropriate to remove 60 Hz interference, it would be possible to have the unit scan approximately 30 temperature points per second. Temperatures could be recorded on a printed tape, or used in a direct calculation, with additional instruments, to provide continual heat balances on the system. The data acquisition portion of the system could be made more elaborate, but the basic requirement is handled by the integrating digital voltmeter for obtaining the respective thermocouple measurements.

H. Utilization of AEDC Induction Power Supply

The induction power supply, being constructed at AEDC, has four push-pull output stages operating in parallel. It utilizes an existing thyratron rectifier direct current power supply with tap changing transformer power control. The design output from the oscillator unit is 24,000 volts rms at 147 amperes. In order to fully utilize the generated power, the load circuit must operate at this voltage directly or operate through an impedance matching transformer.

For use on a variable frequency oscillator, such as the one being constructed at AEDC, the TAFA calculator program had to be modified to allow varying plasma diameters to establish the coil inductance and consequent resonant frequency. The anticipated operating condition was investigated in several different ways with the new program. Figure 25 shows the variation of power to the plasma for two plasma diameters, using 10 or 13 turn coils, as a function of plasma resistivity. The minimum resistivity used was the value for cesium at 200 atm. taken from Reference 23. Figure 26 shows the variation of power as a function of resistivity with the voltage applied to the coil as the variable. This figure is important in establishing the necessary load that must be achieved as the power supply voltage and torch pressure are brought up together during a test run. The family of curves on the figure show how increasing percentages of cesium in the fuel mixture would be used to establish the changes in resistivity necessary to reach high power at high pressure.

Figure 27 shows the variations in the coupled power as a function of plasma diameter and resistivity. These curves provide an important indication of the stability of the plasma operation and its susceptibility to extinguishment with perturbations of the plasma load.

With appropriate ballast resistors for stability of the d.c. arc setup, it would be possible to plan on this unit to supply power at 11,000 volts and 900 amperes. Thus, it is seen that the potential of the facility for high powered hydrogen nozzle testing is significantly greater in the d.c. arc mode of operation than in the oscillator mode of operation. This argument, plus the difficulties involved in designing an appropriate cesium seeder for the induction heated unit, make the use of a d.c. arc gas heater very attractive.

The power control for the unit would be the same one used with the rectifier. A tap changing transformer would be used to regulate the coupled voltage and consequently the power. It is anticipated that the hydrogen heater would be started with an argon plasma and with hydrogen introduced to build up the chamber pressure. Thus, it would be possible to increase pressure, power, and hydrogen gas flow together to achieve the desired operating point.

The overall efficiency of the two modes of operation would not be greatly different. For the d.c. arc operation, the ballast resistor would be designed to drop approximately 35 percent of the input voltage. For the oscillator, approximately 30 percent of the incoming power would be lost at the plates of the oscillator tubes, with an additional 10 percent lost in the induction coil. The two heater designs would have nearly the same losses, with an anticipated 25 percent of the incoming power remaining in the gas stream at the throat of the nozzle. This is an estimate based on past experience with high pressure d.c. arc systems.

CONCLUSIONS

Task I - Design Revision and High Power Testing

1) One additional test period would be required to meet the objectives of the contract, i.e. data with solid feed material and uranium hold-up measurements.

2) Higher powers will be required to obtain the objectives of this task, probably a minimum of 600 kW.

3) The general opinion of the investigators is that the louvered wall concept (Task II) should be investigated and evaluated before proceeding with further work on the porous wall CPS. It is the general consensus that the louvered design or a combination of the louvered-porous system would produce a more stable, lower mixing rate environment. This would more closely meet the objectives of the task.

Task II - Hot Flow Simulation of Cold Tests

A complete design for a louvered wall simulator was finalized and approved by the Project Manager. The simulator is capable of operation under both hot and cold conditions. An added feature is a system for continuous louver adjustment during cold flow operation for optimizing flow patterns.

Task III - Design of A Uranium Feed System

1) When all foreseeable problems in principle are examined, it is apparent that the problem of feeding fuel to the Gas Core Nuclear Rocket is relatively straightforward. However, there are some basic requirements. The feed must come through multiple (24 recommended) feed ports arranged for pure radial injection at

the upstream end of the fireball. The minimum inlet velocity should be such that the adiabatic temperature rise of the fuel exactly matches the initial temperature increase of its surroundings.

2) Using the best estimate which can be made, without detailed calculation, the minimum velocity was found to be 5.2 m sec^{-1} for the assigned mission, a reasonable speed indeed. Feed stream diameters to span the required 22.6 gm to 454 gm/sec flow rates can easily be achieved with streams of reasonable diameter through 2-24 inlet ports.

3) The moderator region is dismissed as intractable. It is isolated from the feed system by cooled shields.

4) Four feed systems are discussed: wire feed, liquid jet feed, pellet feed and cartridge feed. It is apparent that no major critical problems emerge in the four systems presented and all have viable and reasonable fuel magazine schemes.

5) One crucial intangible is whether or not the viscous forces in the fireball can dampen the radial momentum and resultant vortical motion without complete disruption of the fireball. A favorable outcome for this question was assumed in order to proceed, but it requires detailed computation.

Task IV - Design of A Heating System For A Hot Hydrogen Nozzle

1) The first design presented for use at the new 2.4 MW output power supply at AEDC follows the d.c. approach that would use only the high voltage d.c. portion of the power supply. It is based on proven arc constrictor design concepts and embodies

the latest available materials and protection techniques for critical components.

2) The second approach is an r.f. induction heated design which relies on a cesium vapor plus an argon fuel region to provide the necessary plasma resistivity for good coupling efficiency. Several features are included in the design to improve operating efficiency.

3) The only unknowns lie in the area of arc stability at the 200 atm. operating point. The extent of the problem can only be determined by a test program.

4) It is the opinion of the project personnel that both designs could be successfully operated. However, the d.c. approach would involve less technical risk.

APPENDIX A

PLASMA DIAGNOSTICS THROUGH ELECTRICAL SYSTEM MEASUREMENTS

INTRODUCTION

The present combined principles simulator (CPS) design and the proposed GCNR reactor share the common problem of fireball characterization in an opaque wall reactor. It is clearly advantageous to have a passive method of diagnostic characterization remotely situated. Such a method has been suggested by the instrumentation provided by Park-Ohio Industries (TOCCO) for their 9600 Hz supply. It depends on the electrical interaction of the fireball, power supply circuit, and alternating current circuit theory. Note that although the method was suggested by the present instrumentation and frequency regime, it is not limited to that regime. Sprouse[24] has already gone rather far toward developing a suitable framework for its application at radio frequencies.

Specifically, the method hinges on the fact that induction heating is an old art and equations are available that (providing certain reasonable constraints are not violated) relate the voltage across the primary RLC circuit to the power dissipated in the "workpiece" to within 10 percent.[25] It is only necessary to rearrange the equations to uniquely solve for fireball diameter and its electrical conductivity.

The method has been applied ex post facto to one run taken in 1971 in a transparent-walled, water-cooled plasma generator in which the same electrical parameters were measured and the fireball photographed (Figure 28). It appears to give a reasonable estimate of fireball diameter and conductivity although a correction factor is suggested. More recent data obtained in the CPS during the last quarter of 1972 also yield reasonable results for fireball diameter and conductivity (although the fireball cannot now be measured) indicating the potential utility of the method.

We first present the assumptions of the method (including the assumed equivalent primary circuit) together with the equations relating the indicator readings to primary implied

measurables. Further relationships necessary to physically relate the primary measureables to the fireball characteristics are also presented. We indicate how they may be rearranged and solved for the physical quantities of interest. Finally we remark on further work required to establish the method as a primary diagnostic tool.

Glossary

R_A = resistance of lines going to coil

X_A = reactance of lines going to coil

R_p = resistance of coil

X_p = reactance of coil due to flux in windings

X_o = reactance of coil due to flux between windings and fireball

X_s = reflected reactance of fireball

R_s = reflected resistance of fireball

H_o = ampere turns = $f_1 \cdot V_o / X_c \cdot N$

X_c = reactance of capacitor bank $|X_A + X_p + X_o^0|$, ohms

Q = $|X_c|/R$

V_o = rated voltage of power supply

V = $f_1 V_o$ voltage across capacitor

I = computed current in resonant circuit V/X_c (to within 1%)

N = turns in coil

b_1 = diameter of coil (inside), centimeters

a_o = diameter of fireball, centimeters

d_2 = reference depth of fireball $\frac{1}{\sqrt{\pi \mu \sigma f}}$, centimeters

W_o = rated power of generators, watts

$P_{virt}/W_o = f_i$ = virtual power relative to rated

$P_{real}/W_o = f_r$ = real power relative to rated

$P_{plasma}/P_{real} = f_p$ = fraction of real power dissipated in plasma

K_5 = Nagaokas Constant

L = length of coil, centimeters

K_1 = workpiece shortness factor $= K_5 + (1-K_5)(a_o/b_1)^2$

K_2 = load resistance coefficient

$$K_2 = -.05278(a_o/d_2) + .0892(a_o/d_2)^2 - .00480(a_o/d_2)^3$$

$X_L \approx -X_c = X_A + X_p + X_o^0 + \Delta X_o + X_s$

$\Delta X_L = \Delta X_o + X_s$

μ = permeability of space $= 4\pi \times 10^{-7}/39.37 = 3.19 \times 10^{-8}$

ρ_2 = resistivity of fireball, ohm centimeters

σ = conductivity of fireball $ohm^{-1}m^{-1}$

τ = coupling constant

THEORY

A. Assumptions

We assume first of all that the plasma fireball can be represented by a homogeneous right circular cylinder. It is well known that the induction arc is the most nearly homogeneous of all arcs while the nuclear fireball is expected to be even more so. Any singly connected volume can of course be represented as an equivalent right circular cylinder, the more

nearly the actual shapes coincide the better the representation. For the case of the induction arc this is very close to its actual appearance (Figure 28). Within the length of the coil, the fireball is most nearly represented by the frustum of a cone 12.95 cm diameter at the base and 8.90 cm diameter at the top. A cylinder of, say, 10.90 cm diameter would seem to be a reasonable approximation. Given the uncertainties in other diagnostic methods this seems like a conservative assumption. (Should the method evolve into a routine diagnostic tool a "shape factor" could be introduced.)

We assume further that the complete electrical circuit is equivalent to the simplified schematic of Figure 29 for all practical purposes. Note that the very significant transmission line resistance and inductive reactance between the generator and the instrumentation have been omitted. Although they strongly affect the apparent power supply characteristics at the load, the only effect on the load itself is that it must have a slight (~1%) capacitive imbalance to restore the inductive reactance voltage drop. This we ignore.

To continue, the detailed equations on which the following analyses are based depend on negligible magnetic reluctance external to the coil. Conducting end flanges on a plasma torch can change this picture so a "coupling constant," τ, is entered in the theory to accommodate this problem.

Finally we have the constraints of Reference 25 that must be fulfilled for a guaranteed $\pm$10 percent accuracy:

1) Single-layer solenoidal coil wound with rectangular conductor.
2) Cylindrical load telescoped in coil, coaxial with coil.
3) Length of load equal to or greater than length of coil with ends of load flush with ends of coil or extending out of ends of coil.
4) Ratio of inside diameter of coil to length $b_1/L \leq 1.0$.
5) Ratio of coil thickness to length $h/L \leq 0.07$.
6) Ratio of conductor wall thickness to inductor reference dimension $t_1/d_1 \geq 1.35$.

7) Inductor-coil space factor ≥ 0.70.

8) Permeability of coil and load material relative to a vacuum = 1.0.

9) Ratio of inside diameter of coil to reference dimension of coil $b_1/d_1 \geq 3.5$.

10) Ratio of outside diameter of load to reference dimension of load $a_o/d_2 \geq 2.0$.

11) Intercircuit capacitance negligible.

For induction arcs, constraint four is the most nearly apt to be violated but not by much. In any case, no discontinuous anomalies emerge.

The relevant equations from the reference paper are:

$$R_s = \frac{N^2 \pi \rho_2 a_o K_2 K_1^2}{L d_2} \cdot \tau \qquad \text{A1}$$

$$X_s = \frac{N^2 \pi \rho_2 a_o K_1^2}{L d_2} \cdot \tau \qquad \text{A2}$$

$$X_o = \frac{N^2 15.7 f (b_1^2 - a_o^2) K_1 10^{-8}}{L} \cdot \tau = \frac{\tau \cdot N^2 \pi^2 \mu f (b_1^2 - a_o^2) K_1}{2L} \qquad \text{A3}$$

where the workpiece shortness factor is given in terms of Nagaokas Constant (see Figure 30):

$$K_1 = K_5 \left(1 - \frac{a_o^2}{b_1^2}\right) + \frac{a_o^2}{b_1^2} \qquad \text{A4}$$

where the resistance factor, K_2, for a right circular cylinder is given in Figure 31.

B. Analysis

Measured Quantities.- Recall the capacitive reactance is negative imaginary by convention. We assume, in the following, that it is approximately equal in magnitude to the inductive reactance and large compared to the circuit resistance. A known experimental datum is the "number of VAR" of capacitance necessary to nearly bring the circuit into resonance. The capacitive (and hence inductive) reactance follows from:

$$\text{Capacitive reactance} = X_c = - \frac{(\text{rated capacitor voltage})^2}{\text{VAR rating}}$$

$$= - X_L \qquad \text{A5}$$

With no further assumptions, we can determine the reflected resistance of the fireball providing we have voltage and power measurements with and without (superscript ^{0}) the plasma:

$$P_{real}{}^0 = \frac{f_1{}^{0\,2} V_o{}^2}{X_c{}^2} (R_A + R_p) = f_r{}^0 W_o \qquad \text{A6a}$$

$$P_{real} = \frac{f_1{}^2 V_o{}^2}{X_c{}^2} (R_A + R_p + R_s) = f_r W_o \qquad \text{A6b}$$

$$R_s = \frac{X_c{}^2 W_o}{V_o{}^2} \left[\frac{f_r}{f_1{}^2} - \frac{f_r{}^0}{f_1{}^{0\,2}} \right] \qquad \text{A6}$$

Similarly, by operating on the virtual power measurements, we can obtain the overall change in circuit inductive reactance.

$$\Delta X_L = \frac{X_c^2 W_o}{V_o^2} \left[\frac{f_r}{f_1^2} - \frac{f_i^0}{f_1^{0\,2}} \right] \qquad \text{A7}$$

Note that this is not simply reflected reactance but rather its algebraic sum together with the decrease in coil reactance because of the presence of the plasma.

Again, with no furher assumptions, we can easily obtain the efficiency, namely, the fraction of the electrical power going into the plasma vs that lost to all other heat sinks from eqs. A6b and A6.

$$f_p = \frac{R_s}{R_A + R_p + R_s} = \frac{\frac{X_c^2 W_o}{V_o^2} \left[\frac{f_r}{f_1^2} - \frac{f_r^0}{f_0^2} \right]}{f_r \frac{W_o X_c^2}{V_o^2 f_1^2}} = \left[1 - \frac{f_r^0}{f_r} \frac{f_1^2}{f_1^{0\,2}} \right] \qquad \text{A8}$$

Also, by definition

$$Q = X_c / (R_A + R_p + R_s) = X_c / R_s / f_p \qquad \text{A9}$$

C. Derived Quantities

The rigorously defined quantities R_s and ΔX_L may now be used in conjunction with the slightly modified relationships of the reference paper (25) to characterize the fireball. An iterative solution is required. Thus, from eqs. A1 and A2 we find the reflected reactance

$$|X_s| = \frac{R_s}{K_2} = \frac{N^2 \pi \rho_2 a_o K_1^2}{L d_2} \cdot \tau \qquad \text{A10}$$

where the resistance factor K_2 may be represented fairly well up to a value of $a_o/d_2 = 3.5$ by curve fitting:

$$K_2 = a\,(a_o/d_2) + b\,(a_o/d_2)^2 + c\,(a_o/d_2)^3 \qquad A11$$

$$a = -.05278,\ b = .0892,\ c = -.00480$$

Note that a constant, τ, not present in the initial theory has been introduced in eq. A10. This is to account for an expected weakening of the flux in the solenoid due to circulating currents in end flanges and other sources of external reluctance not accommodated in the theory. Indeed, it might make more sense to introduce an inhomogeneity parameter, but that should probably await a clearly recognized need.

By definition, the measureable ΔX_L is

$$\Delta X_L = X_s + \Delta X_o \qquad A12$$

From eq. A3, again introducing τ:

$$\Delta X_o = -\frac{N^2 15.7\, f a_o^2 K_1 10^{-8}}{L} = \frac{N^2 \pi \rho_2 a_o K_1^2}{L d_2} \cdot \frac{a_o/d_2}{2K_1} \cdot \tau \qquad A13$$

So that using this relationship and eq. A2:

$$\Delta X_L = X_s + \Delta X_o = \frac{N^2 \pi \rho_2 a_o K_1^2}{L d_2}\left(1 - \frac{a_o/d_2}{2K_1}\right) = X_s\left(1 - \frac{a_o/d_2}{2K_1}\right) \qquad A14$$

(Note that K_1 has entered the operating relationships and so a value of a_o must be assumed.) This rearranges to given an expression for a_o/d_2 that may be used as a second approximation in eq. A11:

$$a_o/d_2 = \frac{2K_1}{X_s}(X_s - \Delta X_L) \qquad A15$$

Rapidly convergent successive approximation now yields a best value of a_o/d_2 for the assumed fireball diameter a_o. One may then combine eq. A6 together with the definition for the reference depth (eq. A17) to get a second approximation for a_o.

$$a_o = \left\{ \frac{L\,|X_s|}{N^2\pi^2 K_1^{\,2}\mu f\tau_1} \cdot \frac{a_o}{d_2} \right\}^{1/2} \qquad \text{A16}$$

Again the method is rapidly convergent and one has a final value of a_o, a_o/d_2 and thus d_2.

To continue

$$\rho_2 = d_2^{\,2} \cdot \pi \cdot \mu \cdot f \qquad \text{A17}$$

and

$$\sigma = 39.37/\rho_2 \qquad \text{A18}$$

So that not only the fireball size but also its conductivity and hence, for a known substance, the temperature follows immediately.

RESULTS

Inputs and computed results are shown in Tables III-V. In Table III we consider first the transparent-walled, water-cooled torch. Note that the low efficiency probably indicates it was not far from its minimum sustaining power. Fireball radius and (essentially) temperature are computed as a function of the parameter τ. It is seen that a τ of 0.20 gives a fireball diameter in good agreement with visual observation and a temperature quite appropriate to an induction plasma. It is important to note that in every case the Hewlett-Packard 9810 Calculator converges rapidly and unequivocally to the answer. The equations are well posed.

In Table IV we consider three cases for the combined principles simulator (CPS) for three runs of quite different efficiencies. τ has been adjusted to make the temperature of the low efficiency run about the same as that for the water-cooled torch at the same efficiency. It is now much more nearly unity. The pattern of changing fireball parameters with improved loading is quite clear and much as one would expect. The larger and more resistive the fireball, the better the efficiency. (Note that the electrical conductivity changes might reflect contamination changes more than actual changes in temperature.)

In Table V, we consider several points within one startup and run. This gives a singularly clear picture of the evolution of the plasma during the pressure buildup of the starting procedure. (Temperatures are not given here for the sub-atmospheric data because of the rapidly changing but not monitored pressure.) Again the trend is quite interesting. The low pressure arc is unexpectedly efficient while the pronounced increase in temperature with attendant decrease in diameter for high flows is just what one might expect.

DISCUSSION OF RESULTS

It is clear that this scheme of electrical diagnostics is a quick and efficient way of characterizing a fireball, particularly one that for some reason cannot be seen. All other considerations aside, it is almost certainly better than any spectroscopic method the writer is familiar with if the arc has any tendency toward instability.

The greatest drawback of the method is the presence of the adjustable parameter τ. Necessary, for meaningful results, it rather compromises the guarantee of precision built into the source paper. Confidence in this method clearly can only follow extensive testing with mock-up situations such as beakers full of electrolyte adjusted in concentration to have conductivities in the range of plasma interest. These should be "diagnosed" in situ in the same coils, end flanges and nozzles that will be used for the plasma situation. If the parameter τ emerges as a unique meaningful entity in this situation, the method may be applied with confidence.

It is important to realize that the method depends only on the change in resistance and inductance of the coil between plasma and no-plasma conditions. There is no requirement that the plasma power has to come from the coil used. Therefore, a relatively light diagnostic coil may be used for this job and the source of the plasma is immaterial. Note, however, from Figure 31 that the method loses all sensitivity for plasma diameters more than five times the reference depth. This is not really a restriction on the method so much as it is a criterion for selecting the appropriate diagnostic frequencies.

RESUME

It is concluded that with proper in situ calibration using conducting cylinders (such as beakers of electrolyte) to calibrate, this electrical diagnostic method, which depends on the difference in the electrical characteristics of the coil with and without a plasma, should be excellent for the characterization of nuclear or induction type plasmas. Frequencies must be chosen so that the plasma diameter is less than, say, five times the reference depth.

APPENDIX B

MINIMUM SUSTAINING POWER AND MINIMUM SUSTAINING FIELDS FOR THE COMBINED PRINCIPLES SIMULATOR

INTRODUCTION

In its initial operation, (Task I) the combined principles simulator proved to perform in a rather disappointing way. It was found to be hypersensitive to additives in the arc gas--so much so that the smallest air leak made starting impossible and when it operated only a small fraction of the power (20-29 percent) went into the plasma, the remainder going into the coil, etc.

After regarding the initial data, it was concluded that the torch showed the characteristics of operating too close to its minimum sustaining power (MSP) a concept found by TAFA to be useful in scaling induction plasma devices. Thus in future attempts the "plasma off" voltage was raised (by capacitive trimming) to a value far exceeding the rating of the capacitors. Under these circumstances, it was found possible to couple a much higher fraction of the available power into the plasma (>50 percent) indicating operation in a "healthier" regime.

It was felt that the factors determining and limiting the operating point of the device needed clarification and so it was determined to examine it in light of the limits imposed by an available, particularly simple, published theory of the induction plasma generator.[26]

The next section presents the bare outline of the theory and the operating characteristics it generates. This is followed by an interpretation of these curves relating to the present problem. Next the MSP's and MSF's are computed for argon and nitrogen in the CPS and it is shown that although operation on pure nitrogen was precluded by the constraints, the sensitivity displayed to contamination was not inescapable. The blame for this is traced to the use of an improper transmission line connecting the generator and the test site.

THEORY

Basically, the theory[26] represents the arc as an homogeneous right circular cylinder acquiring heat by the well-established principles of induction heating on the one hand and losing it by conduction to the surrounding cold walls on the other. Clearly there is a whole regime of radii and electrical conductivities (i.e., temperatures) for each arc fluid that will satisfy both of these conditions. We supply the remaining condition by requiring the power dissipated in the arc to be a minimum. This is equivalent to the Steenbeck minimum field principle for d.c. arcs and may be shown to be a statement of the second law of the thermodynamics of the steady state. This admits now of analytic solutions relating magnetic field intensities to power dissipated per unit length of arc. The resulting curves, computed at various frequencies for argon and nitrogen in a 2.54 cm torch, are presented in Figure 10. These curves may be scaled to any other size torch by using the $f^{1}/^{2}R$ relationship relating frequency and radius. Thus, if a burner had a 25.4 cm diameter, these curves would still apply but for frequencies only 0.01 those listed in Figure 10.

This theory admittedly ignores two very important heat removal mechanisms, radiation and convection. However, it has been found to reproduce the operating characteristics of argon and nitrogen very well indeed. This is particularly true for the two gases relative to each other in the same torch. However, because of the ignored factors, it requires an adjustment in field strength. The actual fields required are at least an order of magnitude higher in practice than predicted by the theory. This is an adjustment that need be made only for one operating point of a single gas to make the theory completely applicable.

For a full interpretation of Figure 10, the reader is referred to Reference 26. For the present purposes, we need only remark that operation has never been observed to the left of the minima in the curves. This can be shown to be a consequence of a modified Kaufman criterion, but whatever the reason, it defines at once the minimum sustaining power (MSP) densities and (to within the adjustable constant) the minimum sustaining field (MSF) for each gas at each frequency/diameter. These minima have been plotted for a

2.54 cm diameter reactor in Figure 32 (MSP) and in Figure 33 (MSF).

The only other thing to note from Figure 10 is that for every operating power density, there is necessarily a required field and thus for a particular coil a required voltage across it. Operation is not possible unless the power supply is capable of delivering the requisite voltage when that power is being expended in the plasma.

COMBINED PRINCIPLES SIMULATOR (CPS)

The CPS has a heat sink diameter of eight inches (.204 m) and a four turn coil of length 6.45 inches - one inch (.138^5 m). N/L for this coil would be 29 m^{-1}. To find the appropriate characteristics on Figures 32 and 33, we scale the heat sink diameter down to 2.54 cm by the relationship $f^1/^2R$ = constant, i.e. the characteristics of interest would be a 0.615 x 10^6 Hz arc. From Figure 32 we find the minimum sustaining power densities for argon and nitrogen should be 120 kWm^{-1} and 548 kWm^{-1} respectively. For the combined principles simulator, if we assume the arc is about 1-2/3 the length of the coil we might therefore expect minimum sustaining powers of 41 kW (argon) and 186 kW (nitrogen)--in good agreement with the value observed for argon (59 kW, Run 11, Table I). Although the difference is appreciable, it is not by as much as an order of magnitude and it is difficult to see how this accounts for the observed extreme sensitivity of this device to the presence of small amounts of molecular gases. Note that the highest power dissipated in the plasma was observed to be 127 kW, Run 5, Table I.

From Figure 33 we find the minimum sustaining fields for argon and nitrogen to be 0.115 x $10^5/\tau$ ampere turns m^{-1} and 0.3 x $10^5/\tau$ ampere turns m^{-1} respectively. For the CPS then, assuming a τ of 0.078, the minimum coil currents would be 5100 amperes (argon) and 13,250 amperes (nitrogen). (Note that τ was chosen at 0.078 so as to make the voltage requirement measured for the minimum sustaining power for argon agree with that computed. As mentioned above, adjustments of this approximate magnitude are generally required to use this theory.) Because we know the VAR's of capacitance C_{VAR} (coupled for a rated voltage, E_R, of 1600 V) we can directly relate these currents to voltages:

$$X_C = \frac{X_R^2}{C_{VAR}} \qquad B1$$

$$V = IX_C \qquad B2$$

Thus for E_R = 1600 volts, C_{VAR} = 11,205 x 10^3 VAR, X_C = 0.228Ω. The coil voltage required for argon operation is thus 1170 V. That for nitrogen would be 3020 V, nearly twice the rated voltage, but not unreasonable. On the surface, this limitation seems little more likely to have precluded operation with air contamination than the MSP limitation.

We look thus to the power supply characteristics. The tuned circuit, of which the CPS is part, is about 180 KVAR's net capacitive. This is nearly in resonance with the inductance of the long lines from the generator so that under no plasma conditions the voltage is within a few percent of the generator voltage. Note that this is not the same as "no load" situation. Actually more power may be dissipated in the coil with the plasma off than is dissipated in total with the plasma on. This is because the plasma usually reflects as a net decrease in inductance with the perhaps non-intuitive result that the circuit looks less like a capacitance. As a result, the voltage across the circuit drops rapidly (a hyperbolic decrease in the limit of no resistance). This leads to a situation that is at once intuitively difficult to grasp and difficult to apply the usual thermodynamic arguments to. The implications in the present context are however clear.

DISCUSSION

Given the channel model for the induction discharge and the proper scaling relations, we have found it possible to project minimum sustaining powers (MSP) and minimum sustaining fields (MSF) for argon and nitrogen in the combined principles simulator. The observed MSF for argon was used to evaluate an arbitrary constant of the channel model theory, however the observed MSP was in quantitative agreement with that calculated with no adjustment required in the theory. The (probably fortuitously) good agreement, considered in light of previous

successes of the theory, encourages one to accept the same computed quantities for nitrogen in the CPS. Operation with pure nitrogen is thus found only to require 186 kW dissipation in the arc--well within the capabilities of the 350 kW power supply even allowing a fair fraction of dissipated power in the coil and transmission lines. Somewhat less favorable is the calculation that 3020 volts would be required across the coil to sustain operation on nitrogen (as opposed to 1170 V for argon). However, even though the full voltage is not attainable without exceeding the ratings of the capacitors, 2400 V was within reach and so there is no reason here why operation on at least partial nitrogen should have been excluded. This is particularly true when you consider that the power supplies nominally operate with constant voltage ($\pm$ 2 percent) out to full power.

Viewed with hindsight, it is clear that the extreme sensitivity of the CPS to perturbations in gas composition was the result of failing to understand the implications of the inductive reactance of the long lines used to interconnect the test site and the generators. Under no plasma conditions, the resonant torch circuit was trimmed with excess capacitance so that it approached resonance with the transmission and inductance. It may readily be shown that this leads to a hyperbolic increase in voltage across the coil and so it was straightforward to start with any desired voltage. However, the instant the plasma started, it reflected a negative inductive reactance into the torch circuit which is equivalent to taking away capacitance. This causes the voltage to drop (again hyperbolically) to the point where the available field is consistent with the necessarily limited plasma power. Any additions to the plasma that would tend to increase the negative inductive feedback would thus make even less field available. Because the CPS characteristically operated near its MSP, it would then flame out.

A clue that should have alerted us to this problem was the fact that operating with higher starting voltages permitted higher power and more efficient operation. This is much as one would expect from a d.c. arc and its interaction with its power supply. But whereas there is not much that can be done to change the characteristics of a single power supply for a d.c. arc, in this case it would have been simple to e.g., switch in more capacitance after the arc was started. Of

course, this would have necessitated circuit protection in case of unplanned flame out but this is relatively easy to achieve. Alternatively, and far better, the experiment should have been run without the long transmission line or else the line should have been properly compensated along its length according to the well established principles of transmission line theory.

RESUME

In summary then, it is concluded that the high starting voltages necessary to obtain satisfactory efficiencies and the extreme sensitivity of the CPS to air contamination can both be related directly to the inductance inherent in the long transmission line from the generator that was devoid of any capacitive compensation except at the test site itself. It is recommended that in all future tests this unnecessary major perturbations on operation be eliminated or at least controlled.

APPENDIX C

EXPERIMENTAL DETERMINATION OF THE NUMBER DENSITY OF SMOKE PARTICLES AS A FUNCTION OF RADIUS

Given a axially symmetric distribution of smoke in a transparent axially symmetric container, the turbidity of smoke suspension is defined by the relationship[27]

$$\frac{dI}{dy} = -\tau\,(r,\theta)\,I \qquad C1$$

where I is the intensity incident in the y direction. In general, τ will reflect the number density of smoke particles, N, in the suspension and the scattering cross section, ϕ, of each; however, a simple proportionality will be true only in the limit of infinite dilution where multiple scattering of the light disappears as a factor:

$$\underline{\tau \to 0}\ \tau = \phi N \qquad C2$$

It will generally not be necessary to evaluate an absolute value for ϕ as only relative concentrations are relevant in the experiment.

In Figure 34, an experimental configuration is described suitable for the acquisition of the transmitted intensity profile, the data necessary to determine the radial number density distribution. Note, that in addition to minimizing multiple scattered light effects, this configuration has the advantage over photographic techniques in that the well-known non-linearity of the photographic process may be avoided.

Refraction of the laser beam by the curved walls will cause a considerable perturbation near the edges of the distribution. However, it may readily be shown, in a radially symmetric situation, the correct chordal relationships are maintained.[28] Therefore, it is only necessary to introduce an "apparatus function" correction to the transmitted light to account for this potential source of error. Thus, if we scan across the empty vessel we get an apparent source function, B(X). It is only necessary to use this function in place of I_o in the ultimate equations to correct for this edge curvature error.

If we now assume the turbidity to be axisymmetric, we can immediately integrate eq. C1 to get the transmitted intensity J(x):

$$\ln \frac{J(x)}{B(x)} = -\int_{-\sqrt{r^2-x^2}}^{\sqrt{r^2-x^2}} \tau \, dx \qquad C3$$

or making use of the symmetry of the right-hand side of eq. C3 we may write:

$$F(x) = 2 \int_0^{\sqrt{R^2-x^2}} \tau(r) \, dy \qquad C4$$

where:

$$F(x) = \frac{\ln[B(x)/J(x)] + \ln[B(-x)/J(-x)]}{2} \qquad C4'$$

But this is the well-known Abel integral equation. Its solution may be written:[29]

$$\tau(r) = \frac{1}{r} \frac{d}{dr} \int_r^R \frac{F(x) \, x dx}{\sqrt{x^2-r^2}} \qquad C5$$

This completes the formal solution of the problem. Note that the procedure reported here is entirely equivalent to, but rather simpler and more powerful than that reported in Appendix C of the Aerojet Nuclear report.[30]

NUMERICAL EVALUATION

Data from the apparatus of Figure 34 will be in the form of intensity distributions (relative to the reference beam)

of light transmitted through the apparatus with (J(x)) and without (B(x)) the smoke. In general, the distribution will be slightly asymmetric so that the middle is chosen and both sides averaged (e.g., see eq. C4[1]) to get a function suitable for the inversion, eq. C5.[31] There are many ways of performing the inversion, none of them completely satisfactory, but the way found most fruitful by the writer for the usual somewhat crude data[32] is to fit the observed function F(x) to a set of functions that may be analytically integrated in eq. C5. Thus, the unknown error of the inversion is replaced by the well-studied error in least squares curve fitting.

We have chosen the family of all parabolas as a set of basis functions. The calculator was programmed to select the "best", i.e., least squares, coefficients for the first five terms of the expansion:

$$F(x) = \sum_{i=1}^{\infty} C_i (R^2-x^2)^{i-1} \qquad C6$$

These and related functions have been extensively used by workers at the National Bureau of Standards[33] and found to fit most distributions exceedingly well. The series analytically converts into the solution function:

$$\tau(r) = \sum_{i=1}^{5} \lambda_i C_i (R^2-r^2)^{i-3/2} \qquad C7$$

where

$$\lambda_{i+1} = \frac{2^{2i}}{\pi} [(i!)^2/(2i)!] \qquad C8$$

When the program was applied to synthetic trial data,[31] the τ function was reproduced to one part in 10^6.

APPENDIX D

DEVELOPMENT OF MINIMUM VELOCITY EQUATION FOR URANIUM FEED STREAM

Clearly some criterion must be established to ensure the protection of the reactor walls. The criterion that suggests itself is to have the adiabatic temperature rise of the feed stream be such that the initial temperature rise of the feed stream exactly match the temperature profile in the propellant in the vicinity of the wall. This seems a particularly happy choice because if the stream went any slower it would increase heat flux to the wall while if it went any faster it would be heated by conduction from the propellant and it seems unlikely that anything would be gained.

Thus, in the region between the fireball radius, R_N, and the wall, R, temperature is regulated by the radial heat flux and a sort of thermal conductivity (including convective and radiative components). We then write Laplaces equations for spherical radial symmetry:

$$\frac{1}{r^2}\frac{\partial}{\partial r} r^2 \kappa \frac{\partial T}{\partial r} = 0 \qquad \text{D1}$$

The solution is:

$$\frac{\partial T}{\partial r} = \frac{1}{r^2}\frac{1}{\kappa} \int_{T_{wall}}^{T_{mas}} \kappa dt \; \frac{1}{(\frac{1}{R} - \frac{1}{r_N})} \qquad \text{D2}$$

At the wall, this reduces to:

$$\left.\frac{\partial T}{\partial r}\right|_{r=R} = - \frac{1}{\kappa_{wall}} \frac{r_N}{R(R-r_N)} \cdot \int_{T_{wall}}^{T_N} \kappa dT \qquad \text{D3}$$

But for the constant velocity feed stream (one dimensional), we may write the substantive derivative:

$$\frac{DT}{dt} = \frac{\partial T}{\partial t} + \frac{\partial T}{\partial r}\frac{dr}{dt} \qquad D4$$

A steady state is achieved if $\partial T/\partial t = 0$, then one can immediately write:

$$\frac{DT}{dt} = \frac{\eta}{c} = \left.\frac{\partial T}{\partial r}\right|_{r=R} \cdot vel \qquad D5$$

or

$$vel = \frac{\eta}{c}\frac{\kappa_{wall}}{S_N} R \frac{(R-r_N)}{r_N} \qquad D6$$

where S_N is the Schmitz heat flow potential[34] of the propellant at the boundary of the nuclear core (Figure 19).

$$S_N = \int_{T_{wall}}^{T_N} \kappa dt \qquad D7$$

Thermal conductivities computed for pure hydrogen at 500 atm. by N. T. Grier (Figure 3) were used to compute Figure 19.

REFERENCES

1. Poole, John W.; and Vogel, Charles E.: Induction Simulation of Gas Core Nuclear Engine. NASA CR-2155, February 1973.

2. American Lava Corporation: Mechanical and Electrical Properties of AlSiMag Ceramics, Chart No. 691.

3. Poole, John W.; and Vogel, Charles E.: Induction Torches and Low Frequency Tests. NASA CR-2053, May 1972.

4. Vogel, Charles E.; Poole, John W.; and Dundas, Peter H.: Radiation Measurements and Low Frequency and High Pressure Investigations of Induction Heated Plasma. NASA CR-1804, May 1971.

5. Dundas, P.H.: Induction Plasma Heating: Measurement of Gas Concentrations, Temperatures, and Stagnation Heads in a Binary Plasma System. NASA CR-1527, February 1970.

6. Whitmarsh, Charles L., Jr.: Neutronics Analysis of an Open-Cycle High-Impulse Gas-Core Reactor Concept. NASA TMX-2534, April 1972.

7. Ragsdale, Robert G.: Are Gas-Core Nuclear Rockets Attainable? AIAA Paper No. 68-570, Am. Inst. Aeron. and Astronaut., 4th Propulsion Joint Specialist Conference (Cleveland, Ohio), June 1968.

8. Cordfunke, E.H.: The Chemistry of Uranium in Nuclear Technology. Vol. 13.-Topics in Organic and General Chemistry. Am. Elsevier (New York), 1970.

9. Putre, Henry A.: Effect of Buoyancy on Fuel Containment In An Open-Cycle Gas-Core Nuclear Rocket Engine. NASA TMX-67924, 1971.

10. Lamb, H.: Hydrodynamics. Sixth Edition, Dover Publishing Company, 1945.

11. Anon.: The Technology of Nuclear Reactor Safety, Vol. I, Reactor Physics and Control. MIT Press, Table 4-4.

12. Anon.: Nuclear Engineering Handbook. McGraw-Hill Book Co. (New York), 1958, pp. 10-106-10-108.

13. Birkhoff, G.; and Zarantonello, E.H.: Jets, Wakes, and Cavities. Academic Press (New York), 1957, p. 15.

14. Anon: Reactor Handbook, Vol. I "Materials". Interscience Publication (New York), 1960.

15. Poole, John W.; and Vogel, Charles E.: Induction Plasma Nozzle Tests. NASA CR-1765, April 1971.

16. Carter, Arlen F.; Weaver, Willard R.; McFarland, Donald R.; and Wood, George P.: Development and Initial Operating Characteristics of the 20-Megawatt Linear Plasma Accelerator Facility. NASA TN D-6547, December 1971.

17. Anon.: Experiments to Establish Current Carrying Capacity of Thermionic-Emitting Cathodes. AVSSD-0043-67-RR (Contract No. NAS2-3379), AVCO Corp., Jan. 30, 1967. (Available as NASA CR-73186)

18. Dethlefsen, R.: Investigation of Electrode Erosion in High Current Electric Arcs. ARL 68-0112, Aerospace Research Laboratories, June 1968.

19. Watson, V.R.; and Pegot, E.B.: Numerical Calculations for the Characteristics of a Gas Flowing Axially Through a Constricted Arc. NASA TN D-4042, June 1967.

20. Klein, J.F.; and Roman, W.C.: Results of Experiments to Simulate Radiant Heating of Propellant in a Nuclear Light Bulb Engine Using a D.C. Arc Radiant Energy Source. Report J-910900-1, United Aircraft Research Laboratory, September 1970.

21. Roman, W.C.: Experimental Investigation of a High Intensity R-F Radiant Energy Source to Simulate the Thermal Environment in a Nuclear Light Bulb Engine. Report J-910900-4, United Aircraft Research Laboratories, September 1970.

22. Stone, J.P.; et al: High Temperature Vapor Pressures of Sodium, Potassium, and Cesium. J. Chem. Eng. Data, Vol. 11, no. 3, July 1966, pp. 315-320.

23. Kulik, P.P.: Dense (Non-ideal) Plasma Fundamental Properties. AIAA Paper 72-414, Moscow Aviation Institute, April 1972.

24. Sprouse, J.A.: Solenoids Excited at Radio-Frequencies in the Presence of Plasmas. AEDC-TR-70-206, Arnold Engineering Development Center, October 1970.

25. Vaughan, J.T.; and Williamson, J.W.: Design of Induction-Heating Coils for Cylindrical Nonmagnetic Loads. AIEE Paper 45-107, 1945.

26. Freeman, M.P.; and Chase, J.D.: Energy-Transfer Mechanism and Typical Operating Characteristics for the Thermal RF Plasma Generator. J. Appl. Phys., vol. 39, no. 1, January 1968, pp. 180-190.

27. Heller, Wilfred: Elements of the Theory of Light Scattering. I. Scattering in Gases, Liquids, Solutions, and Dispersion of Small Particles. Record of Chem. Prog. 20, 209, 1959.

28. Stokes, A.D.: Optics of Circular Tubes Used for Plasma Confinement. J. Opt. Soc. Am. 57, 1100, 1967.

29. Tatchmarsh, E.C.: Introduction to the Theory of Fourier Integrals. Second Edition, Oxford University Press (New York), 1948, p. 331.

30. Kunze, J.F.; Suckling, D.H.; and Cooper, C.G.: Phase I Topical Report, Flowing Gas, Non-Nuclear Experiments on The Gas Core Reactor. NASA CR-120824, February 1972.

31. Freeman, M.P., and Katz, S.: Determination of a Radiance-Coefficient Profile from the Observed Asymmetric Radiance Distribution of an Optically Thin Radiating Medium. J. Opt. Soc. Am., 53, 1172, 1963.

32. Wiese, W. L.; Paquette, D.R.; and Solarske, J.E.: Profiles of Stark-Broadened Balmer Lines in a Hydrogen Plasma. Phys. Rev., 129, 1225, 1963.

33. Popenoe, C.H.; and Shumakrer, J.B. Jr.: Arc Measurement of Some Argon Transition Probabilities. J. Research. NBS 69A, 495, 1965.

34. Schmitz, G.: Zur Theorie der Wandstabilisierten Bogensaule. Z. Naturforsch. 5a, 571, 1950.

TABLE I

TEST RESULTS - HIGH POWER TESTS

Run No.		20/72 15	21/72 1	21/72 2	21/72 3	21/72 4	21/72 5	21/72 7	21/72 8	21/72 9	21/72 11	21/72 12	21/72 13
Meter Readings (percent)													
	V	102.00	93.00	73.00	68.00	72.00	72.00	74.00	95.00	86.00	73.00	107.00	105.00
	A	81.00	78.00	67.00	58.00	59.00	63.00	62.00	79.00	71.00	65.00	90.00	91.00
	kW	85.00	80.00	65.00	64.00	62.00	68.00	65.00	79.00	72.00	50.00	95.00	100.00
	KVAR	12.50	24.00	11.00	9.00	9.00	8.00	9.00	24.00	17.00	22.00	29.00	34.00
Differential Temperature													
Coil	°K	32.78	23.33	16.11	15.56	15.00	16.67	17.78	25.00	21.67	17.78	36.11	34.44
Torch	°K	7.28	3.89	4.44	5.44	5.00	5.00	5.00	2.78	3.89	5.00	5.00	6.11
Nozzle	°K	11.28	6.28	7.56	8.89	8.06	8.67	8.33	3.89	6.22	6.67	7.67	8.72
Operating Conditions													
	V	816.00	744.00	584.00	544.00	576.00	576.00	592.00	760.00	688.00	584.00	856.00	840.00
	A	354.78	341.64	293.46	254.04	258.42	275.94	271.56	346.02	310.98	284.70	394.20	398.58
	kW	297.50	280.00	227.50	224.00	217.00	238.00	227.50	276.50	252.00	175.00	332.50	350.00
	KVAR	43.75	84.00	38.50	31.50	31.50	31.50	28.00	31.50	84.00	59.50	101.50	119.00
	ø	8.37	16.70	9.61	8.00	8.26	6.71	7.88	16.90	13.28	23.75	16.98	18.78
Losses													
Coil	kW	138.24	98.41	67.95	65.60	63.26	70.29	74.98	105.44	91.38	74.98	152.30	145.27
	%	46.47	35.15	29.87	29.29	29.15	29.53	32.96	38.13	36.26	42.84	45.80	41.50
Torch	kW	12.10	6.47	7.39	9.06	8.32	8.32	8.32	4.62	6.47	6.47	8.32	10.16
	%	4.07	2.31	3.25	4.04	3.83	3.49	3.66	1.67	2.57	3.70	2.50	2.90
Nozzle	kW	8.85	4.93	5.93	6.98	6.32	6.80	6.54	3.05	4.88	5.23	6.02	6.85
	%	2.98	1.76	2.61	3.11	2.91	2.86	2.87	1.10	1.94	2.99	1.81	1.96
Buss & Capacitors	kW	80.40	66.84	41.18	35.73	40.06	40.06	42.32	69.75	57.16	41.18	88.48	85.20
	%	27.03	23.87	18.10	15.95	18.46	16.83	18.60	25.22	22.68	23.53	26.61	24.34
Total	kW	239.59	176.64	122.45	117.37	117.96	125.47	132.15	182.85	159.88	127.86	255.11	247.48
	%	80.54	63.09	53.82	52.40	54.36	52.72	58.09	66.13	63.45	73.06	76.72	70.71
Power to Exhaust Gas													
	kW	57.91	103.36	105.05	106.63	99.04	112.53	95.35	93.65	92.12	47.14	77.39	102.52
	%	19.46	36.91	46.18	47.60	45.64	47.28	41.91	33.87	36.55	26.95	23.28	29.29
Gas Flow													
	Wall g/sec	22.24	11.38	11.38	11.38	11.38	11.38	11.38	15.93	15.93	11.38	13.94	14.76
	Core g/sec	0.88	0.46	0.46	0.46	0.46	0.46	0.46	0.46	0.46	0.41	0.41	0.41
Exhaust Gas Enthalpy													
	MJ/kgm*	2.50	8.71	8.85	8.98	8.34	9.48	8.03	5.70	5.60	3.97	5.37	6.74

*4.30×10^2 to convert to Btu/lb.

TABLE II

PHYSICAL CONSTANTS OF URANIUM[10]

Atomic Weight	238.03
Density (298°K)	
x-ray	19.214
Exp.	19.05 ± .02
Phase Transformations	
α-β	940.9°K
β-γ	1048 °K
Melting Point	1405.5°K
Heat of Fusion	2500-2900 cal/g atom
Heat of Sublimation (0°K)	129.0 kcal/mole
Specific Heat	6.594 cal/° mole
Thermal Conductivity	0.060 cal/cm sec deg

TABLE III

TRANSPARENT-WALLED, WATER-COOLED TORCH
THE EFFECT OF τ ON COMPUTED FIREBALL DIAMETER AND CONDUCTIVITY

Parameters:				
No. of turns	5			
Length of coil	17.75 cm			
Inside diameter of coil	18.40 cm			
Nagaokas Constant	0.68			
VARS of capacity	11,120,000 VAR			
Capacity rated - volts	1600 V			
Power supply rated power	350,000 W			
Power supply rated voltage (xformed)	1400 V			
Frequency	9600 Hz			
Observation:				
Fireball was a conic frustum of 8.90 cm diameter to 12.95 cm diameter. (Average D = 10.91 cm)				
Measureables: (fractional)				
Voltage (plasma off)	0.993			
Real power (plasma off)	0.68			
Virtual power (plasma off)	0.26			
Voltage (plasma on)	0.948			
Real power (plasma on)	0.79			
Virtual power (plasma on)	0.1508			
Computed Measureables:				
Power (watts)	276,500			
Fraction of real power in plasma (efficiency)	0.214			
Q of circuit with arc on	27.7			
Coil current (amperes)	5771			
Derived Quantities:				
τ	0.10	0.20	0.30	0.40
Fireball diameter (cm)	13.65	10.95	9.50	8.55
Fireball conductivity ($ohm^{-1}m^{-1}$)	3644	4958	6177	7356
Ratio of diameter to reference depth	1.60	1.50	1.46	1.43
Implied temperature for argon ($^{\circ}K$)	11,000	12,600	14,100	15,300

TABLE IV

COMBINED PRINCIPLES SIMULATOR

Parameters:			
No. of turns	4		
Length of coil	16.4 cm		
Inside diameter of coil	25.60 cm		
Nagaokas Constant	0.585		
VARS of capacity	11,205,000 VAR		
Capacity rated - volts	1600 V		
Power supply rated power	350,000 W		
Power supply rated voltage	1600 V		
Frequency	9600 Hz		
τ	0.65		
Run Identification:	21/72 #1	20/72 #15	21/72 #5
Measureables: (fractional)			
Voltage (plasma off)	1.025	1.18	1.17
Real power (plasma off)	0.79	0.87	0.92
Virtual power (plasma off)	0.28	0.21	0.25
Voltage (plasma on)	0.93	1.02	0.72
Real power (plasma on)	0.80	0.85	0.68
Virtual power (plasma on)	0.24	0.12	0.08
Computed Measurables:			
Power (watts)	280,000	297,500	238,000
Fraction of real power in plasma (efficiency)	0.18	0.235	0.488
Q of circuit with arc on	34.6	39.2	24.4
Coil current (amperes)	6513	7143	5042
Derived Quantities:			
Fireball diameter (cm)	0.69	9.21	13.85
Fireball conductivity ($ohm^{-1}m^{-1}$)	5666	4958	2729
Ratio of diameter to reference depth	1.27	1.26	1.41
Implied temperature for argon (°K)	13,300	12,600	9,800

TABLE V

COMBINED PRINCIPLES SIMULATOR
EVOLUTION OF THE FIREBALL DURING STARTUP - RUN 13/72 #32

Parameters: Same as for Table IV				
Time in Run: (sec)	9	11	17	26.5
Description:	Glow	Low Pressure Arc	Atmospheric Arc	High Flow
Measureables: (fractional)				
Voltage (plasma off)	0.95[2]	0.95[5]	0.96	0.96
Real power (plasma off)	0.79[5]	0.79	0.78	0.76
Virtual power (plasma off)	0.25	0.24[5]	0.23	0.21
Voltage (plasma on)	0.86	0.44	0.71	0.83
Real power (plasma on)	0.76	0.37	0.66	0.73
Virtual power (plasma on)	0.17[5]	0.03	0.09	0.13[5]
Computed Measureables:				
Power (watts)	266,000	129,500	231,000	255,500
Fraction of real power in plasma (efficiency)	0.14[7]	0.54[7]	0.35	0.22[5]
Q of circuit with arc on	31.1	16.8	24.4	30.2
Coil current (amperes)	6023	3081	4972	5812
Derived Quantities:				
Fireball diameter (cm)	8.46	16.27	12.52	9.95
Fireball conductivity ($ohm^{-1}m^{-1}$)	5687	2091	3065	4384
Ratio of diameter to reference depth	1.24	1.44	1.35	1.28
Implied temperature for argon (°K)	----	----	10,300	12,000

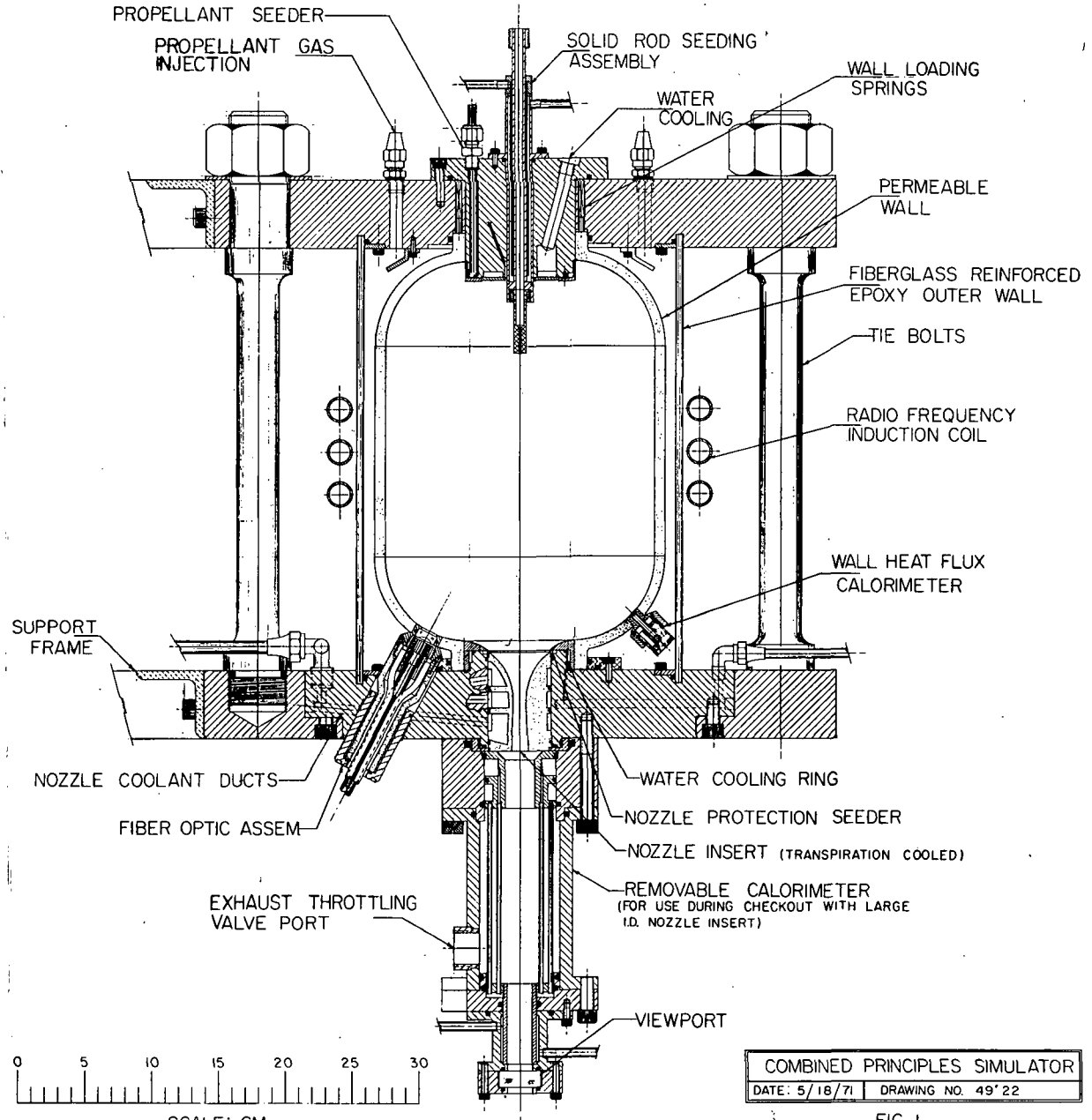

COMBINED PRINCIPLES SIMULATOR	
DATE: 5/18/71	DRAWING NO. 49'22

FIG. 1

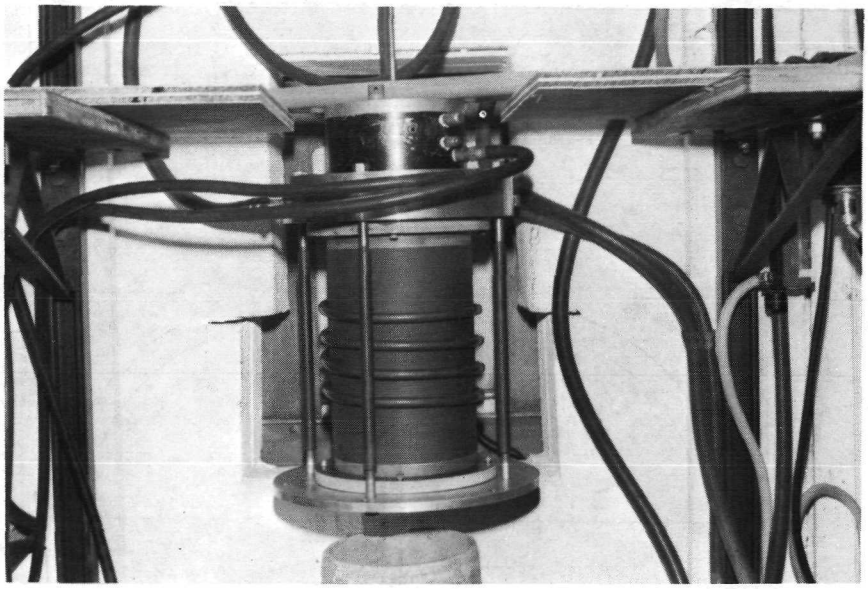

SET-UP FOR PERMEABLE WALL TEST
Figure 2

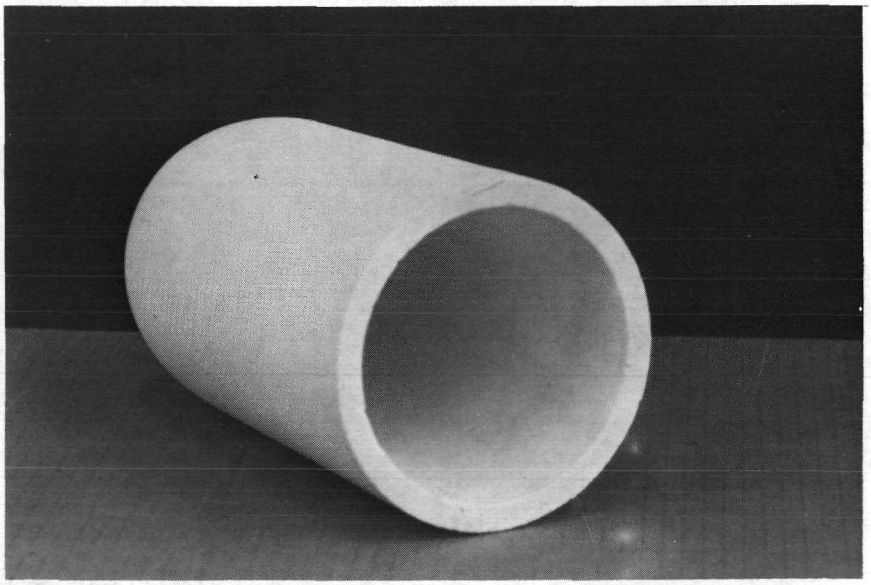

PERMEABLE FUSED SILICA TEST PIECE
Figure 3

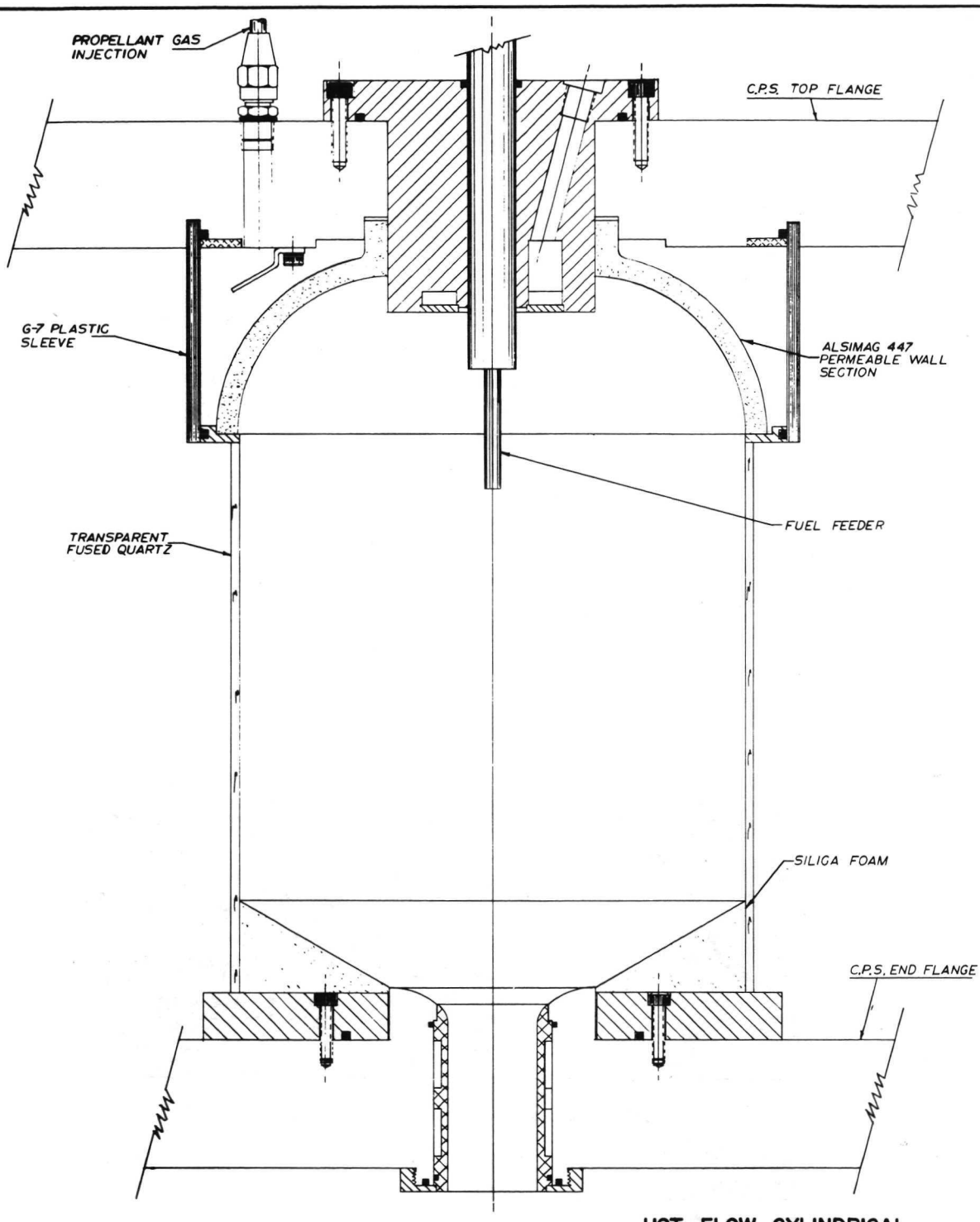

HOT FLOW CYLINDRICAL WALL PROPELLANT SEEDING TEST DEVICE

FIG. 4

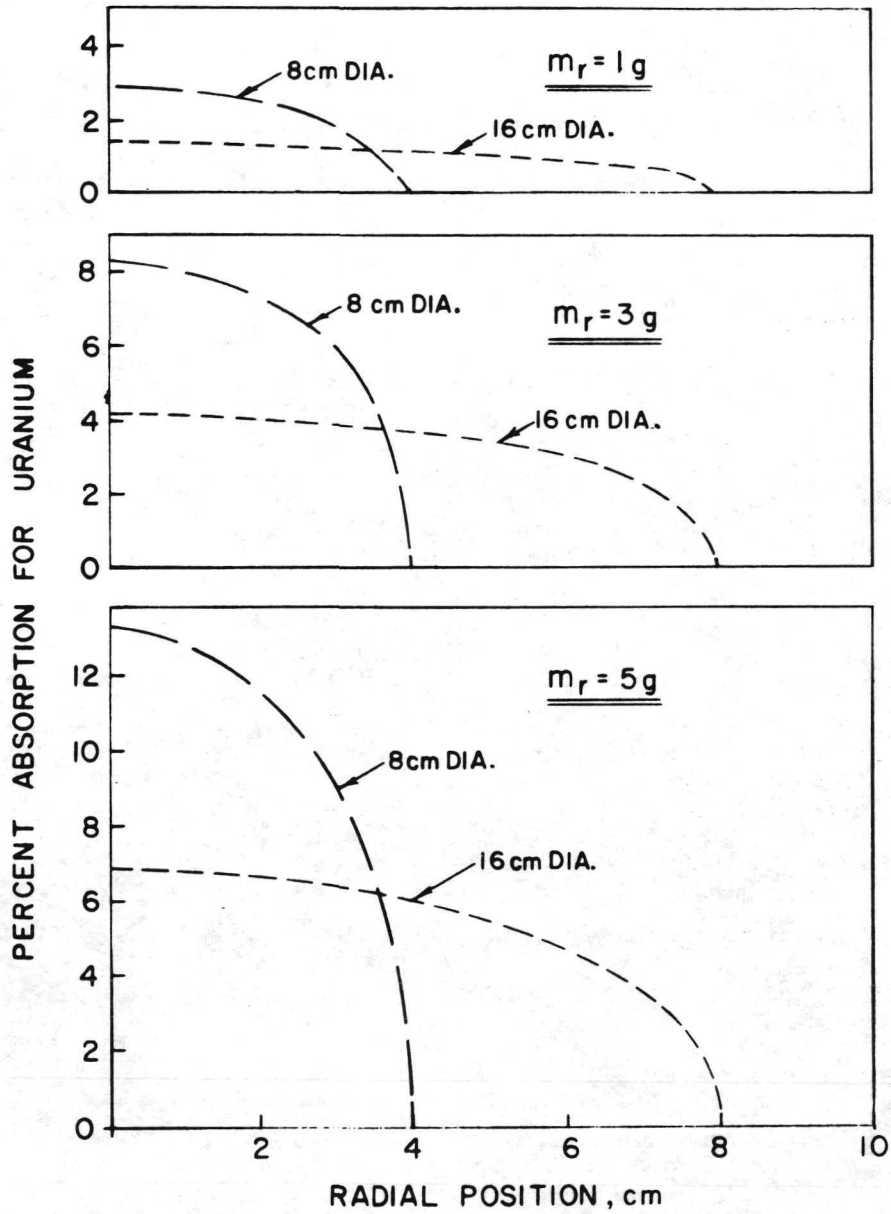

CALCULATED X-RAY ABSORPTION FOR VARIOUS URANIUM MASS RETENTION VALUES (m_r) FOR THE COMBINED PRINCIPLES SIMULATOR AS A FUNCTION OF RADIAL POSITION

FIG. 5

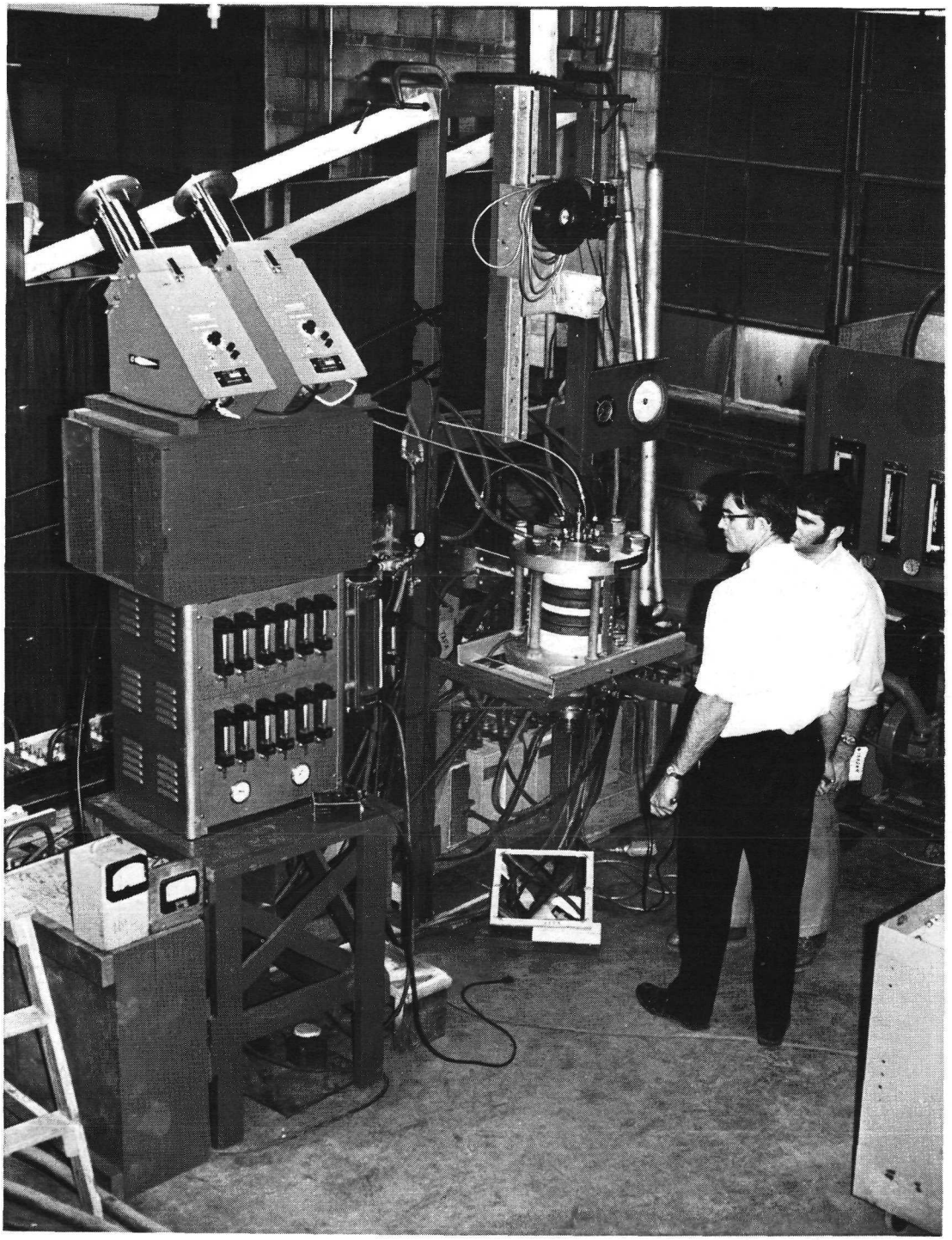

CPS SETUP SHOWING SEED FEEDERS (UPPER LEFT),
GAS CONTROL PANEL AND URANIUM WIRE FEED

FIGURE 6

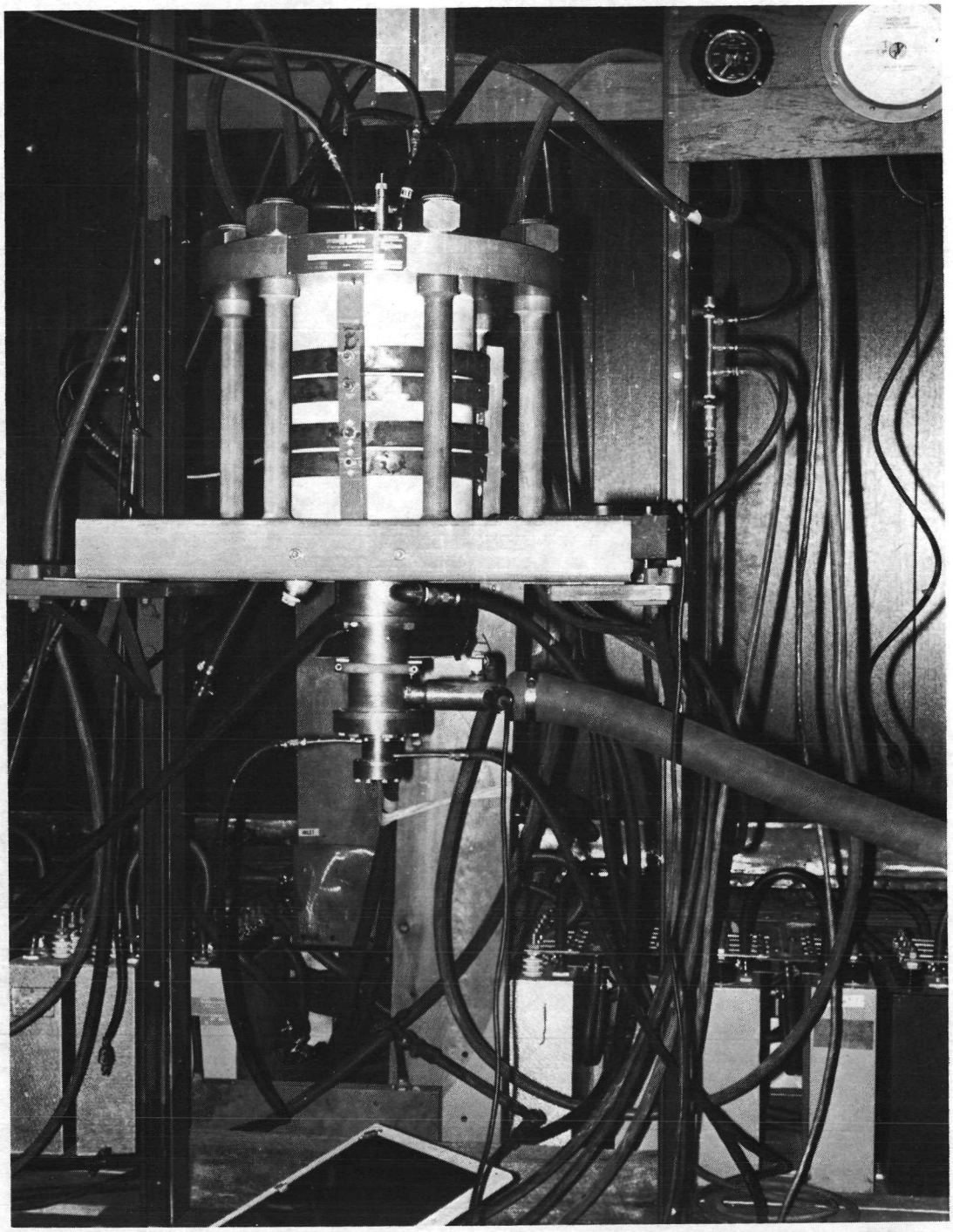

CPS SHOWING SPLIT COIL AND EXIT HEAT EXCHANGER

FIGURE 7

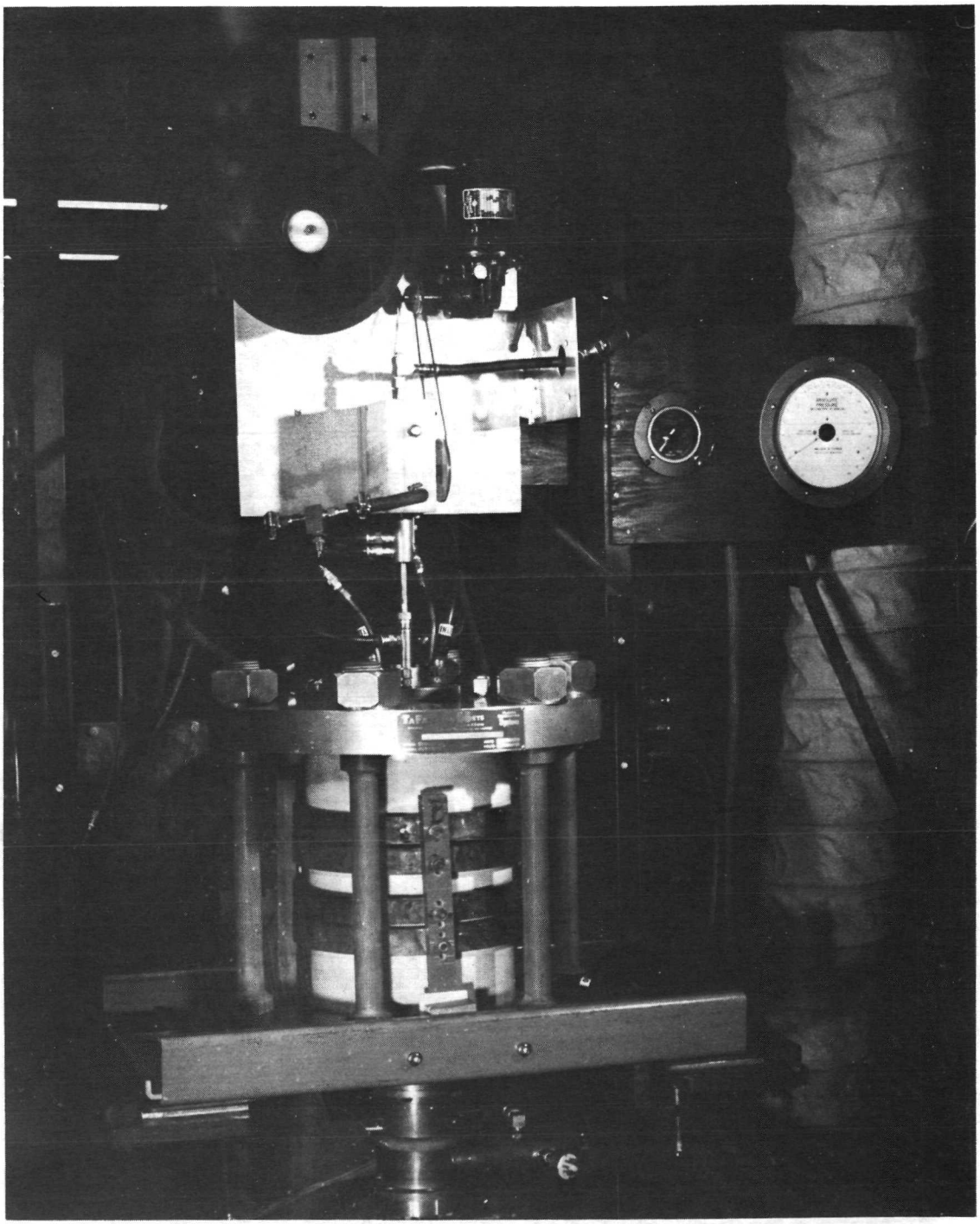

URANIUM WIRE FEED ASSEMBLY CONNECTED TO CPS

FIGURE 8

PLASMA EXHAUSTING FROM CPS WITH CALORIMETER REMOVED

FIGURE 9

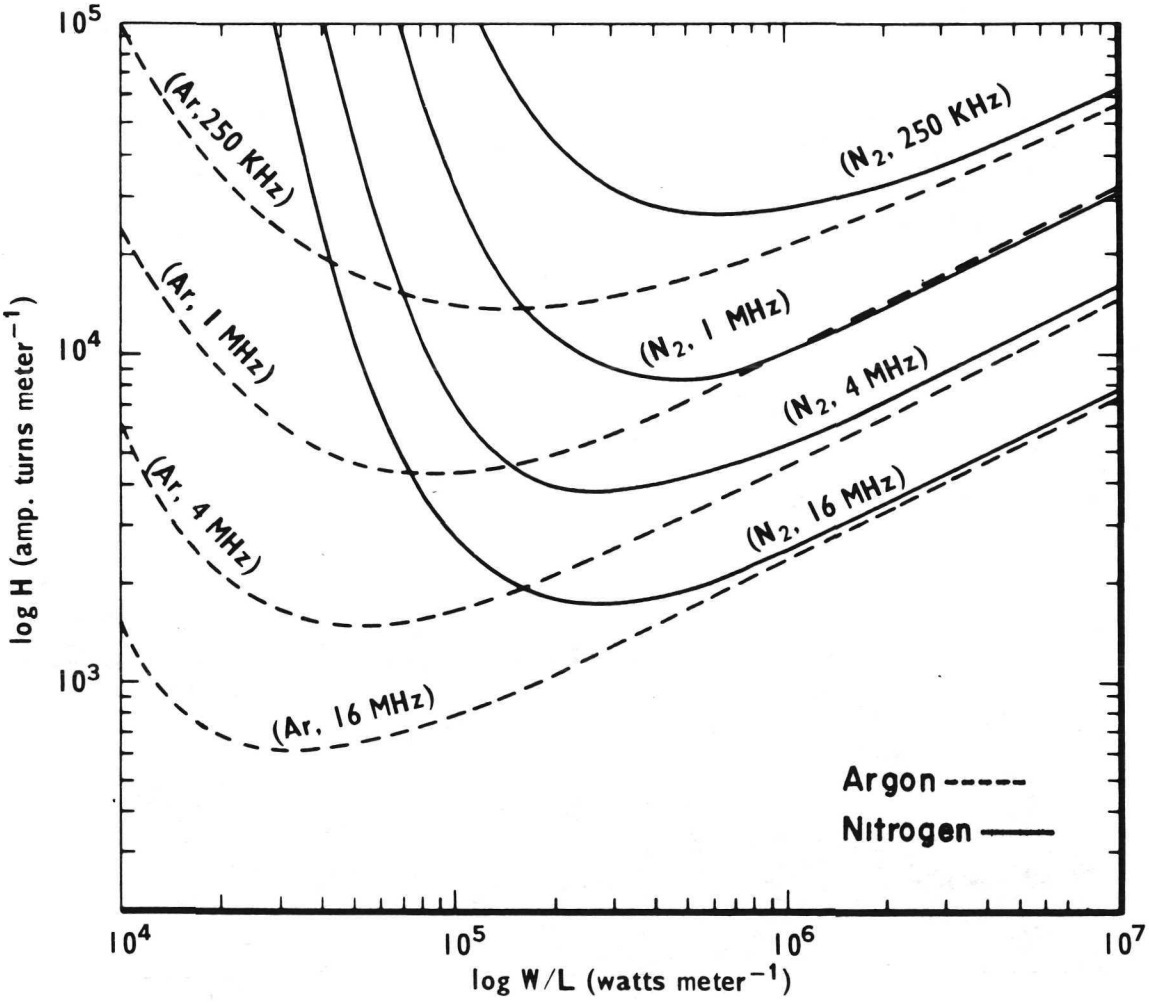

Theoretical Curves Of Magnetic Field Strength vs Linear Power Density In A 2.54 cm. Torch At Various Frequencies

Figure 10

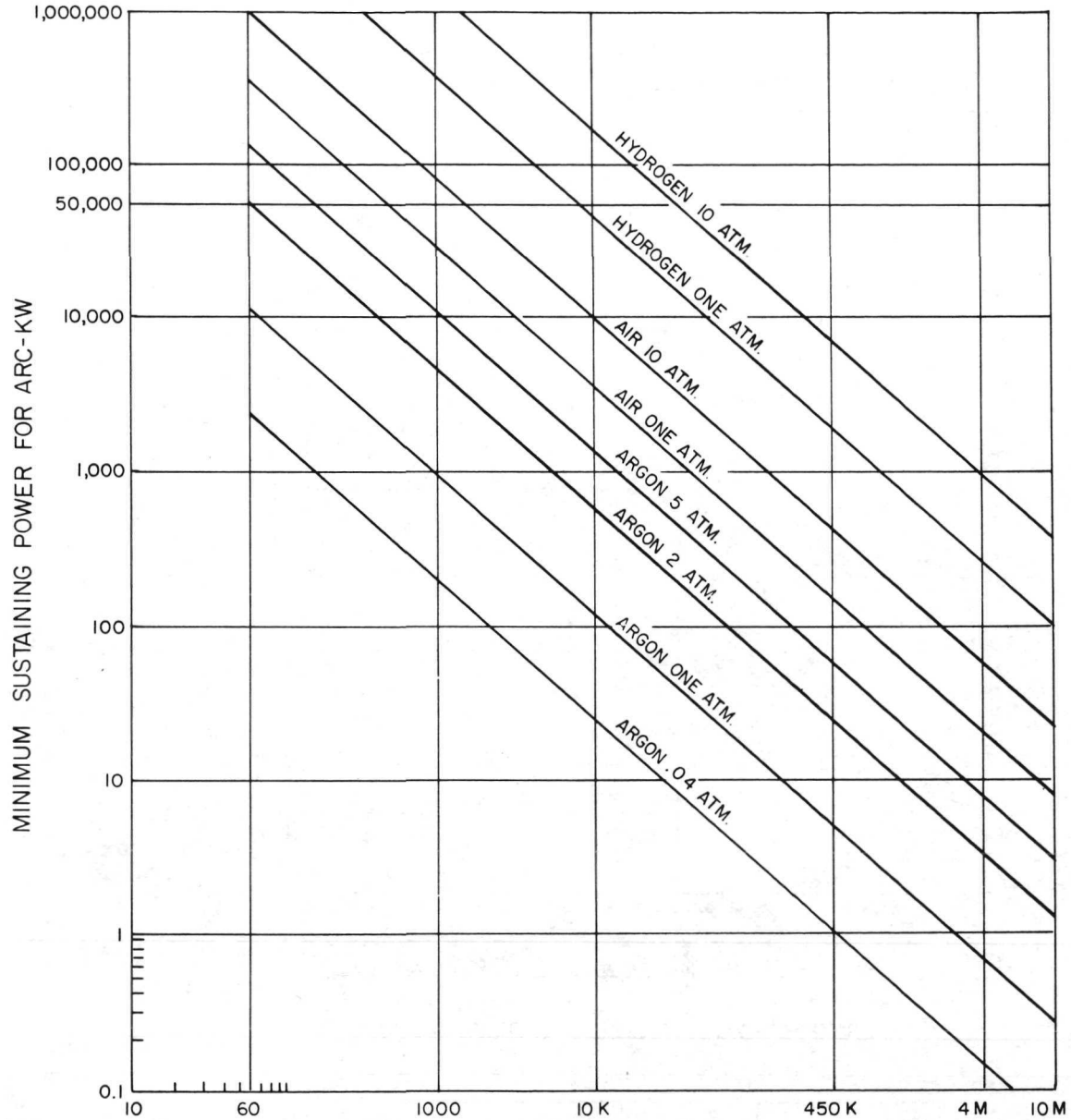

MINIMUM SUSTAINING POWER FOR INDUCTION ARCS

Figure 11

ENERGY DISTRIBUTION IN A 10,000 HERTZ
51 cm. INDUCTION PLASMA SYSTEM

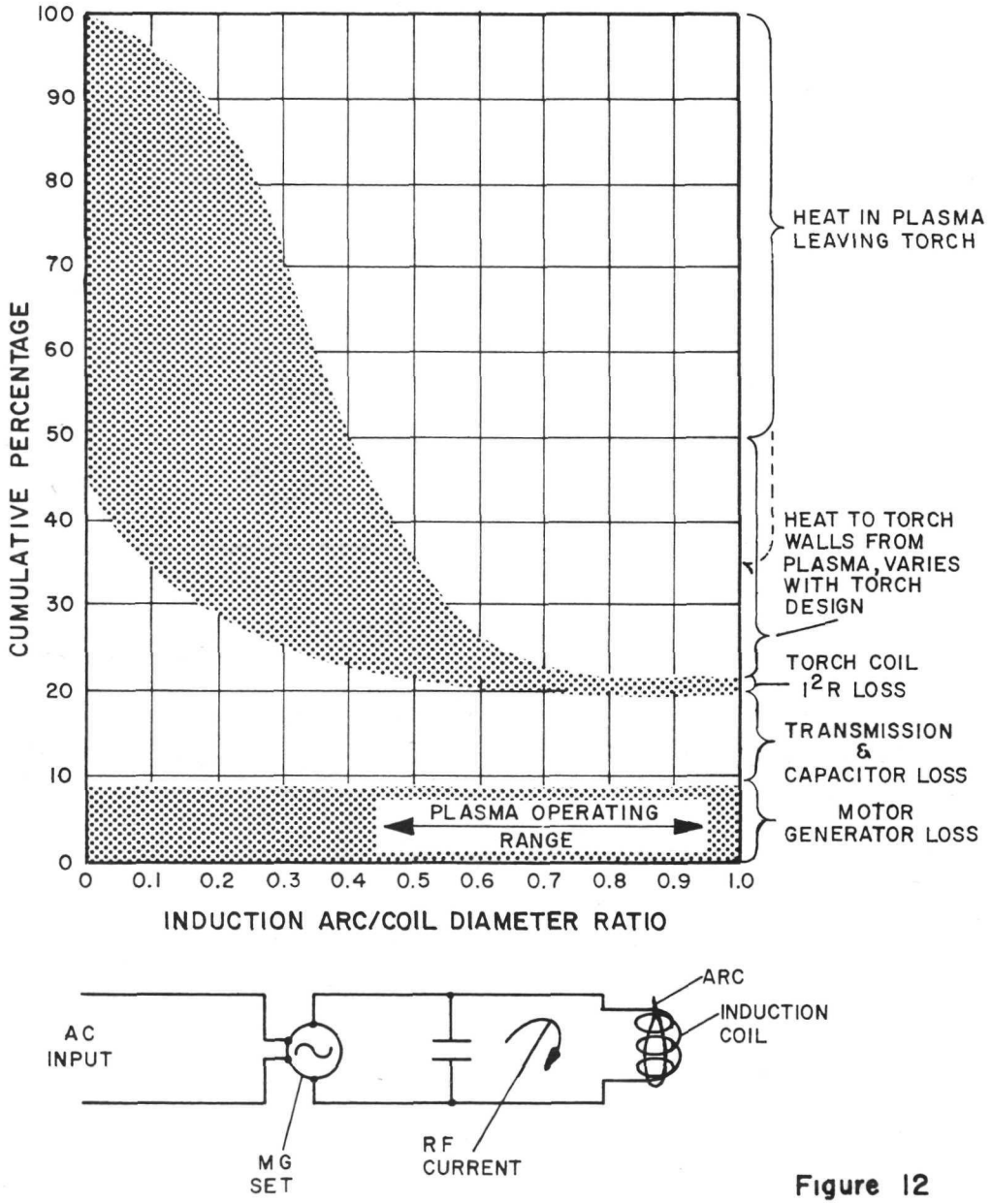

Figure 12

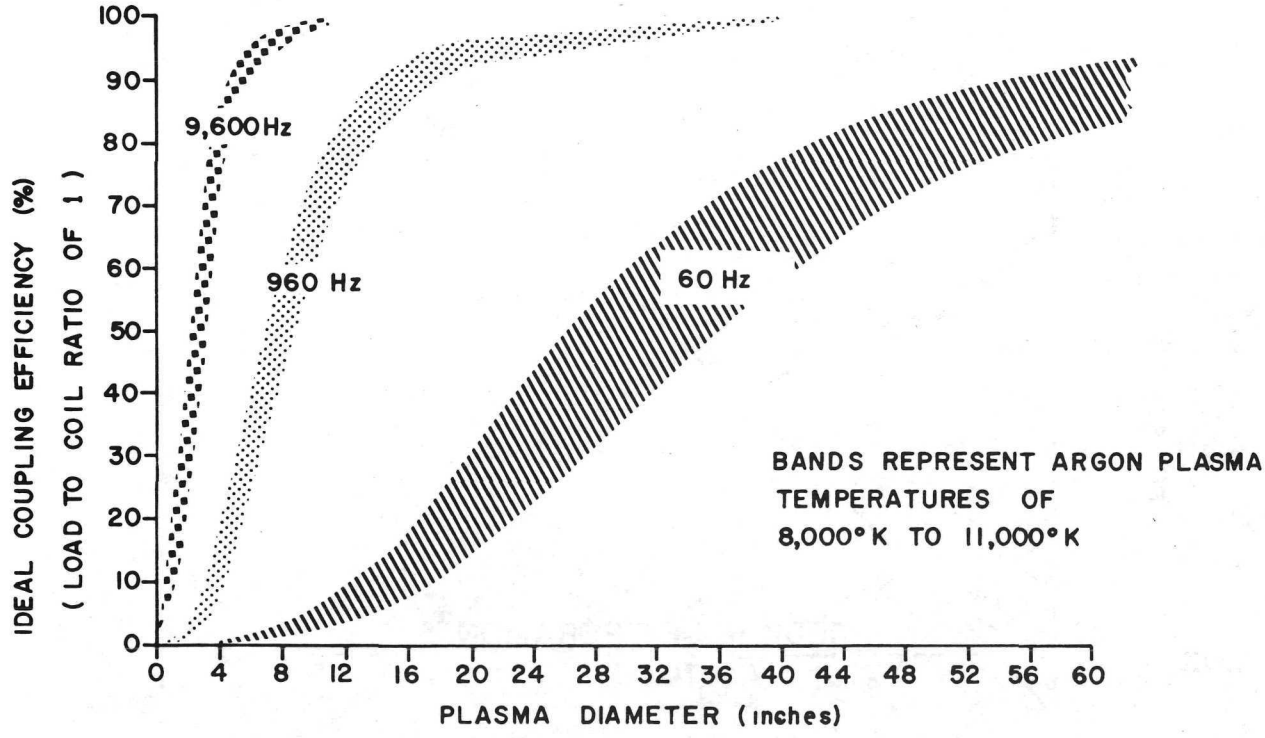

IDEAL COUPLING EFFICIENCY AS A FUNCTION OF PLASMA DIAMETER

(Ref. 4)

Figure 13

C.P.S. STABILITY LIMITS AT 1 ATMOSPHERE

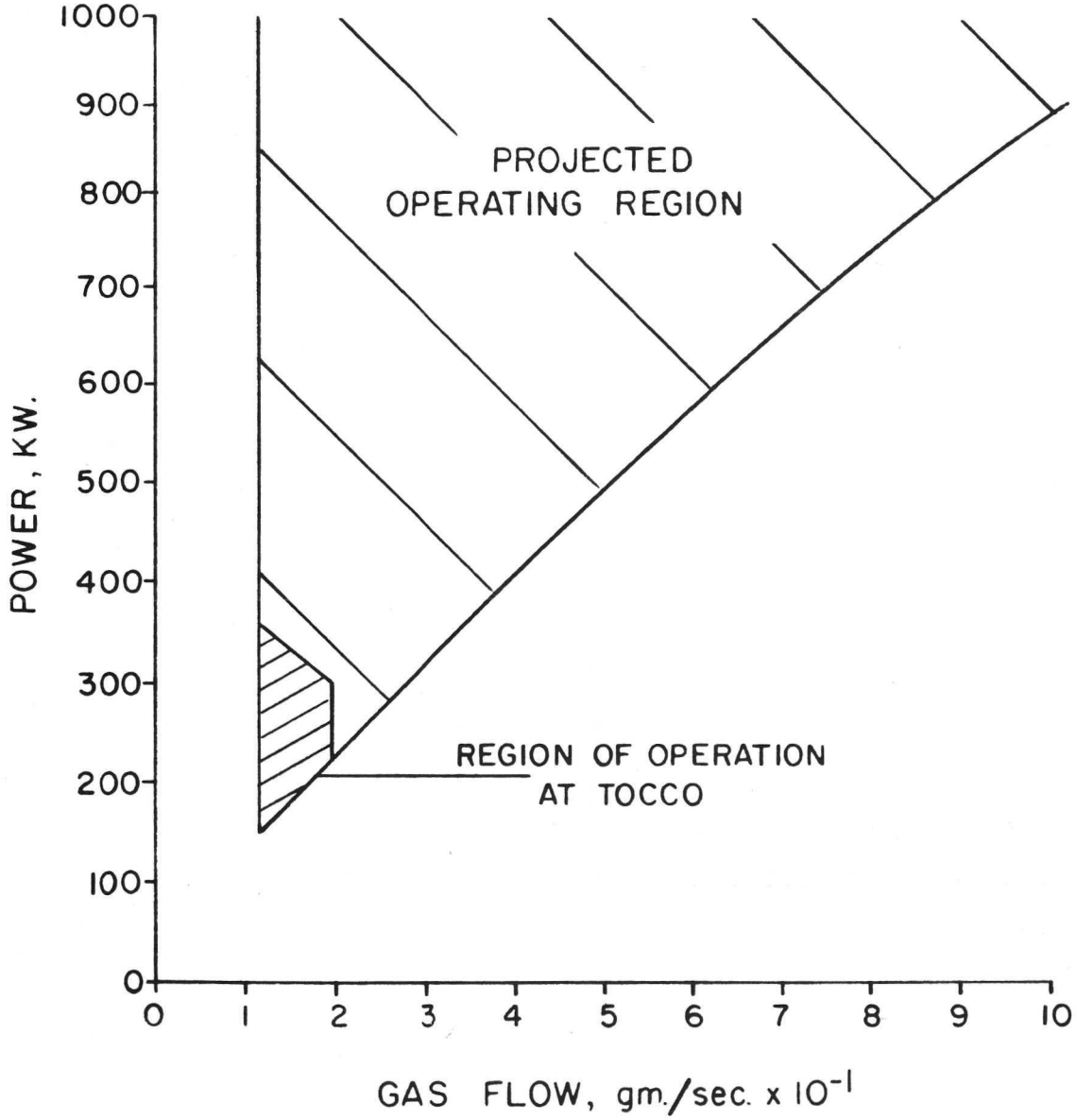

Figure 14

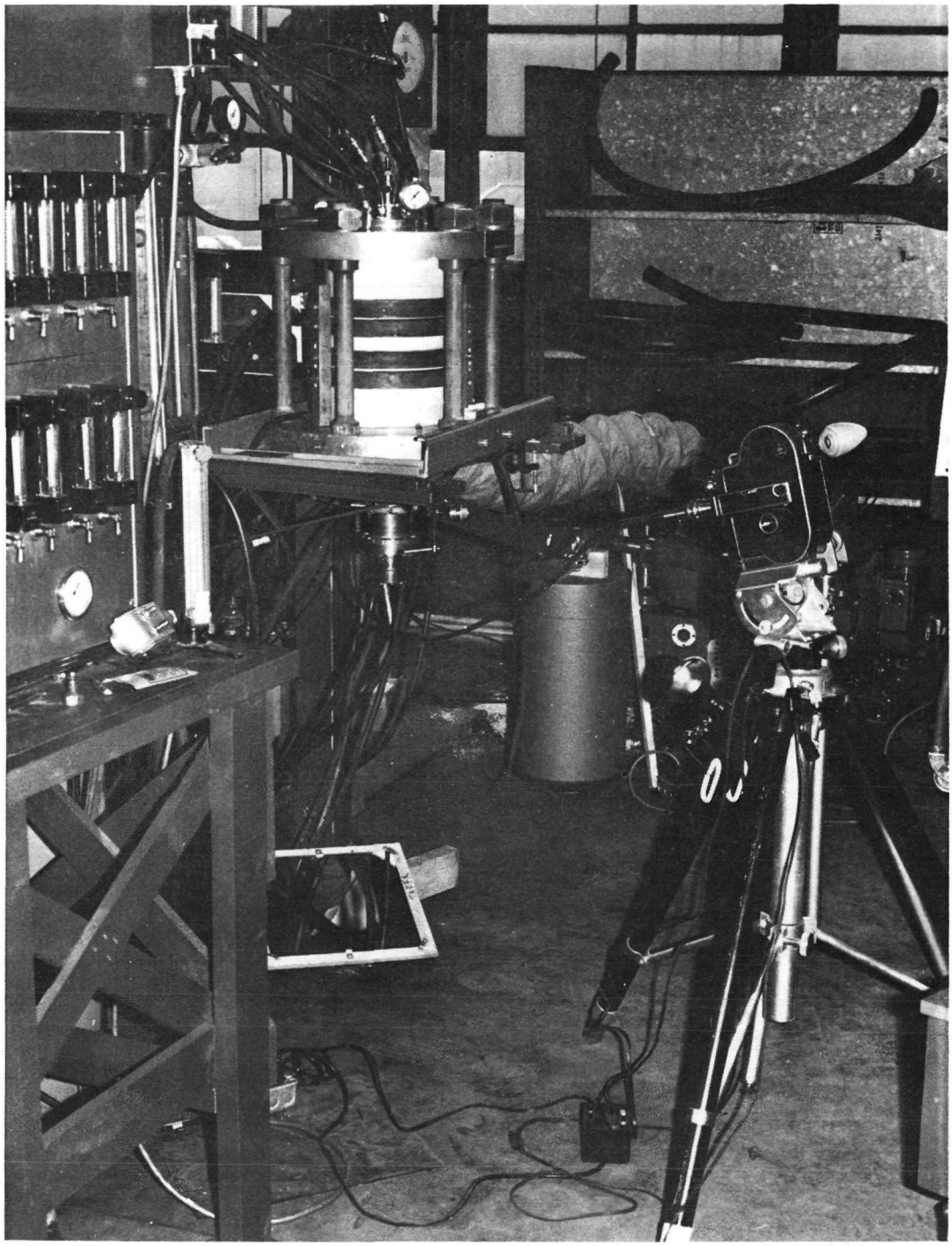

FIBER OPTICS ATTACHED TO CPS AND BOLEX CAMERA

FIGURE 15

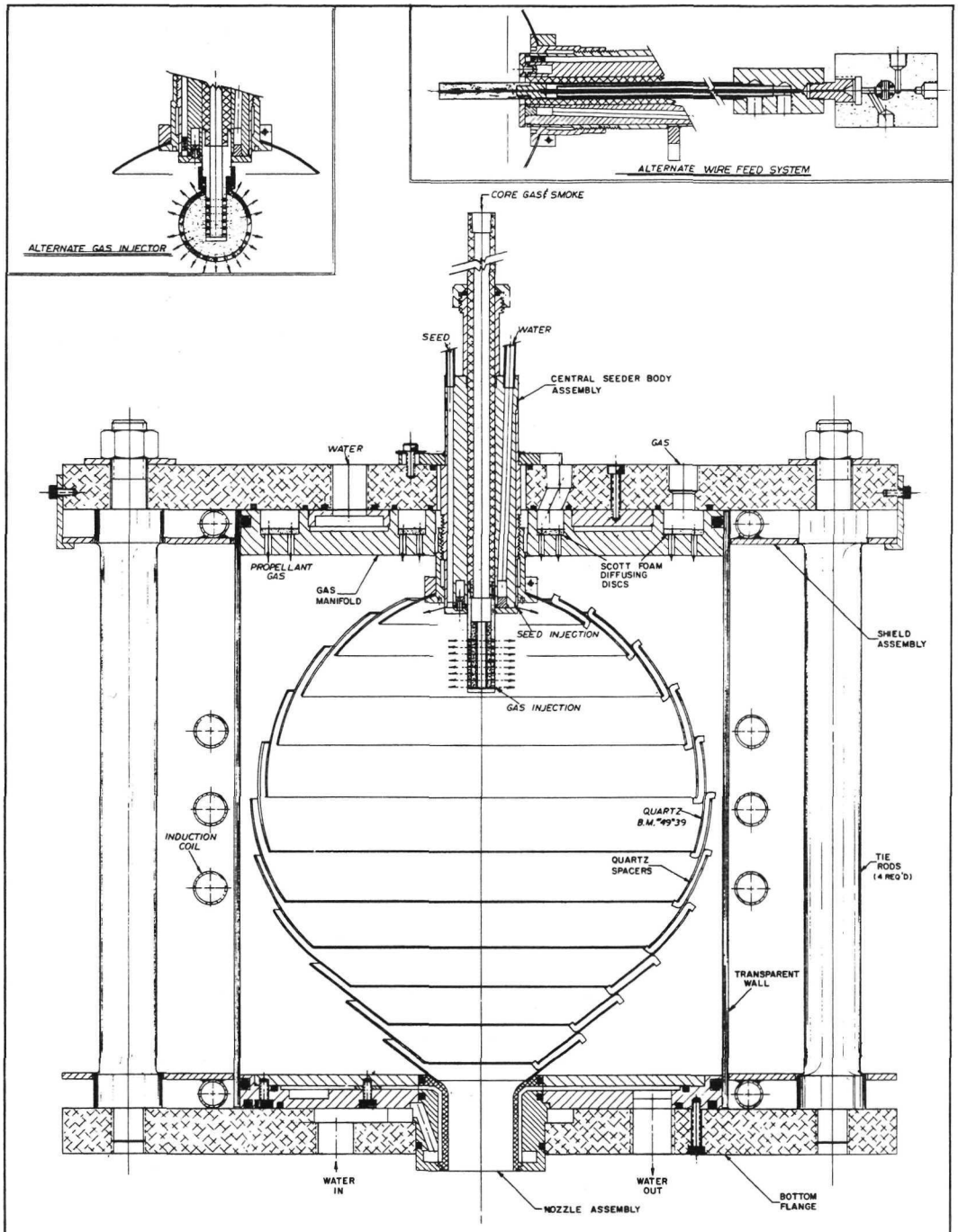

PROPOSED LOUVERED INNER WALL DESIGN

OVERALL VIEW ILLUSTRATING THE ARRANGEMENT OF THE QUARTZ LOUVERED INNER WALL WITH ALTERNATE GAS AND WIRE FEED SYSTEMS

FIG.16

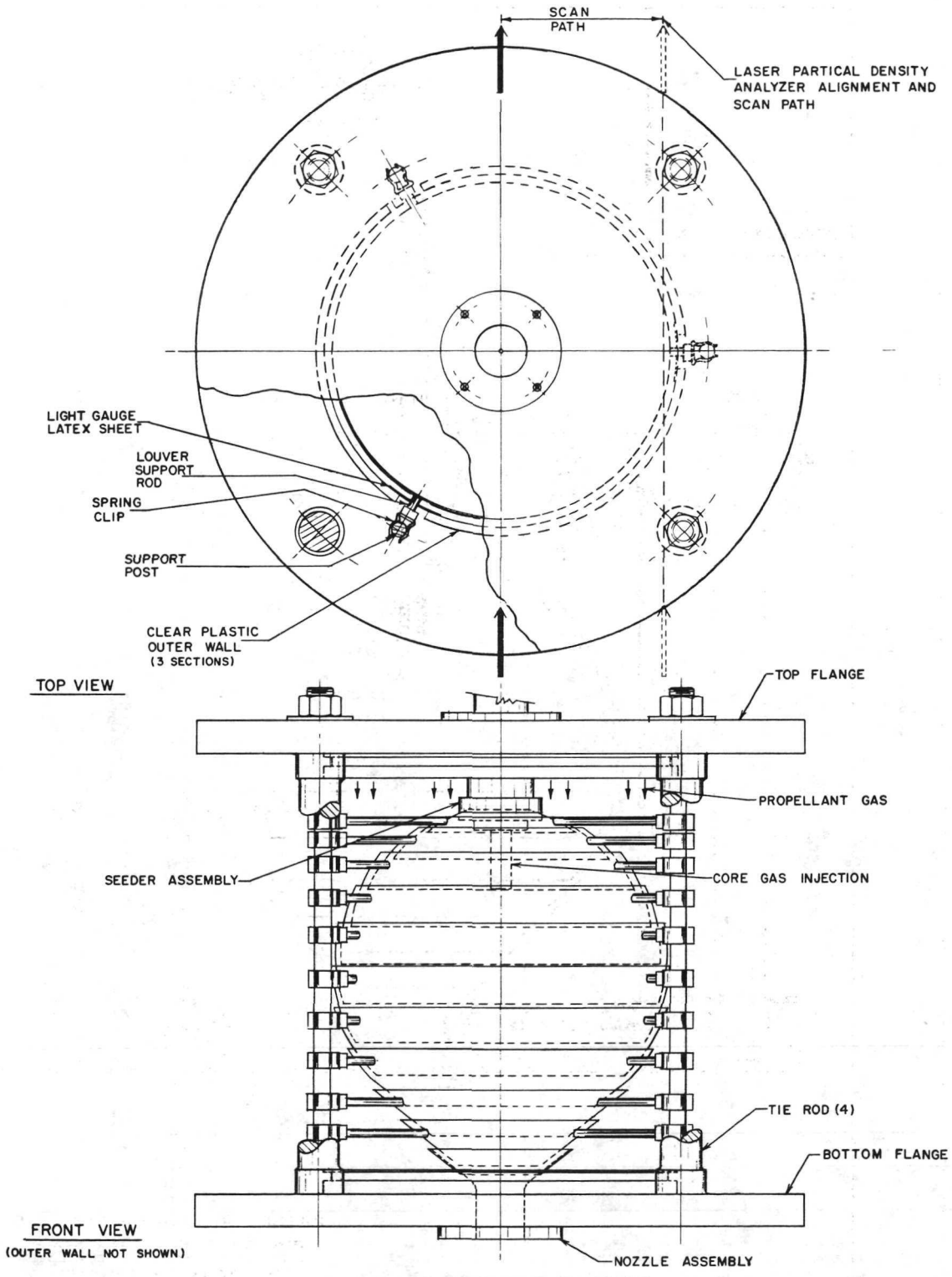

LOUVER ADJUSTMENT FIXTURE
ASSEMBLY

Figure 17

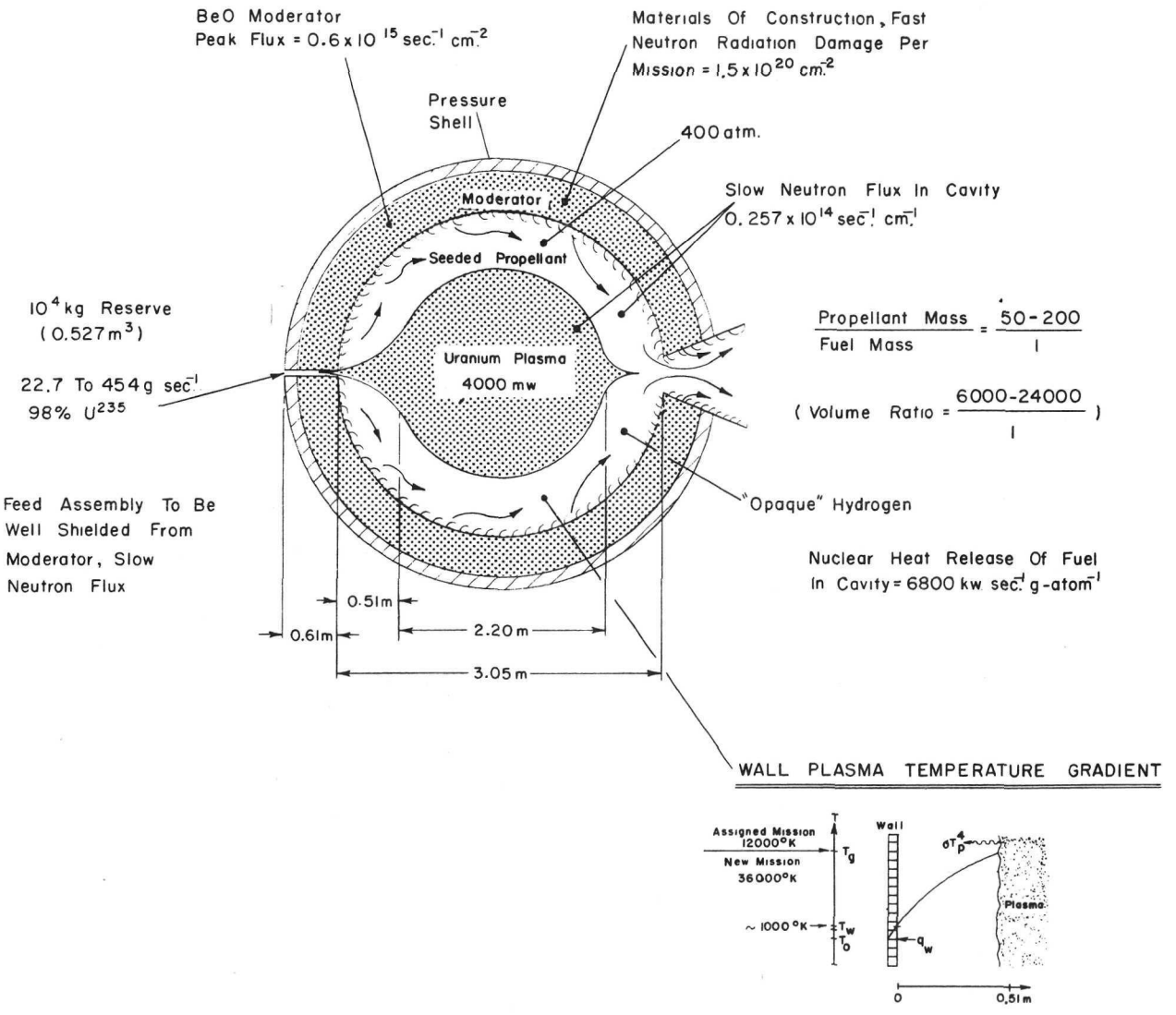

FINAL TASK III SPECIFICATIONS

Figure 18

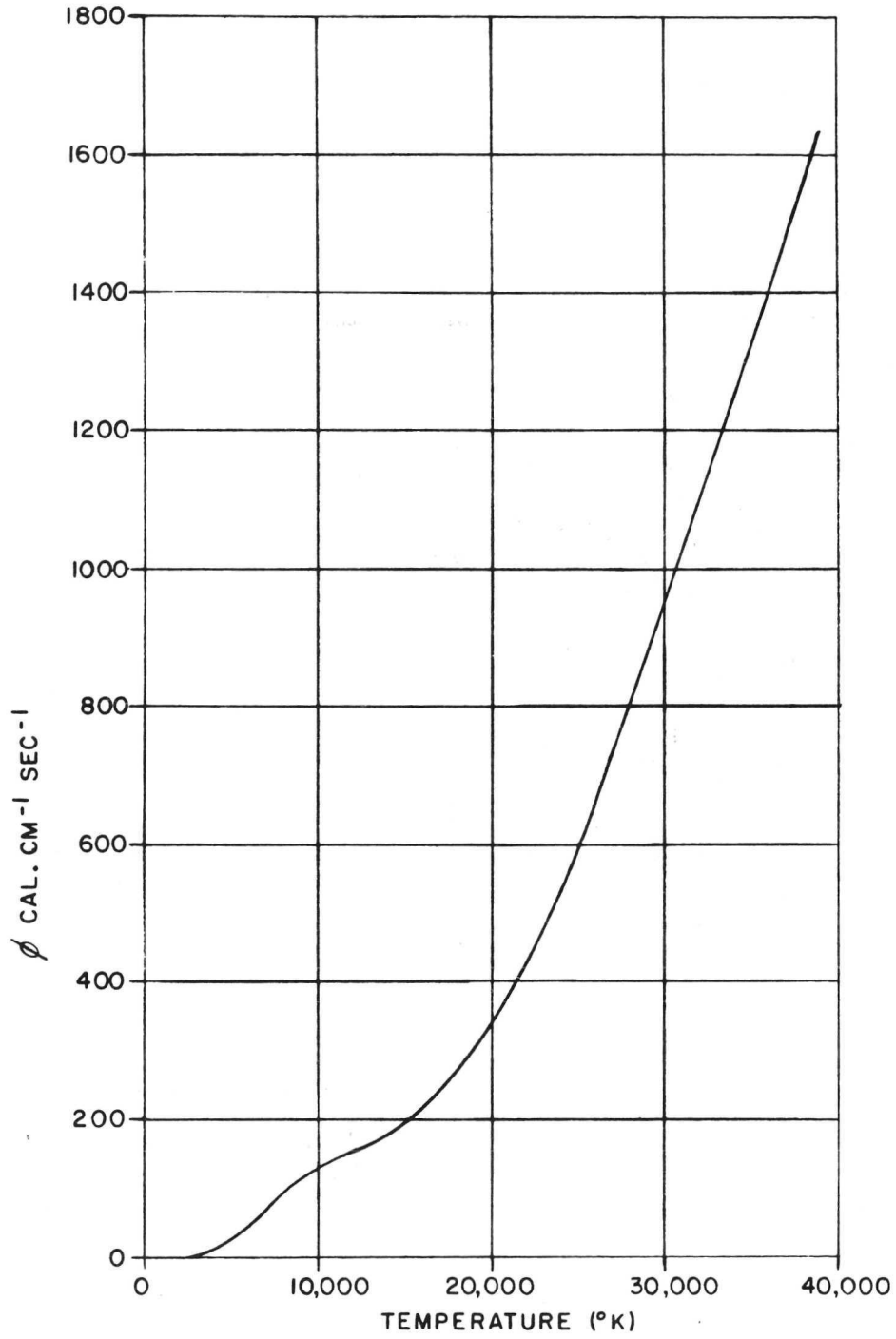

SCHMITZ HEAT FLOW POTENTIAL FOR HYDROGEN AT 500 ATMOSPHERES (REFERRED TO 1000° K)

FIG.19

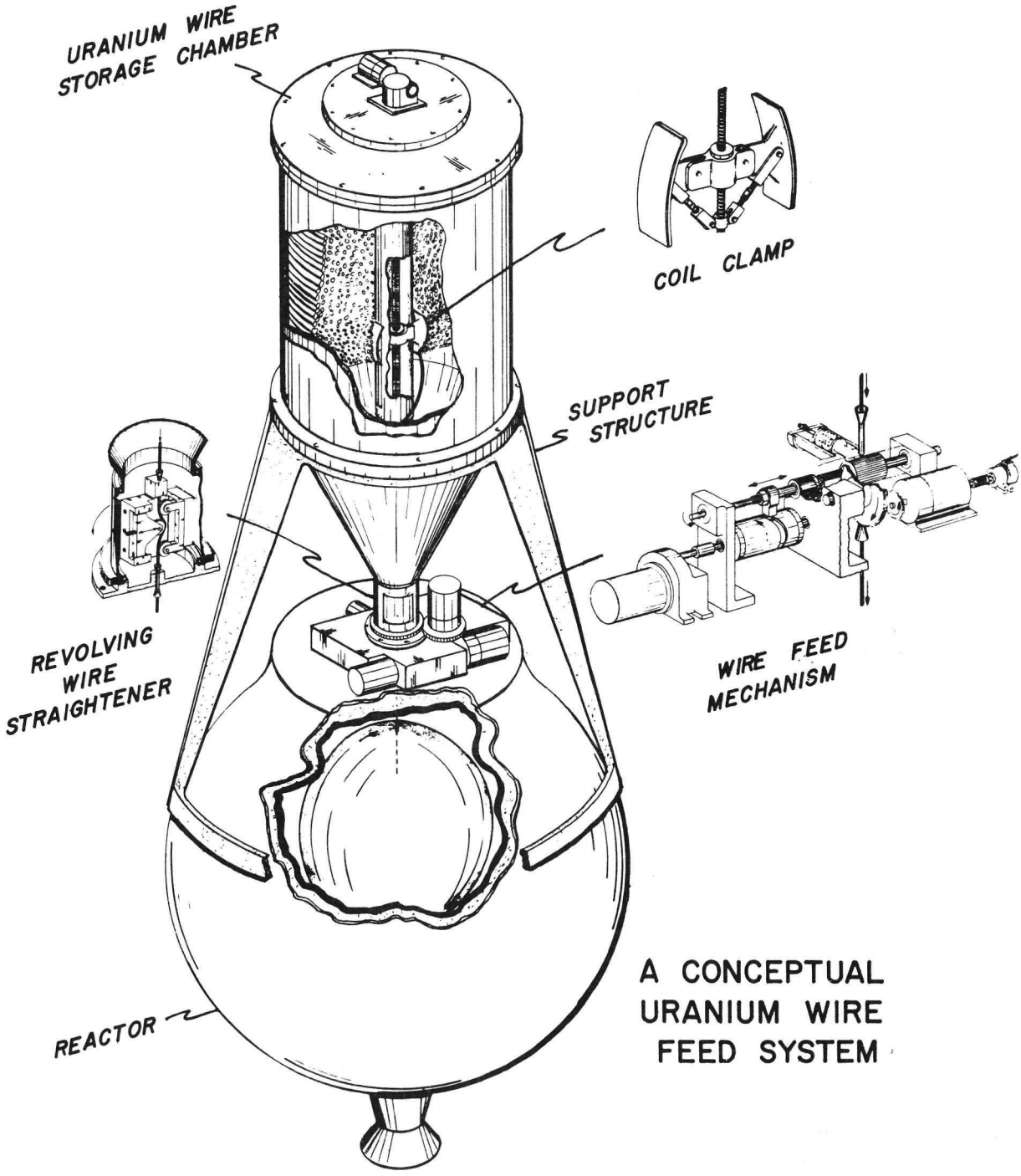
URANIUM WIRE STORAGE CHAMBER
COIL CLAMP
SUPPORT STRUCTURE
REVOLVING WIRE STRAIGHTENER
WIRE FEED MECHANISM
REACTOR
A CONCEPTUAL URANIUM WIRE FEED SYSTEM

Figure 20

CONCEPTUAL URANIUM LIQUID JET FEED SYSTEM

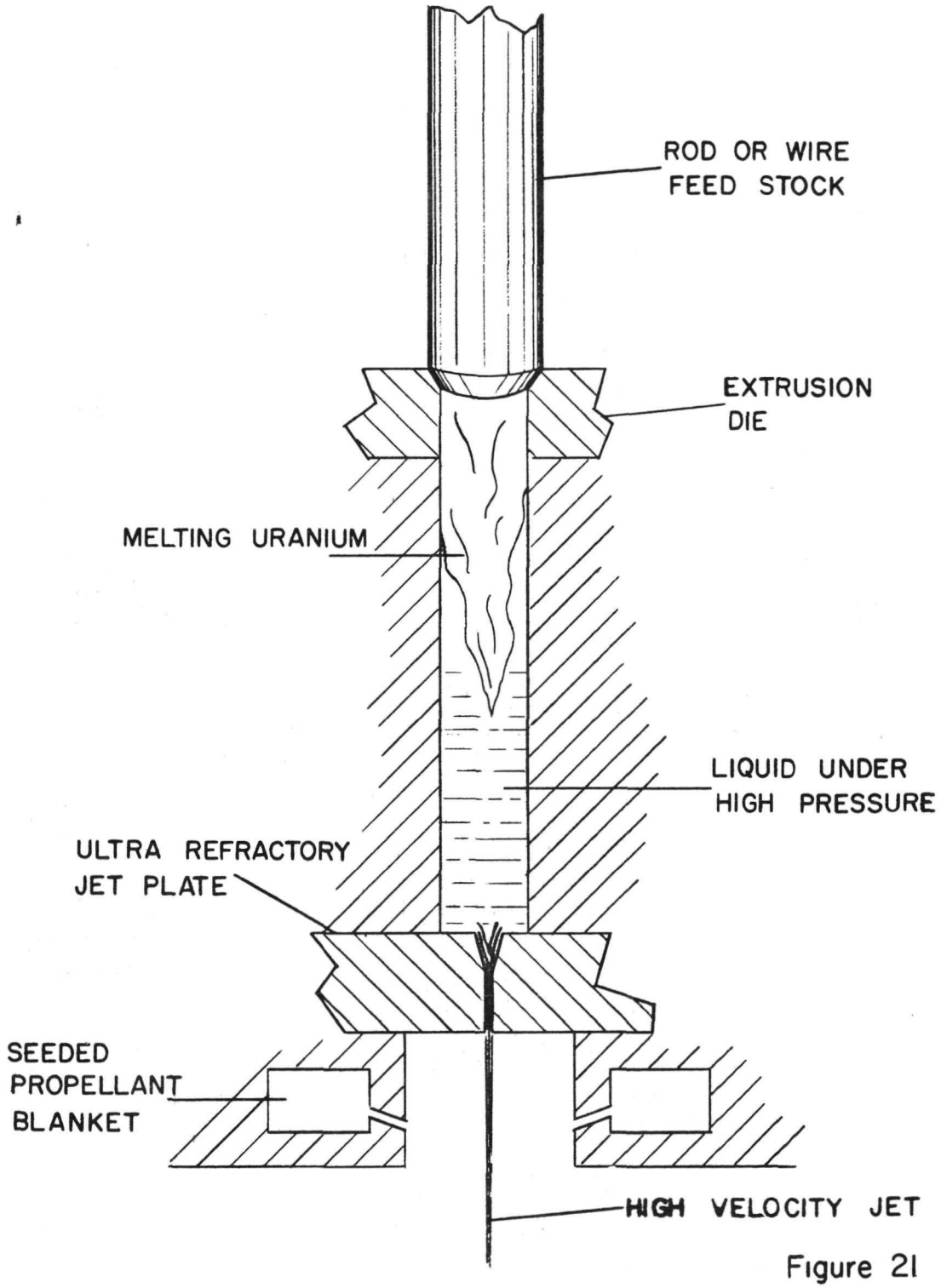

Figure 21

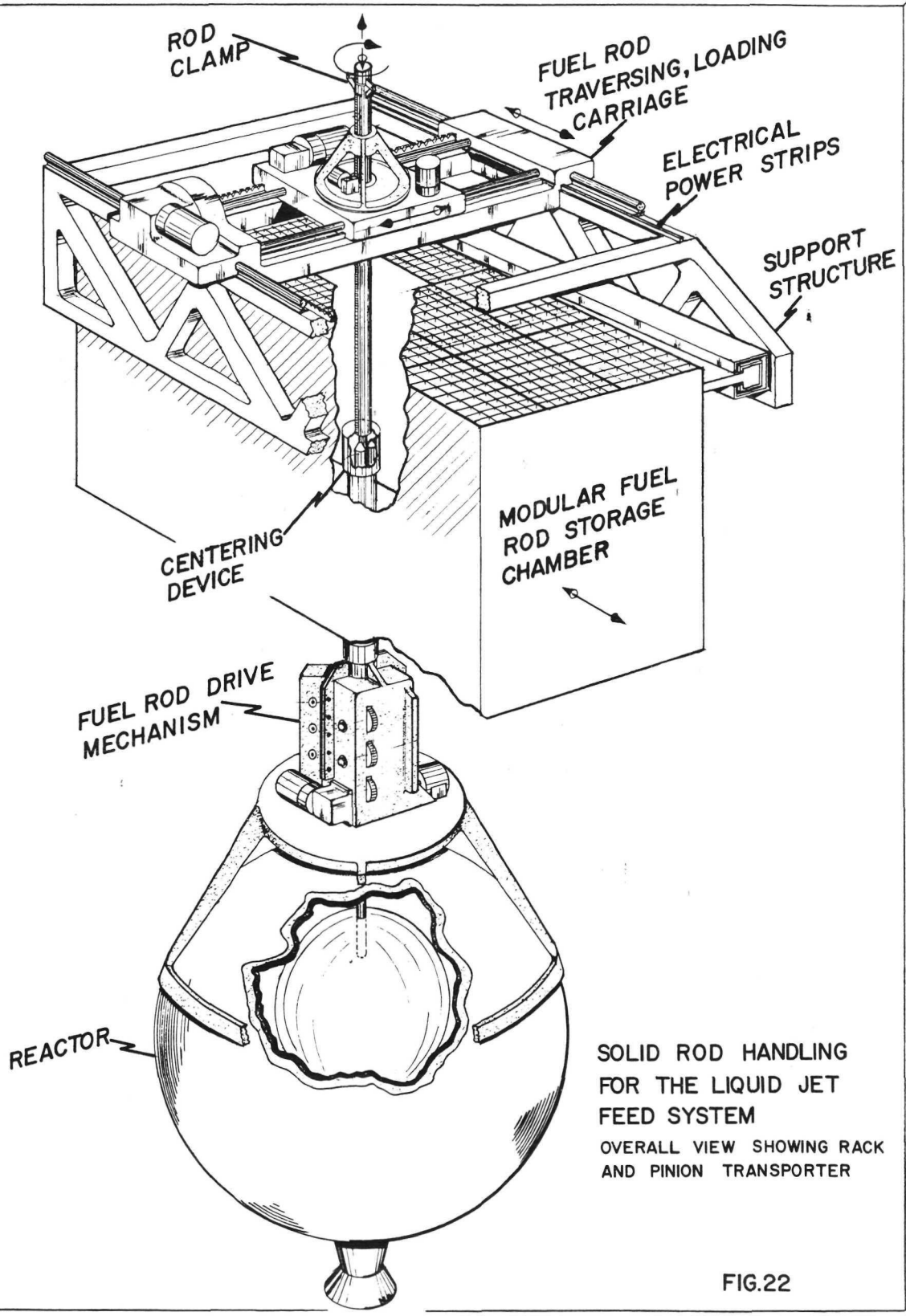

SOLID ROD HANDLING FOR THE LIQUID JET FEED SYSTEM

OVERALL VIEW SHOWING RACK AND PINION TRANSPORTER

FIG.22

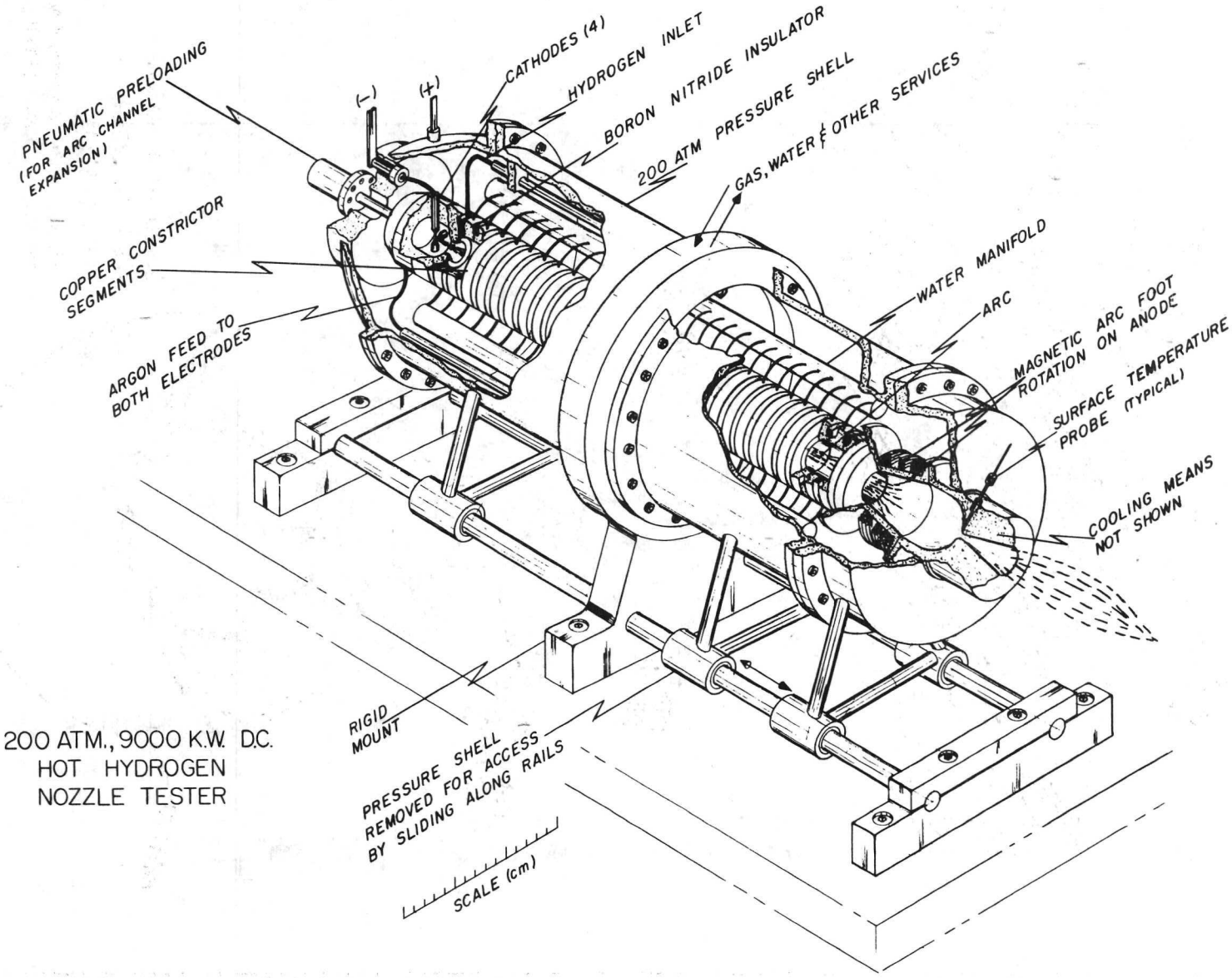
PNEUMATIC PRELOADING (FOR ARC CHANNEL EXPANSION)
(−)
(+)
CATHODES (4)
HYDROGEN INLET
BORON NITRIDE INSULATOR
200 ATM PRESSURE SHELL
GAS, WATER & OTHER SERVICES
COPPER CONSTRICTOR SEGMENTS
ARGON FEED TO BOTH ELECTRODES
WATER MANIFOLD
ARC
MAGNETIC ARC FOOT ROTATION ON ANODE
SURFACE TEMPERATURE PROBE (TYPICAL)
COOLING MEANS NOT SHOWN
RIGID MOUNT
PRESSURE SHELL REMOVED FOR ACCESS BY SLIDING ALONG RAILS
SCALE (cm)
200 ATM., 9000 K.W. D.C.
HOT HYDROGEN
NOZZLE TESTER

Figure 23

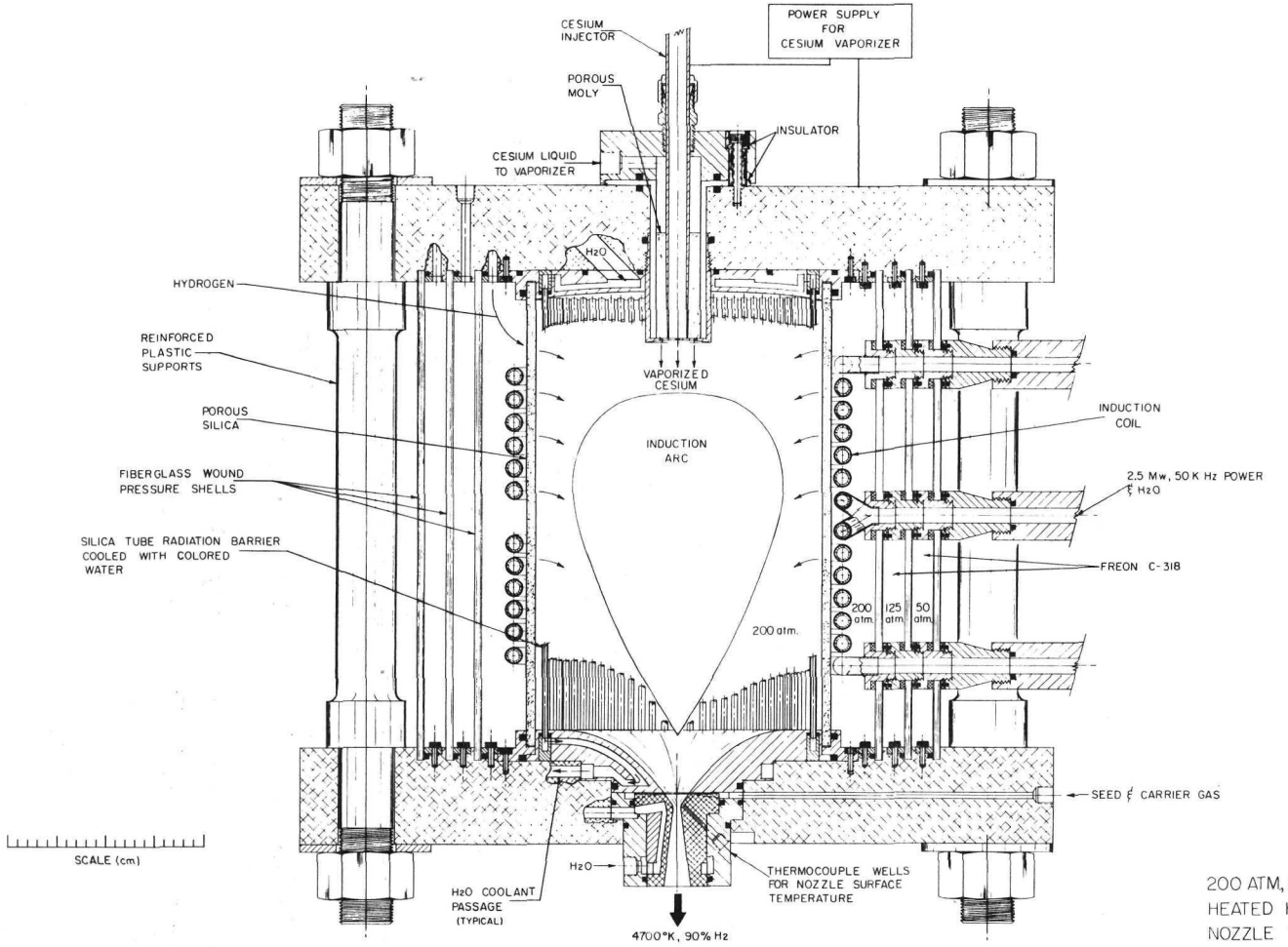

200 ATM, 2500 K.W. INDUCTION HEATED HOT HYDROGEN NOZZLE TESTER

Figure 24

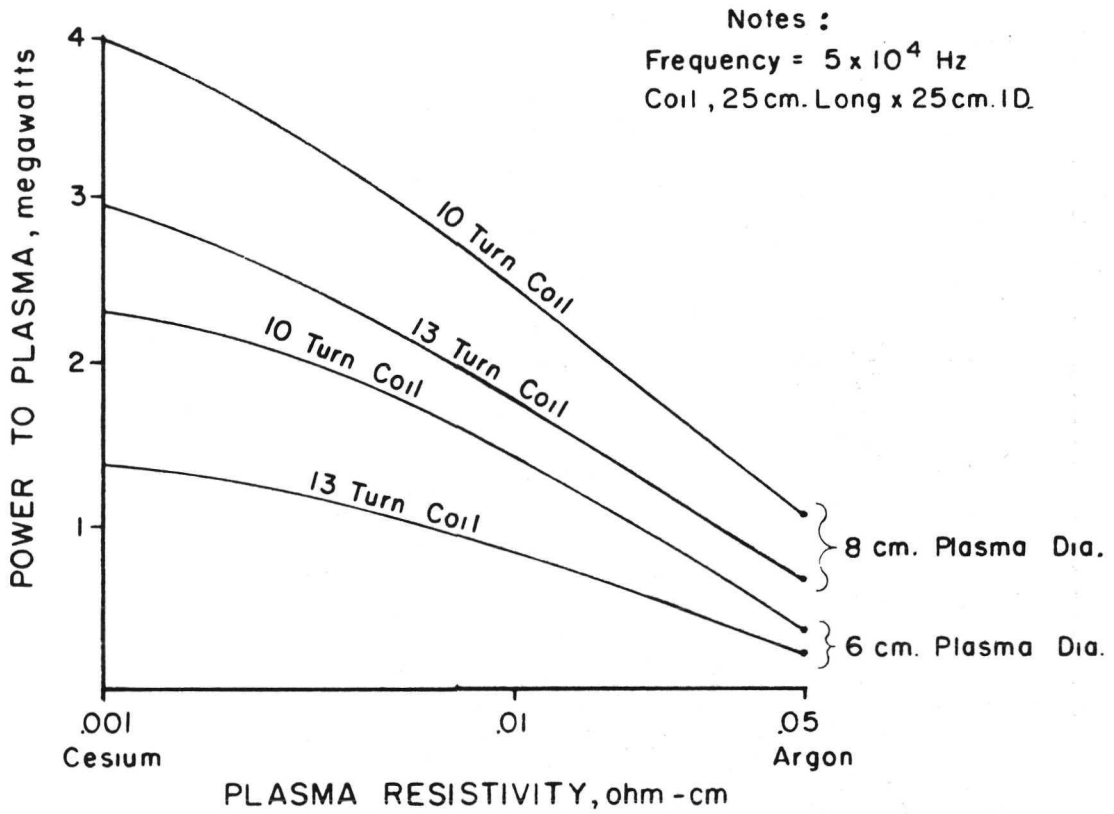

Effects Of Plasma Resistivity And Coil Turns On Power Coupled To The Plasma

Figure 25

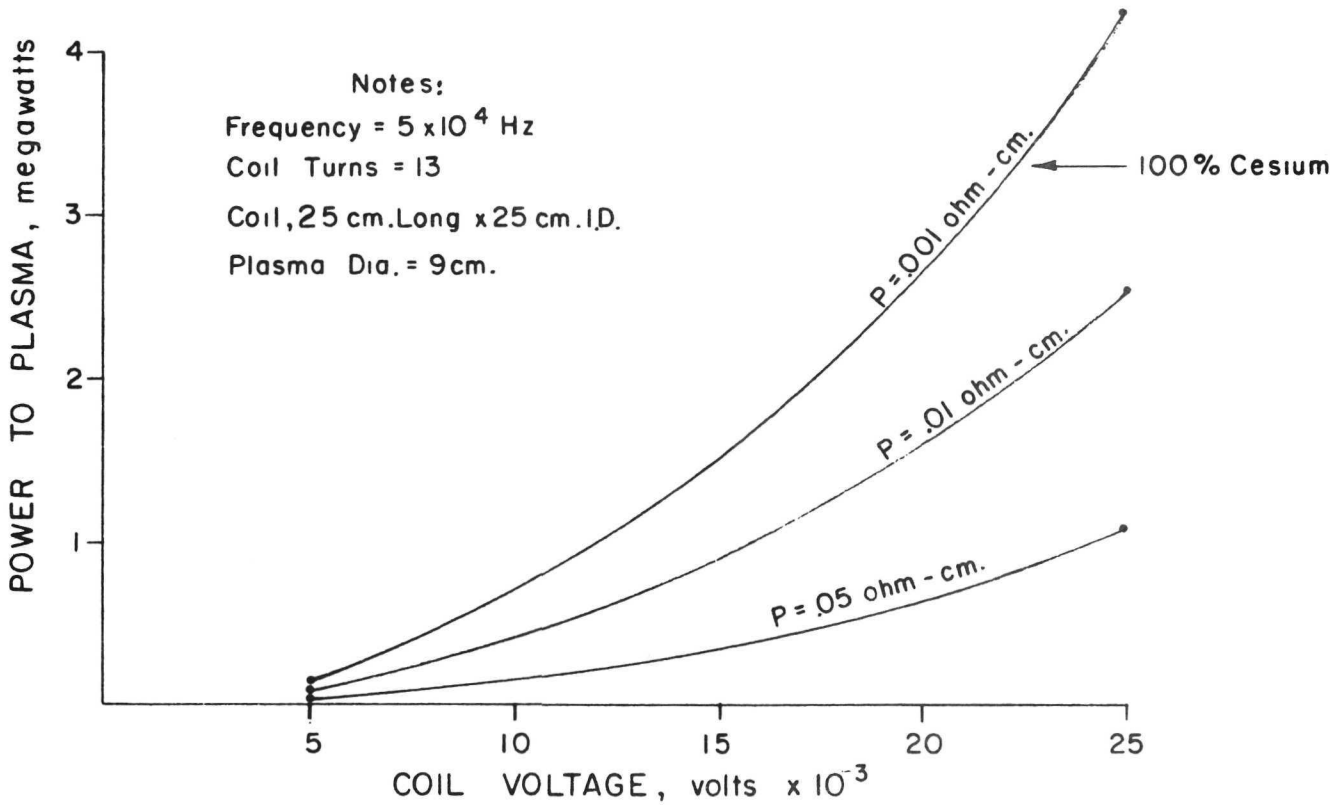

Effects Of Coil Voltage And Plasma Resistivity On Power Coupled To The Plasma

Figure 26

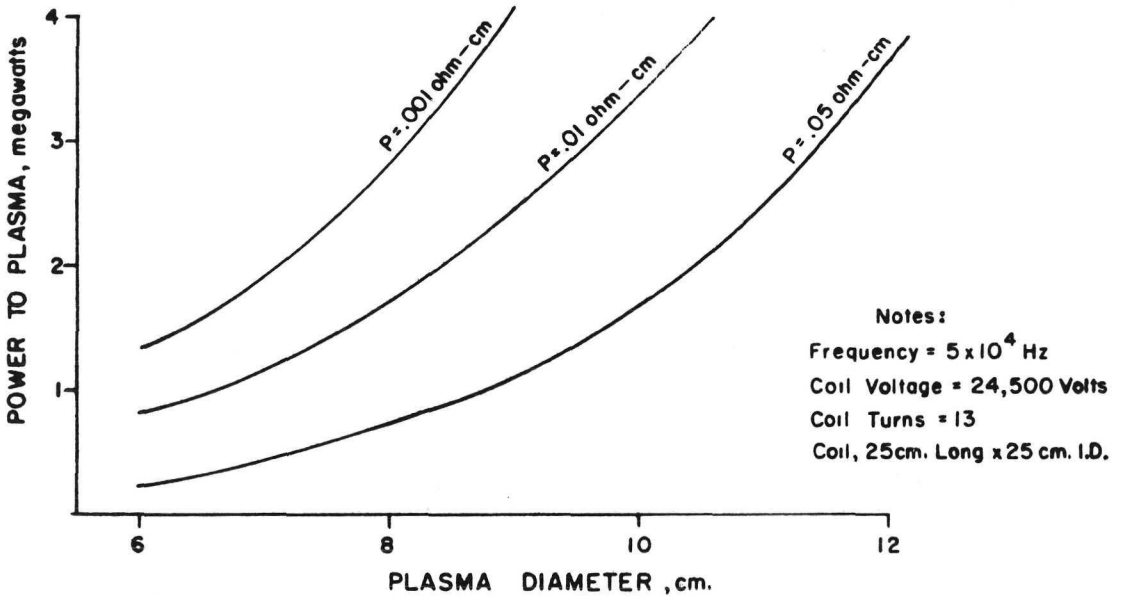

Effects Of Plasma Diameter And Resistivity On Power Coupled To The Plasma

Figure 27

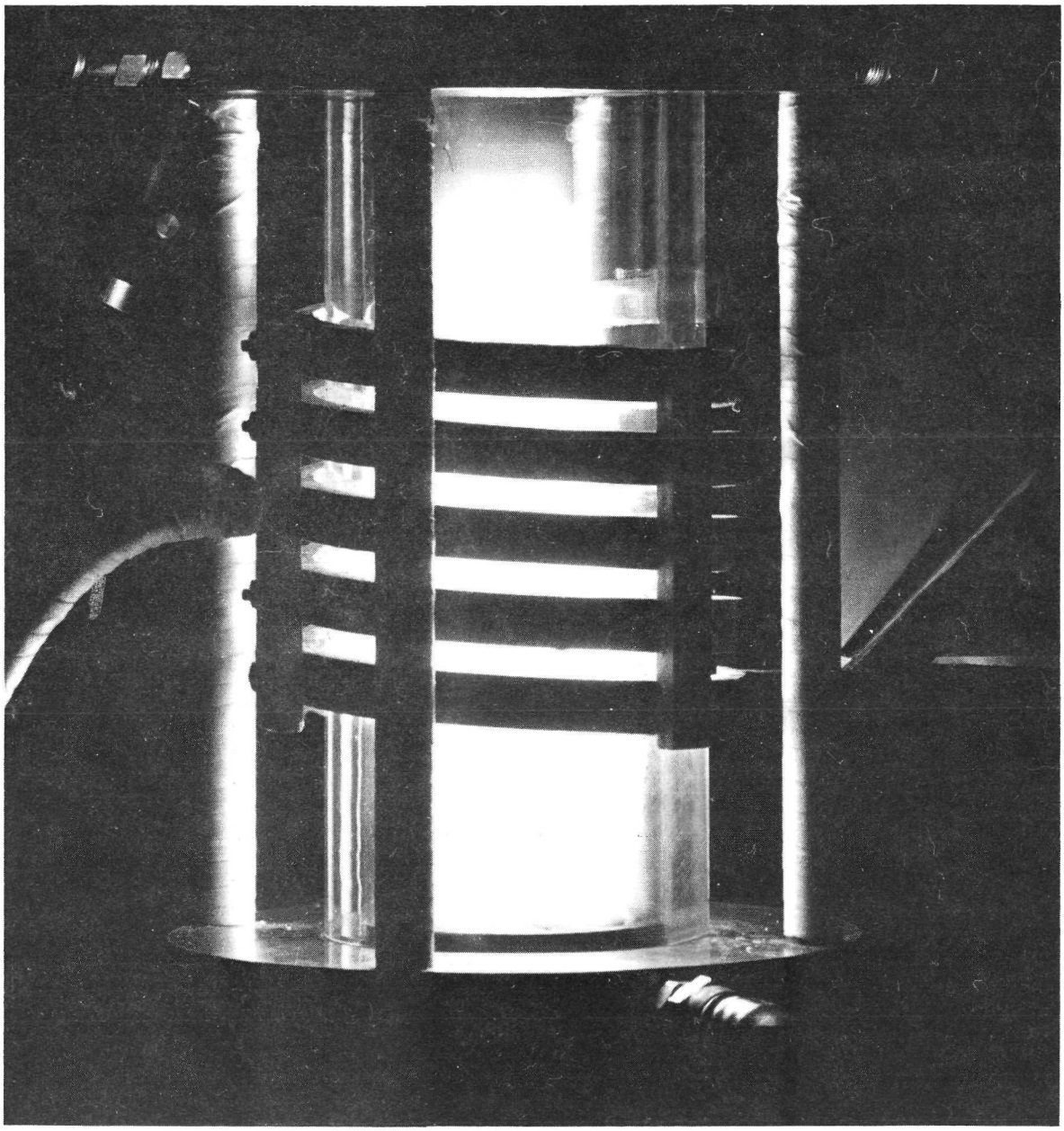

FIGURE 28 PHOTOGRAPH OF THE TRANSPARENT-WALLED WATER-COOLED 9600 Hz INDUCTION TORCH

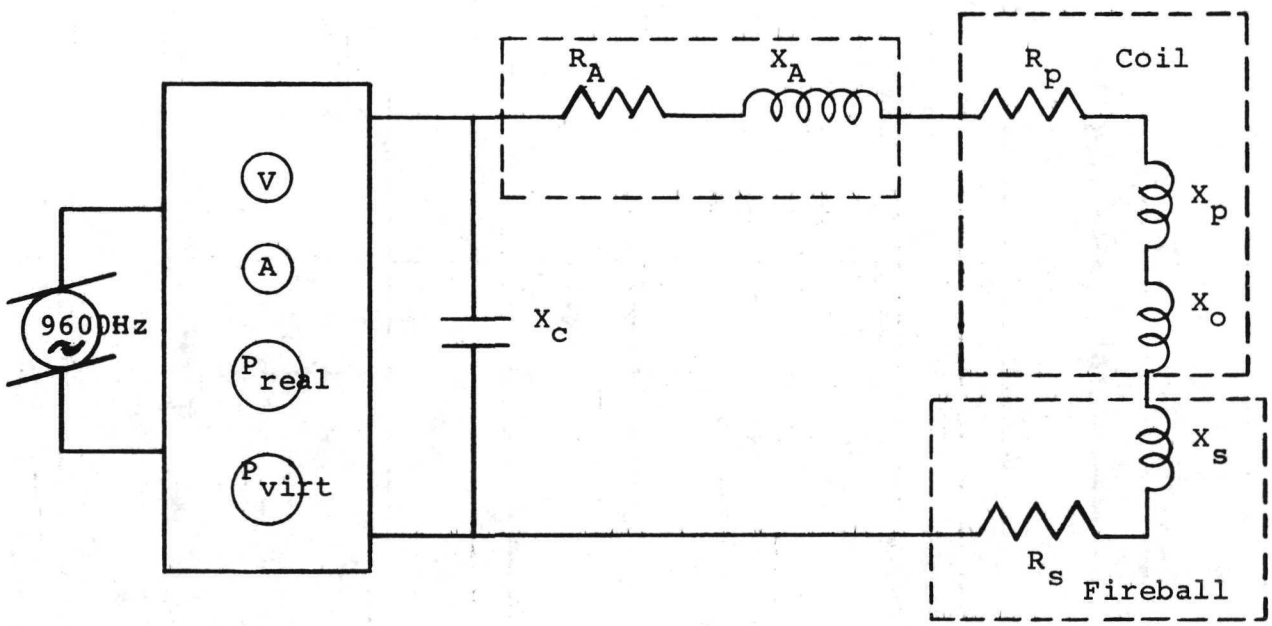

SCHEMATIC REPRESENTATION OF AN EQUIVALENT ELECTRICAL CIRCUIT SHOWING REFLECTED IMPEDANCE

FIGURE 29

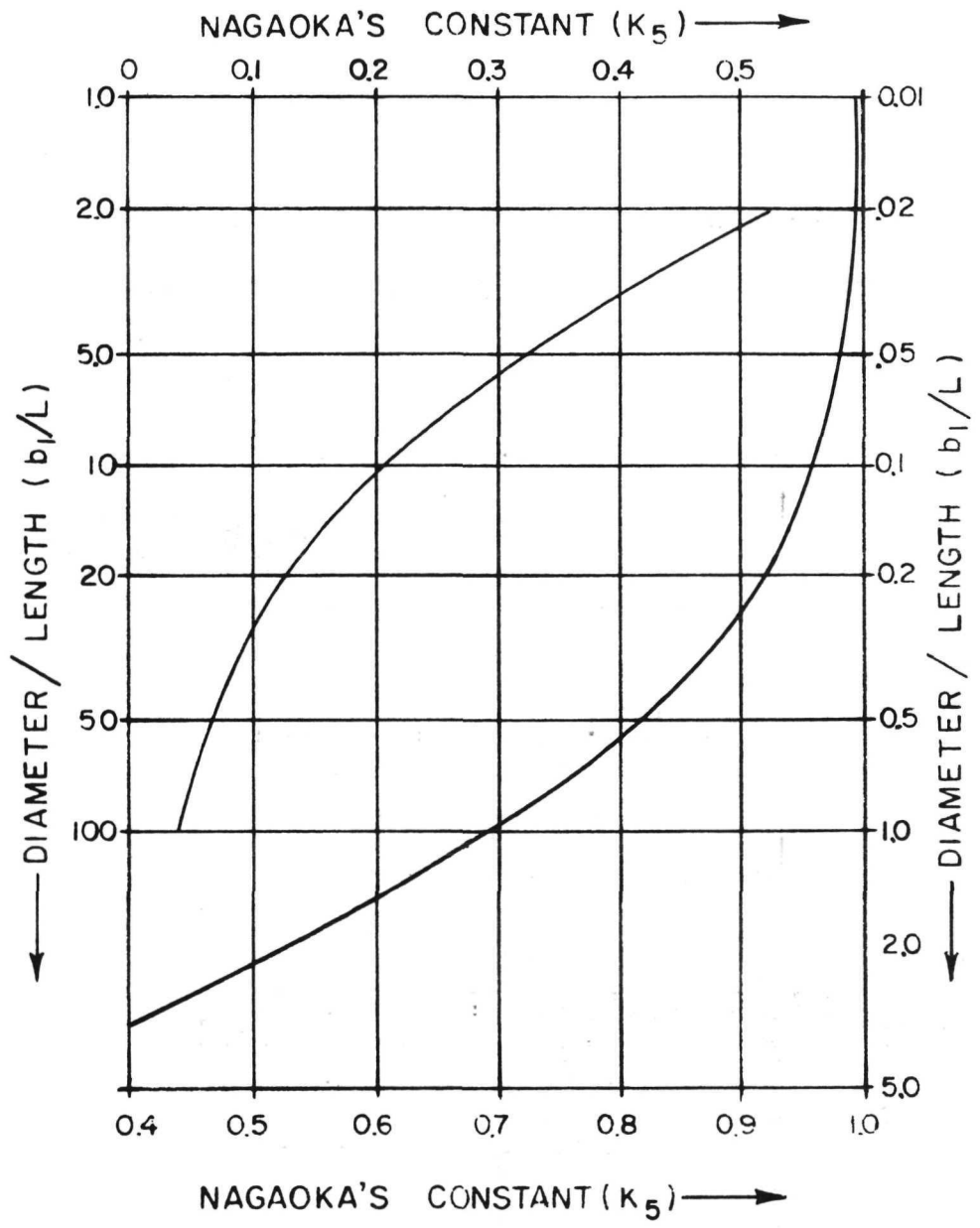

Nagaoka's Constant (K_5) For A Wide Range Of d/l
(Ref. 9)

Figure 30

Load Resistance Factor As A Function Of Plasma Diameter To Reference Depth Ratio

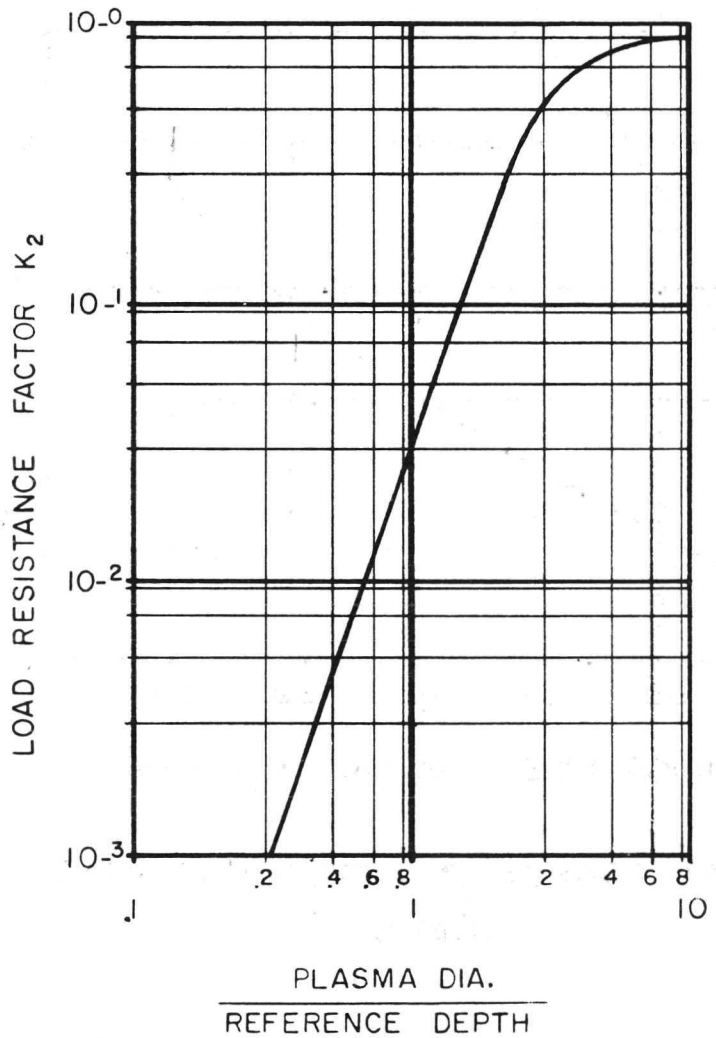

Figure 31

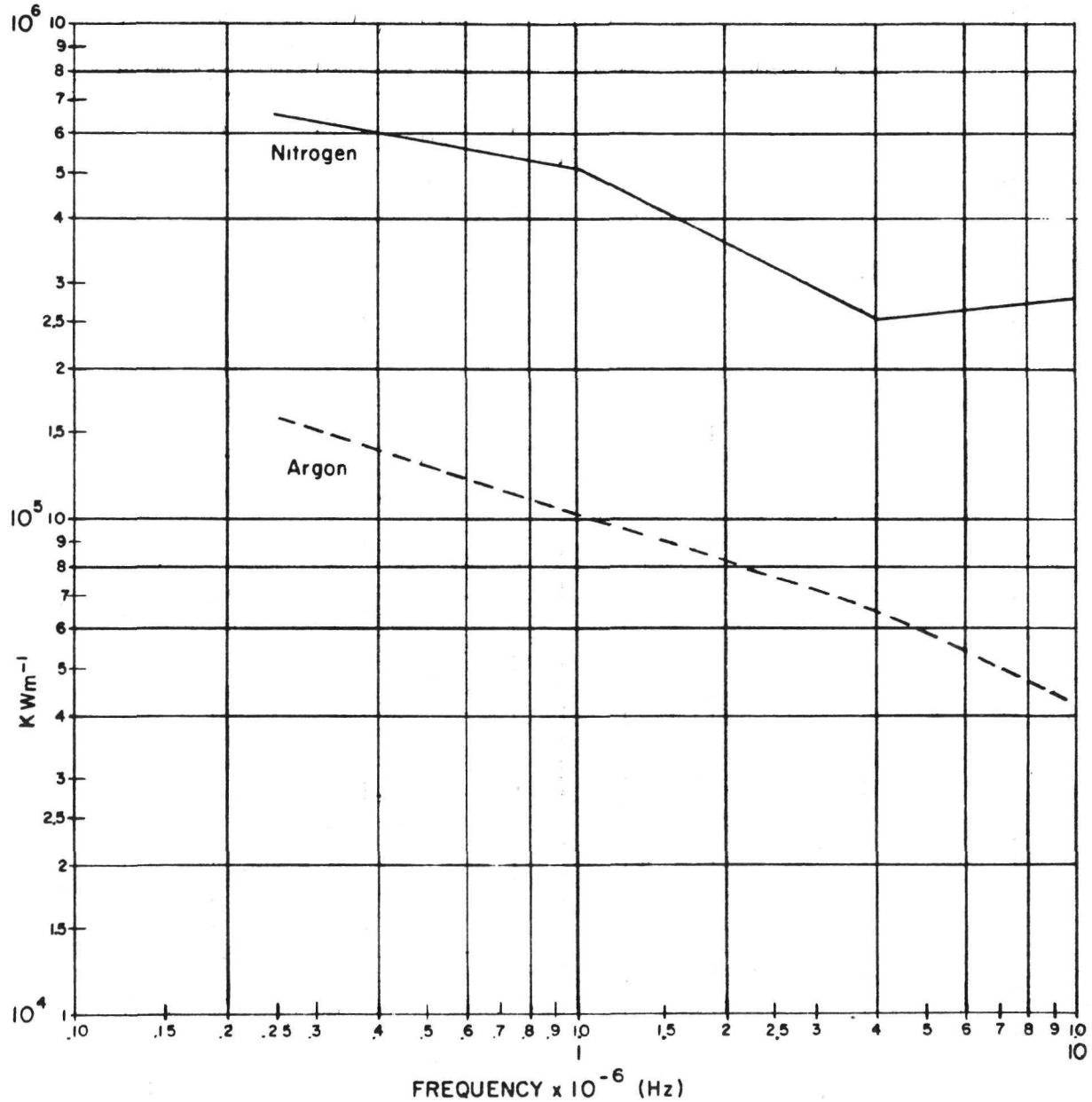

Minimum Sustaining Power Density vs Frequency In A 2.54 cm. Torch. Broken Line Interpolation From Figure 10

Figure 32

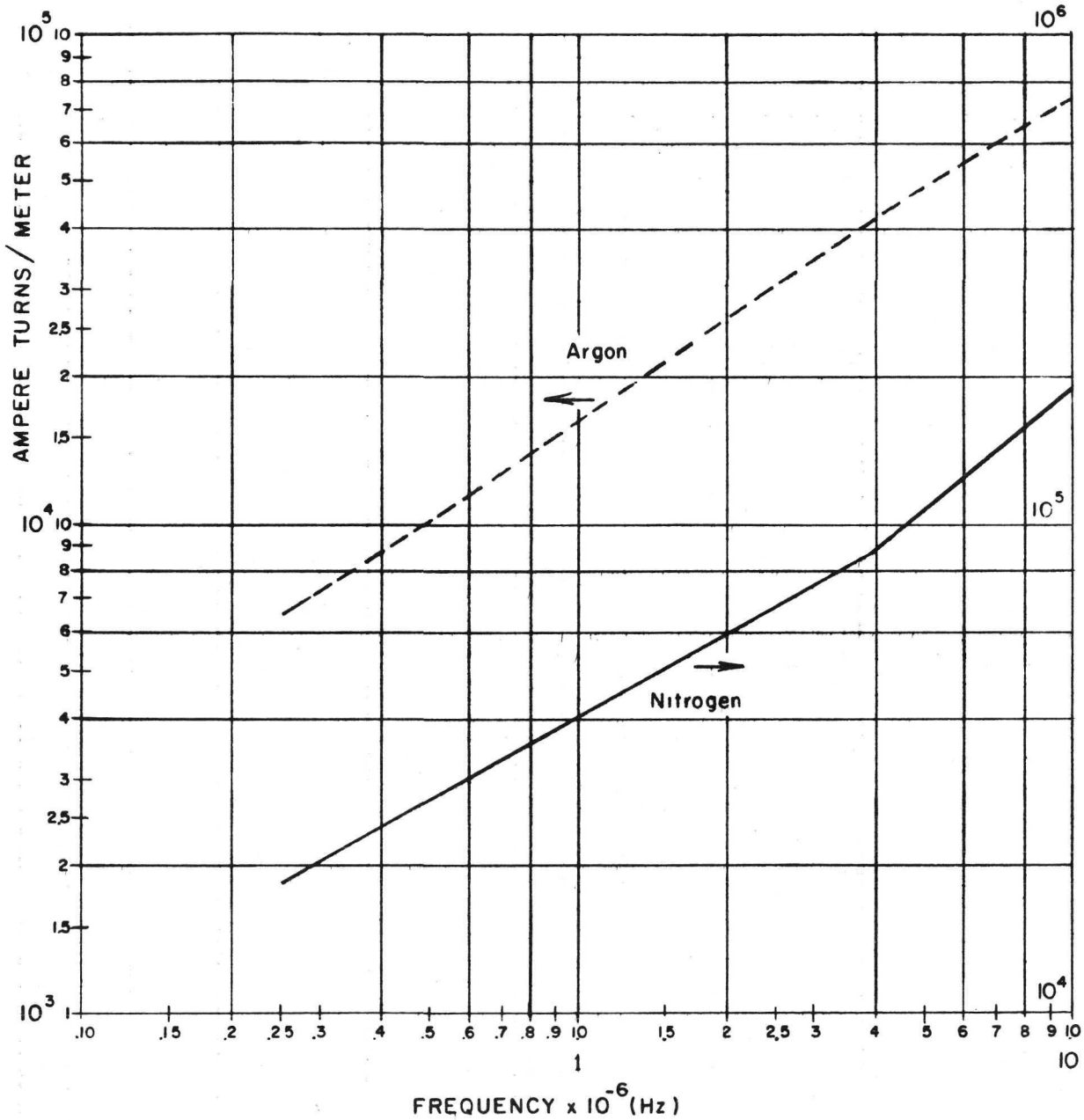

Minimum Sustaining Fields vs Frequency In A 2.54 cm. Torch

Broken Line Interpolation From Figure 10

Figure 33

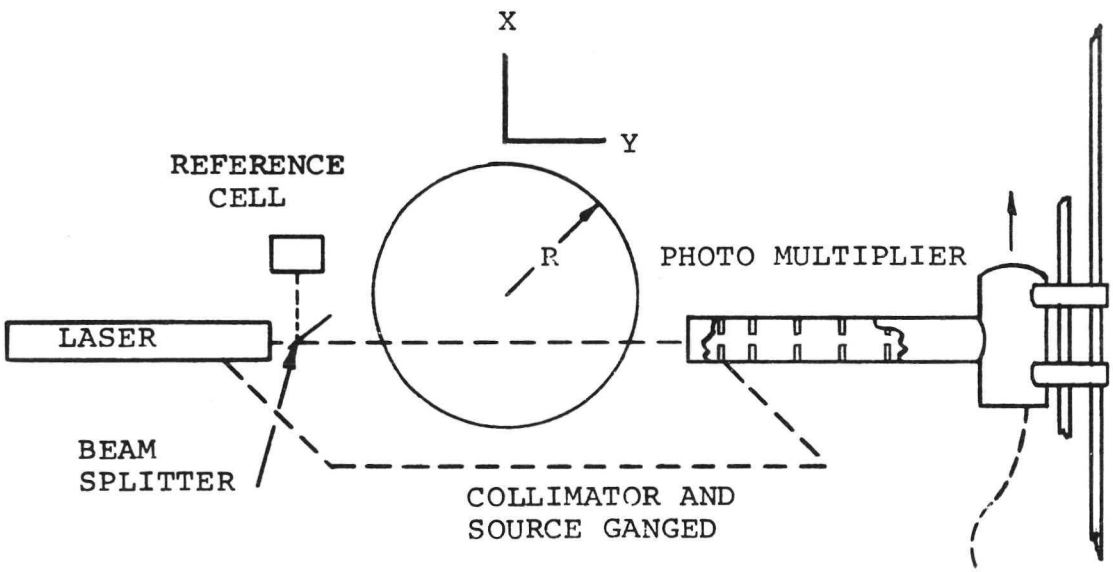

SCHEMATIC REPRESENTATION OF APPARATUS SUITABLE FOR RADIAL SMOKE PARTICLE NUMBER DENSITY DETERMINATIONS

FIGURE 34

☆U.S. GOVERNMENT PRINTING OFFICE: 1973-739-153/41

NATIONAL AERONAUTICS AND SPACE ADMINISTRATION
WASHINGTON, D.C. 20546

OFFICIAL BUSINESS
PENALTY FOR PRIVATE USE $300

SPECIAL FOURTH-CLASS RATE BOOK

POSTAGE AND FEES PAID
NATIONAL AERONAUTICS AND SPACE ADMINISTRATION
451

U.S.MAIL

POSTMASTER: If Undeliverable (Section 158 Postal Manual) Do Not Return

"The aeronautical and space activities of the United States shall be conducted so as to contribute . . . to the expansion of human knowledge of phenomena in the atmosphere and space. The Administration shall provide for the widest practicable and appropriate dissemination of information concerning its activities and the results thereof."

—NATIONAL AERONAUTICS AND SPACE ACT OF 1958

NASA SCIENTIFIC AND TECHNICAL PUBLICATIONS

TECHNICAL REPORTS: Scientific and technical information considered important, complete, and a lasting contribution to existing knowledge.

TECHNICAL NOTES: Information less broad in scope but nevertheless of importance as a contribution to existing knowledge.

TECHNICAL MEMORANDUMS: Information receiving limited distribution because of preliminary data, security classification, or other reasons. Also includes conference proceedings with either limited or unlimited distribution.

CONTRACTOR REPORTS: Scientific and technical information generated under a NASA contract or grant and considered an important contribution to existing knowledge.

TECHNICAL TRANSLATIONS: Information published in a foreign language considered to merit NASA distribution in English.

SPECIAL PUBLICATIONS: Information derived from or of value to NASA activities. Publications include final reports of major projects, monographs, data compilations, handbooks, sourcebooks, and special bibliographies.

TECHNOLOGY UTILIZATION PUBLICATIONS: Information on technology used by NASA that may be of particular interest in commercial and other non-aerospace applications. Publications include Tech Briefs, Technology Utilization Reports and Technology Surveys.

Details on the availability of these publications may be obtained from:

SCIENTIFIC AND TECHNICAL INFORMATION OFFICE

NATIONAL AERONAUTICS AND SPACE ADMINISTRATION

Washington, D.C. 20546